PARAMETER ESTIMATION AND OPTIMAL SUPERVISORY CONTROL OF CHILLED WATER PLANTS

by

BARRETT A. FLAKE

A dissertation submitted in partial fulfillment
of the requirement for the degree of

DOCTOR OF PHILOSOPHY
(Mechanical Engineering)

at the

UNIVERSITY OF WISCONSIN-MADISON

1998

© Copyright by Barrett A. Flake 1998
All Rights Reserved

PARAMETER ESTIMATION AND OPTIMAL SUPERVISORY CONTROL OF CHILLED WATER PLANTS

Barrett A. Flake

Under the supervision of Professor John W. Mitchell
at the University of Wisconsin–Madison

The objective of the work is to develop methods for minimizing the energy costs of chilled water systems through optimal control. The general approach includes the following tasks: 1) proposing a system of parametric models that represent the real chilled water system, 2) determining model parameters from measured data, and 3) subjecting the system of parametric models to an optimization algorithm.

A comprehensive approach for determining the optimal control for any general chilled water system is developed. The general system presents a difficult problem for parameter estimation and optimization because of discontinuous variables and nonlinear relationships between input and output variables. Various methods for parametric estimation and control optimization are presented and demonstrated on simulated and actual plant models.

The actual plant model consists of interconnected component models, including an electric motor driven chiller, a steam turbine driven chiller and associated steam condenser, and a multi-cell cooling tower. Different parameter estimation methods using measured plant data are applied and compared. Optimal supervisory control is determined through application of the simulated annealing method to the model. The dependence of optimal control settings upon independent variables (e.g. chilled water return temperature and ambient wet bulb temperature) is investigated. Cost savings of optimal over conventional control strategies are calculated and compared.

Contents

Abstract i

List of Figures ix

List of Tables xv

Nomenclature xvii

CHAPTER 1 Introduction 1

1.1 Motivation 1
1.2 HVAC System Description 2
1.3 System Optimization – A Simplified Example 4
1.4 Summary 6

CHAPTER 2 Literature Review 9

2.1 Introduction 9
2.2 Optimal Control Applied to HVAC Systems 10
2.3 Summary 18

CHAPTER 3 Parameter Estimation 19

3.1 Model Choice Considerations 19
3.2 Parametric Models 21
3.2.1 Multivariate Model Representation 21
3.2.2 Multiresponse Regression Models 22
3.3 Parameter Estimation Methods 24
3.3.1 Probability Review 24
3.3.2 Parameter Estimation by Least Squares 26
3.3.3 Other Estimation Methods 28
3.3.4 The Determinant Criterion 29
3.3.5 Linear Dependencies in $R^{\mathrm{T}}R$ 29
3.4 Parameter Identifiability Problems 32
3.4.1 Overparameterization 32
3.4.2 Parameter Variance 34
3.4.3 Parameter Identification Problems Summary 36
3.5 Example Chilled Water Plant 37
3.5.1 Chilled Water System Simulation with TRNSYS 37
3.5.2 Example System Description 37
3.5.3 Minimization Algorithms Used 39
3.5.4 Parameter Identifiability Problems with the Cooling Tower Model 42
3.5.5 Starting Values 45
3.5.6 Explanation of Tables of Regression Results 45
3.5.7 Method Comparisons 48
3.5.8 Residual Plots 56
3.5.9 Example Problem Parameter Variance Estimates 60
3.5.10 Outliers 61
3.6 Summary 64

CHAPTER 4 Parameter Estimation - Walnut Street Plant 67

4.1 Central Plant Description 67
4.2 Data Measurements 70
4.3 TRNSYS Walnut Street Plant Model 72
4.4 Component Models 74
4.4.1 Chiller Model 74
4.4.2 Steam Turbine Model 76
4.4.3 Heat Exchanger (Surface Condenser) Model 77
4.4.4 Cooling Tower Model 79
4.5 Parameter Estimation for the Walnut Street Plant Model 80
4.5.1 Parameter Estimation Methods 80
4.5.2 Parameter Estimation Results - Composite Model 84
4.5.3 Parameter Estimation Results - Individual Components and Subsystems 88
4.5.4 Use of Manufacturer's Data for Parameter Estimates 90
4.5.5 Parameter Estimation Summary 94

CHAPTER 5 Optimal Supervisory Control 99

5.1 The Optimal Control Problem 99
5.2 The Steady State Optimal Control Problem 101
5.2.1 Local Loop/Supervisory Control 101
5.2.2 The Steady State Approximation 102
5.2.3 Application of the Steady State Approximation to a Chilled Water System 103
5.3 Optimization Problem 105
5.3.1 Classification of the Optimization Problem 106
5.4 Simulated Annealing 106
5.4.1 Background 106
5.4.2 Methodology 107

5.4.3 Implementing Simulated Annealing with TRNSYS 109
5.4.4 Constraints 111
5.5 Implementation of Optimal Control in a Chilled Water System 111
5.6 Summary 113

CHAPTER 6 Optimal Supervisory Control -Walnut Street Plant 115

6.1 Problem Description 115
6.2 Conventional Control 117
6.3 Optimal Supervisory Control Results 118
6.4 Demand Charges 124
6.5 Optimal Supervisory Control with Demand Charges 128
6.6 Priority Control 132
6.7 Optimal Control with Tchws = 7.2 °C (45.0 °F) 134
6.8 Chiller Part Load Performance and Optimal Control 136
6.9 Summary 139

CHAPTER 7 Conclusions 141

7.1 Modeling and Parameter Estimation 141
7.1.1 Modeling 142
7.1.2 Regression Methods 142
7.1.3 Walnut Street Plant Parameter Estimation 143
7.2 Optimization 144
7.2.1 The Optimization Problem 144
7.2.2 Simulated Annealing Method 145
7.2.3 Optimal Control of the Walnut Street Plant 145
7.3 Summary 147

CHAPTER 8 Recommendations 149

8.1 Modeling and Parameter Estimation 149

8.1.1 Data Acquisition 149

8.1.2 Model Comparisons 150

8.1.3 Overparameterization and Parameter Variance 150

8.1.4 Updating Parameter Estimates 151

8.1.5 Integrated System Optimization and Parameter Estimation 152

8.2 Optimal Control 152

8.2.1 Optimal Control Strategies 152

8.2.2 Demand Charges and Dynamic Optimization 153

8.2.3 Extension and Application of Optimal Control Methods 154

8.2.4 Recommended Application of Optimal Control Results. 155

Bibliography 157

List of Figures

FIGURE 1.2.1: System for cooling a conditioned space. Energy consuming components are marked with an asterisk (*). The combined system of compressor, condenser, expansion valve and evaporator constitute a “chiller”. 3

FIGURE 1.3.1: Relationship between component power and temperatures in a simple vapor compression refrigeration system. 5

FIGURE 1.3.2: Dependence of total power (evaporator fan, compressor and condenser fan) upon evaporator and condenser fan power. 6

FIGURE 3.2.1: Block diagram showing interconnections of a multicomponent system. 22

FIGURE 3.3.1: Example cumulative probability density function. 24

FIGURE 3.3.2: Example probability density function (pdf). 25

FIGURE 3.3.3: Inlet and outlet temperatures for a counter flow heat exchanger. 30

FIGURE 3.4.1: Plot of Equation 3.4.3 for β_3= 8.75 (solid line) and β_3 = 1.25 (dashed line). 33

FIGURE 3.5.1: Block diagram showing interconnections in the example system. 38

FIGURE 3.5.2: Objective function surface in terms of parameters c and n for the cooling tower parameter estimation example. 44

FIGURE 3.5.3: Enlargement of objective function surface in FIGURE 3.5.2. 44

FIGURE 3.5.4: Error vs. "true" steam flow rate values over the initial 240 points of simulated measured data. The random error has a standard deviation of 100. 58

FIGURE 3.5.5: Residuals (measured - predicted values) of steam flow rate for the initial 240 data points. Estimation method used weighted least squares with the Levenberg-Marquardt minimization algorithm and four responses in the objective function. The residuals have a standard deviation of 136.5. 58

FIGURE 3.5.6: Steam flow rate errors vs. predicted values over the second set of 240 observations. Parameter estimates used in generating these data are from the application of ordinary least squares and the SQP algorithm. 59

FIGURE 3.5.7: Steam flow rate errors vs. predicted values over the second set of 240 observations. Parameter estimates used to generate these residuals are the result of using four regressor variables in a weighted least squares objective function and the Levenburg-Marquardt algorithm (ODRPACK). 59

FIGURE 3.5.8: Plot of residuals of hot well temperatures resulting from regression. Twelve outliers, evident in the plot, were included in the measured data. 64

FIGURE 4.1.1: Walnut Street chilled water plant schematic. 68

FIGURE 4.2.1: Log sheet for chiller #4 (electric motor driven) on July 11, 1994. 71

FIGURE 4.3.1: Walnut Street TRNSYS model wiring diagram showing input and output connections of the component variables. 73

FIGURE 4.4.1: Diagram of TRNSYS chiller component model. 75

FIGURE 4.4.2: Diagram of steam turbine and surface condenser. 78

FIGURE 4.5.1: Diagram showing interconnections of the chiller/steam turbine/surface condenser subsystem. 83

FIGURE 4.5.2: Steam flow rate and electric power residuals standard deviations resulting from applying the determinant criterion and least squares with various responses. 87

FIGURE 4.5.3: Steam mass flow rate residuals from composite model predictions using parameters estimated from subsystem component models. 91

FIGURE 4.5.4: Electric chiller power residuals from composite model predictions using parameters estimated from subsystem component models. 91

FIGURE 4.5.5: Measured and predicted steam mass flow rate with parameters estimated using subsystem component models. 92

FIGURE 4.5.6: Measured and predicted electric chiller power with parameters estimated using subsystem component models. 92

FIGURE 4.5.7: Residual plot for cooling tower water outlet temperature with parameters estimated from measured data. 95

FIGURE 4.5.8: Residual plot for cooling tower water outlet temperature with parameters estimated from manufacturer's data. 95

FIGURE 4.5.9: Measured and model predicted cooling tower water outlet temperature using parameters estimated from measured data. 96

FIGURE 4.5.10: Measured and model predicted cooling tower water outlet temperature using parameters estimated from measured data. 96

FIGURE 5.2.1: Local loop control of coil discharge air temperature. 102

FIGURE 5.2.2: a.) Optimal trajectory of a dynamic system. b.) Discrete approximation to optimal trajectory. c.) System response showing near steady state behavior of system over interval ΔT. 103

FIGURE 5.4.1: The simulated annealing algorithm given by Corana et al. [Cor78] 109

FIGURE 5.4.2: System of chilled water components within TRNSYS. 110

FIGURE 5.4.3: Implementation of SIMANN optimization algorithm with TRNSYS. 112

FIGURE 6.2.1: Steam and electricity costs under conventional control. 119

FIGURE 6.2.2: Chilled water return temperature and supply temperatures from the steam and electric chillers (#3 and #4) under conventional control. 119

FIGURE 6.2.3: Cooling tower fan speeds under conventional control. 120

FIGURE 6.3.1: Optimal chilled water temperatures from both chillers as a function of chilled water return temperature. Electric costs are 4.40¢/kW·hr. 121

FIGURE 6.3.2: Optimal chilled water temperatures from both chillers as a function of chilled water return temperature. Electric costs are 2.64¢/kW·hr. 121

FIGURE 6.3.3: Total cost as a function of $T_{chw\ \#3}$ at different cooling tower fan speeds. Independent variables: T_{chwr} = 9.2 °C, T_{db} = 18.3 °C, k_{elec} = $0.0264/kW·hr. 122

FIGURE 6.3.4: Total cost as a function of $T_{chw\ \#3}$ at different cooling tower fan speeds. Independent variables: T_{chwr} = 11.3 °C, T_{wb} = 25.6 °C, k_{elec}= $0.0444/kW·hr. 122

FIGURE 6.3.5: Steam and electric chiller energy costs with cooling tower fans at full speed. Independent variable values are the same as given in FIGURE 6.3.4. 123

FIGURE 6.3.6: Optimal cooling tower fan speed control vs. chilled water return temperature and wet bulb temperature. Electrical cost is $0.0264/kW·hr. 125

FIGURE 6.3.7: Optimal cooling tower fan speed control vs. chilled water return temperature and wet bulb temperature. Electrical cost is $0.0440/kW·hr. 125

FIGURE 6.3.8: Conventional cooling tower fan speed control vs. chilled water return temperature and wet bulb temperature. 126

FIGURE 6.3.9: Hourly savings of optimal control over conventional control. 126

FIGURE 6.5.1: Total cost versus chilled water supply temperature from chiller #3. In this case, there is a demand charge for electric power requirement exceeding 3951 kW. 129

FIGURE 6.5.2: Rank ordered optimal hourly power demand. No demand charges were included in the optimization. 131

FIGURE 6.5.3: Rank ordered demand with optimal peak demand limit included in the optimization. 132

FIGURE 6.6.1: Chilled water supply temperatures and load fraction for steam priority chiller control. 133

FIGURE 6.7.1: Optimal chilled water supply temperatures of the steam and electric chiller versus chilled water return temperature. The mixed chilled water supply temperature is fixed to be 7.2 °C. 137

FIGURE 6.7.2: Optimal fraction of total load met by chillers #3 and #4 versus chilled water return temperature. 138

FIGURE 6.8.1: Typical part load performance for an electrically driven chiller at constant entering condenser water temperature. 138

List of Tables

TABLE 3.5.1 Parameter Starting Values and Bounds 46

TABLE 3.5.2 Example System Regression Results - Ordinary Least Squares, Six Responses 50

TABLE 3.5.3 Example System Regression Results - Ordinary Least Squares, Four and Three Responses 51

TABLE 3.5.4 Example System Regression Results - Weighted Least Squares 53

TABLE 3.5.5 Example System Regression Results - Determinant Criterion 54

TABLE 3.5.6 Parameter Variance and Bias Estimates for the Example Problem 61

TABLE 3.5.7 Example System Regression Results - Outliers Included in Data 63

TABLE 4.5.1 List of parameters used in the composite chilled water plant model 81

TABLE 4.5.2 Problem configurations used in parameter estimation runs 84

TABLE 4.5.3 Walnut Street Regression Results 86

TABLE 4.5.4 Estimated Cooling Tower Parameters 93

TABLE 4.5.5 Estimation Results Using Manufacturer's and Measured Data 94

TABLE 6.1.1 Independent and Control Variables 116

TABLE 6.7.1 Comparison of costs under different operating strategies 136

Nomenclature

Roman symbols

c		control variable
c_p	[kJ/kg K]	constant pressure specific heat
C_r	[-]	ratio of heat capacitance
E	[volts]	voltage
f_{hw}	[-]	hot well heat transfer factor
h	[kJ/kg]	enthalpy
H_i		system interconnection matrix
I	[amps]	current
J		objective function
k	[$/energy unit]	cost per unit energy
$\dot{m}$	[kg/hr]	mass flow rate
Ntu	[-]	number of transfer units
p	[Pa]	pressure
pf	[-]	power factor
P	[kW]	power
$\dot{Q}$	[kJ/hr]	heat transfer rate

r		residual in predicted value
R		residual matrix
t	[hr]	time
T	[°C]	temperature
UA	[kJ/hr K]	overall heat transfer coefficient
V	[m^3/hr]	maximum cooling tower volumetric flowrate
V		covariance matrix
w		data weight
W		weighting matrix
x		input variable
X	[-]	normalized chiller temperature difference
$\tilde{y}$		measured response value
$\hat{y}$		true response value
y		predicted response (output) variable
Y	[-]	normalized compressor power

Greek symbols

β		model parameter
γ	[-]	cooling tower fan speed control variable
ε	[-]	heat transfer effectiveness
ε	[-]	error in predicted value
η	[-]	efficiency
λ		Lagrange multiplier
ρ	[kg/m^3]	density
ω	[$kg_{water}/kg_{dry\ air}$]	air humidity ratio

CHAPTER 1

Introduction

1.1 Motivation

Energy used to maintain comfortable living and working environments represents a large fraction of total energy usage. According to the United States Department of Energy (DOE), energy consumption in commercial and residential buildings represented 36% of the United States total energy use in 1996 [DOE97]. Associated with the very large energy requirements are large energy costs. For example, a large central heating and chilled water plant serving the University of Wisconsin-Madison campus has annual fuel costs exceeding $5 million. Consequently, there is great interest in minimizing energy costs.

In an effort to reduce energy costs, the performance of compressors, fans, heat exchangers and other components used in heating and cooling systems has been greatly improved. However, even if these devices operate at their limiting thermodynamic efficiency, more can be done to reduce energy costs. Maximizing individual component efficiency does not necessarily result in the collection or system of components operates at minimum cost. Another opportunity for minimizing energy costs lies in the *supervisory control* of the system of components. Heating and cooling systems are typically controlled to maintain temperature and humidity levels. Since there may be

many control settings that meet these environmental requirements, there exists an opportunity to find a set of *optimum supervisory control* settings that minimize energy costs. The means of determining these optimum control settings is the goal of this work.

1.2 HVAC System Description

A heating, ventilating and air conditioning (HVAC) system may be generally described as a system for transporting heat and moisture into or out of conditioned spaces. In usual practice, the moisture transport is associated with either humidification or dehumidification of an air stream by evaporation or condensation. Thus, the moisture transport can also be included as a heat transport process associated with the phase change (i.e. latent heat or latent load). HVAC systems also function to ventilate conditioned spaces, diluting indoor air contaminants with filtered outdoor air. Although any general HVAC system that heats, cools or ventilates may be the object of optimal control, this work focuses on the more complex cooling or "air conditioning" systems. The methods developed are general, however, and are applicable to optimal control of heating and ventilating systems as well.

At any level of complexity, from a window unit to a large scale chilled water plant, the primary system function is to move heat (e.g. a cooling "load") between some conditioned space and some lower temperature sink. Heat enters the conditioned space from any number of sources and must be removed at the same rate in order to maintain comfortable conditions. The source of cooling (or heat sink) may be a chilled water coil or an evaporator of a vapor compression refrigeration cycle. Heat transferred to an evaporator of a refrigeration cycle is further transported to the environment along with energy input to the cycle.

In moving the heat from the spaces to the lower temperature sinks and to the environment, heat is exchanged between different fluids. Consider the system shown in Figure 1.2.1, used to provide chilled water for cooling a conditioned space. The heat entering the conditioned space is transported via a moist air stream to the chilled water at the chilled water coil. Next, the heat is transported via the chilled water to the refrigerant at the chiller evaporator. Then the heat is rejected, along with the energy input of the compressor, to water moving through the condenser.

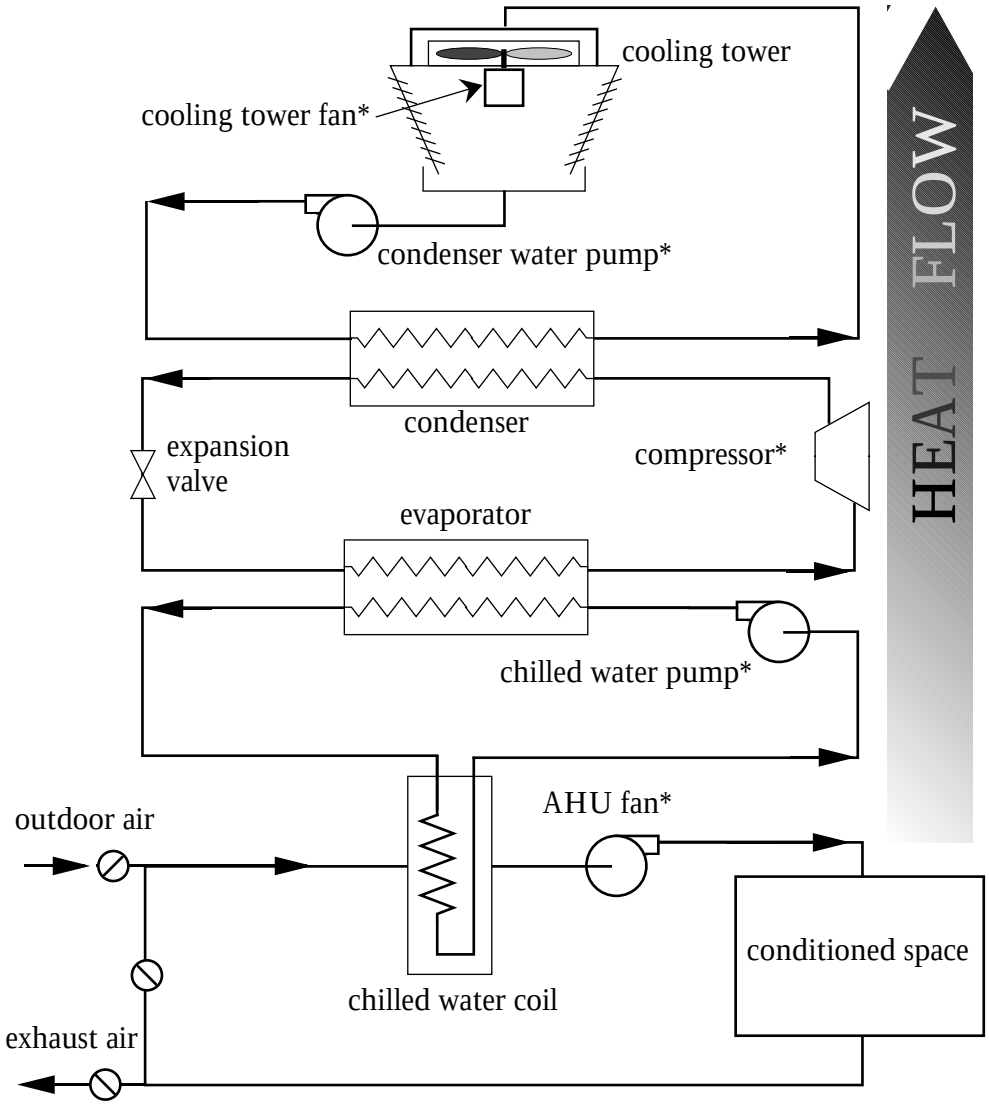

FIGURE 1.2.1: System for cooling a conditioned space. Energy consuming components are marked with an asterisk (*). The combined system of compressor, condenser, expansion valve and evaporator constitute a “chiller”.

The resulting additional heat in the condenser water is rejected to the environment by transfer to an airstream moving through the cooling tower.

Discounting any natural convection driven loops, at every stage of the heat transport process a work input is required to move the fluid. Energy costs associated with operating the system

include not only the cost of energy input for the cooling cycle, but also all the fans and pumps used to transport heat through the system. For systems with widely distributed flows, the pumping and fan costs can easily be as much as the costs for operating the compressor.

1.3 System Optimization–A Simplified Example

Although the cooling load for the conditioned spaces is fixed for any given environmental conditions, the flow rates of the working fluids in the transport loops are not. An equivalent amount of heat may be transported at a higher or lower flow rate with a corresponding decrease or increase in temperature difference. In a system capable of variable flow rates, the opportunity for optimization lies by finding the flow rates which minimize total energy costs.

Considering a single fluid loop, minimum pumping cost occurs at the lowest flow rate at which the load can be transferred at the heat exchangers. However, the temperature difference in any single loop cannot change independently of the other energy consuming components. Lower pumping costs may require larger costs in other loops. The dependence of cooling cycle energy costs upon pumping or fan costs can be explained by considering the simple system in Figure 1.3.1. The temperature differences of the evaporator, condenser and the cooling cycle are given in relationship to one another. The temperature of the conditioned space T_{space}, the ambient (outdoor) temperature T_{amb}, and the space cooling load $\dot{Q}_{evap}$, are fixed, while the evaporator and condensing temperatures (T_{evap} ,T_{cond}) can vary.

For this system, the total energy cost is the sum of three component costs: the evaporator fan, the cooling cycle compressor and the condenser fan. The relationships between temperature differences and component energy costs are given by simplified models shown in the figure. Compressor power is given in terms of the condensing and evaporating temperatures, as in a Carnot refrigeration cycle. For constant specific heat and constant effectiveness, heat transfer at the evaporator and condenser is proportional to the product of air mass flow rate and the difference in incoming fluid temperatures. Fan power has a simple cubic dependence upon air mass flow rate. Note that for the evaporator and condenser fans, as their energy input decreases, the flow rates decrease, and to maintain the same heat transfer, the temperature differences must increase. The

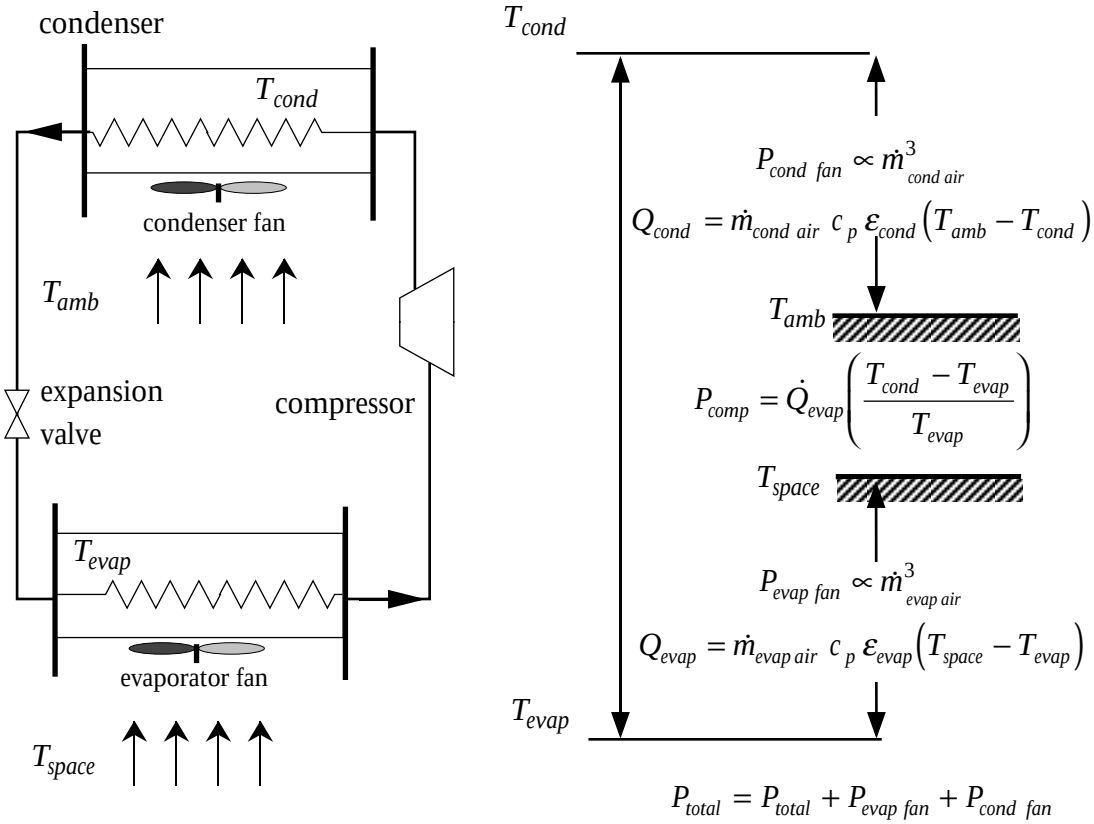

FIGURE 1.3.1: Relationship between component power and temperatures in a simple vapor compression refrigeration system.

converse is true for the cooling cycle - an increase in temperature difference over which the cycle must transport heat corresponds to an increase in energy input and therefore energy costs. The optimization problem for this example system is to find what combination of evaporator and condenser flow rates (or equivalently, evaporator and condenser fan powers) result in the total system energy cost being minimized.

The inverse relationship between the power input to the fans and power required for the thermodynamic cycle yields a convex dependence of total power upon either fan power. The refrigeration cycle is more efficient when operating over smaller temperature differences. However, to achieve the lower temperature differences in the heat exchangers, the flow rates and therefore the pump and fan power must be larger. A contour plot representative of the total power in terms of

evaporator and condenser fan power is given in Figure 1.3.2. The optimum operating point occurs

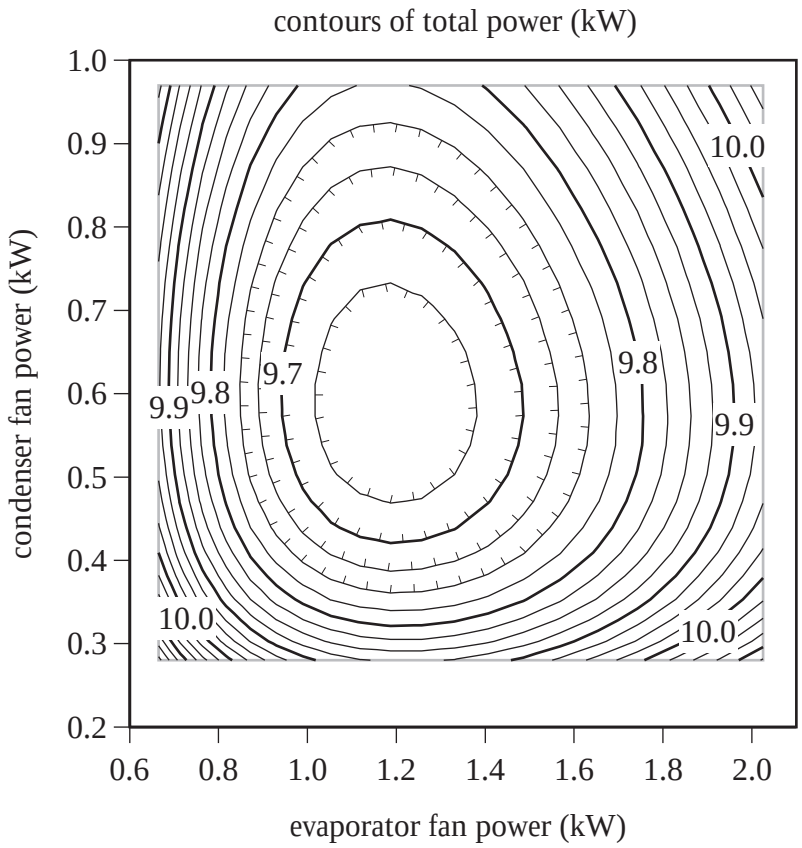

FIGURE 1.3.2: Dependence of total power (evaporator fan, compressor and condenser fan) upon evaporator and condenser fan power.

where an incremental increase in fan cost is equivalent to the incremental reduction in cooling cycle power cost.

1.4 Summary

The objective of this thesis is to develop a means for determining values of controlled variables that minimize total energy costs for a general chilled water system. A general system represents a much more difficult optimization problem than shown in the example. Major difficulties include matching model predictions to real system performance and solving a multidimensional, con-

strained optimization problem with both continuous and discrete variables. Some of these difficulties are described in the review of published reports on HVAC system optimization given in Chapter 2. Methods for modeling and model parameter estimation are given in Chapter 3. These methods are applied to finding parameter estimates for chilled water plant model in Chapter 4. The supervisory optimal control problem and methods of its solution are discussed in Chapter 5. Optimal supervisory control for a chilled water plant on the University of Wisconsin campus is explored in Chapter 6. Conclusions and recommendations are discussed in the final chapters.

CHAPTER 2

Literature Review

2.1 Introduction

Optimization or minimization of operating costs associated with HVAC systems has been addressed in the technical literature only in recent years. To some extent, the knowledge and technology for implementing at least some form of optimal control has existed since the advent of commercial air conditioning and refrigeration earlier this century. However, reports concerning optimal control of HVAC systems are not found in the literature dated prior to the mid-1970s. As the primary if not sole driving force behind the implementation of any new technology is economic, the "energy crisis" of the early 1970s no doubt spurred the increased interest in minimizing energy costs.

Presented here is a review of literature that addresses optimal control applied to the operation of HVAC systems. Much work has also been published on the application of optimization methods in the general area of process control and on application to specific non-HVAC systems. Work not specifically related to HVAC systems is reviewed as necessary to support the proposed methodology.

2.2 Optimal Control Applied to HVAC Systems

The paper by Zimmer discusses a basic approach of proposing a parametric model, determining the model parameters and subjecting the model to an optimization method for minimizing costs associated with a system of chillers. [Zim76] The proposed application included multiple chillers driven by differing energy sources with differing costs. Quadratic models of individual chiller operating cost in terms of load were used with a minimization method given by Nelder and Mead [Nel65] to determine optimal loading of the chillers. The Nelder-Mead method is a downhill search method for multidimensional minimization involving only function evaluations. Zimmer modified the original Nelder-Mead method to handle constraints by using a penalty function. Coefficients for the models of chiller costs in terms of load were fit from data collected from the subject system. The chiller loads were constrained to be between some given maximum and minimum; however, the approach did not consider the possibility of changing the on/off status of a chiller. Also, the models for costs did not account for variations in condenser temperature or flow rates. The primary conclusion drawn was that it is sometimes best to operate the chillers at equal incremental costs when not limited by the maximum or minimum load constraints. Incremental cost is described as the resulting increase in chiller energy cost for an increment in chiller load. Reduction in annual energy costs were anticipated to be only 1-3% for the application of the given optimization methodology.

In some reports, general recommendations toward reducing chiller system energy are presented as resulting in an "optimized" system. Such a report is given by Lipták in which a number of heuristic optimization rules are given, many of which appear to be shortsighted. [Lip77] For example, he advocates minimizing chiller COP by running at a maximum feasible chilled water temperature and minimizing the cooling tower water temperature. The corresponding increases in pump and fan power are neglected. A number of credible suggestions are offered however, such as recovering heat from the condenser and discriminating between the chilled water loads to determine the maximum chilled water set point.

A rare report of actual implementation of optimization methods to a refrigeration system is given by Chun and Norden. [Chu82] The report details the operation, management and control

of a large (14,200 ton) chilled water system supporting a large textile plant. Again, the basic approach included using a parametric model in an optimization algorithm. For this application, chiller power was modeled by a linear combination of five measured variables. The Nelder-Mead simplex algorithm was used to determine the chilled water supply temperatures for the individual chillers that minimize total system operating costs. In order to determine the model parameters, factorial experiments were run with each of the dependent variables varied over a range of conditions. If the difference between predicted and actual compressor work exceeded some limit, the models were updated with another set of experiments.

The Nelder-Mead simplex algorithm was modified for their problem to handle constraints by adding a penalty, equal to the square of the constraint violation, to the objective function. Minimization was done only in terms of chilled water temperatures (continuous variables) and did not consider different combinations of operating chillers (integer variables). Chun's report did provide an estimate of the potential savings by optimizing systems of chillers. A comparison of annual energy usage for the refrigeration system showed a 12.5% decrease after implementing the optimization strategy.

Methods for improvement rather than optimization of chiller energy usage are presented by Thielman. [The83] Recommendations are made for varying chilled water supply and condenser water supply temperatures based on external forcing variables, such as load and wet bulb temperature. However, the dependence of compressor power upon chilled water and condenser water temperatures and flows is not investigated. These ideas are centered on reducing chiller power consumption rather than total system power. Using an energy management and control system (EMCS) to sequence the operation of multiple chillers is advocated. It is assumed that the optimal schedule for sequencing as a function of load is known a priori.

A multilevel optimization approach is used by Enterline [Ent84] where groups of components are optimized without considering the dependence between the components. For example, the optimum chilled water set point is the maximum temperature that can meet all required loads. This local optimization does not consider the resulting increase in pumping costs. A coordinating or supervisory controller determines the optimum chilled water temperature from a proposed

model relating chiller power and chilled water pumping power. An on-line control strategy is used where the gradient of chiller plus pump power with respect to chilled water temperature is continuously evaluated. This gradient is an input to the supervisory controller, which then determines the optimal chilled water set point. However, the supervisory controller did not account for pumping and fan costs on the condenser side of the chiller. Optimal load allocation among parallel chillers was determined with quadratic models of individual chiller utility cost in terms of load. The quadratic cost models were of limited use, as they did not account for the dependence of chiller costs on evaporator or condenser temperatures.

Hackner investigated optimal control for a specific building and supporting chilled water plant by simulation. [Hac85] The study included finding optimum combinations of some discrete control variables such as number of operating chillers or speeds of cooling tower fans. Optimal chilled water supply temperatures and supply air temperatures were determined by running the simulation over a wide range of conditions. The run of 40,000 combinations required to determine the optimum conditions was considered impractical for performing on-line control given the computational power available at the time. Resulting energy reduction was reported to be 19% compared to operating the plant with fixed set points.

Johnson advocated using programmable controllers to reset system set points such as chilled water and condenser water temperature and implementation of a chiller sequencing schedule. [Joh85] The optimal chiller sequence schedule in terms of load is derived in the manner of Hackner. [Hac85] The thrust of Johnson's work gives some means of exploiting the capabilities of programmable controllers in reducing system energy costs. The means of determining optimal values of set points used by the programmable controllers is not investigated.

Spethman demonstrated how to find the optimum combination of chillers and their respective loads from performance graphs.[Spe85] Methods are shown for cases of both similar and dissimilar chiller characteristics. An algorithm is proposed for finding the minimum cost for operating three chillers with dissimilar characteristics. However, this algorithm could not be extended to the general case. Auxiliary pumping and fan costs were not included in the analysis.

A simulation of a 1.4 million square foot commercial facility was used by Lau to determine optimal control strategies for the specific case. [Lau85] Models for the building's multiple chiller chilled water plant were fit with real system data. The optimum conditions for minimizing plant energy costs were found by exercising the simulation over ranges of five variables: wet bulb temperature, chilled water load, cooling tower fan speeds, condenser pump flow and number of operating chillers. Optimization of these variables demonstrated a 1.4% reduction in energy costs compared to existing control practices at the plant. However, the chilled water supply temperature was not considered in the global type search.

Braun [Bra89] presented two approaches or methodologies for finding optimal values of control variables in a chilled water system. A modular, component based method is given where the cost functions of individual models are assumed to be quadratic. Other component output variables are assumed to be linear functions of inputs. It is assumed that the sum of the component costs is quadratic in terms of the control variables, and ordinary gradients are used to define the optimum values of these variables. Equality and inequality constraints are incorporated with Lagrangian multipliers. The general functions presented for the component models include discrete or non-continuous dependent variables. As the gradient methods used cannot be applied to the nonsmooth functions resulting from the discrete variables, a combinatorial approach is recommended. The optimization problem is solved in terms of the continuous variables for every feasible combination of discrete variables and the combination yielding the minimum cost is selected.

The quadratic cost function and linear output models are extended to the case of nonlinear optimization through an iterative technique. The quadratic and linear models then represent local approximations to the nonlinear models. Under an assumption of convexity, this method is shown to converge to the optimum.

A second approach to the problem of determining optimum control variables considers the collection of components as a single system where the system cost is modelled as quadratic in the controlled and uncontrolled variables. The uncontrolled variables are considered to be measurable inputs that affect the performance of the system such as chilled water load and wet bulb tempera-

ture. This formulation somewhat simplifies the optimization problem, as an analytical expression of the optimum can be derived by equating the Jacobian of the system cost function to zero. Discrete variables are again considered in a combinatorial sense where the analytical expression for zero gradient is evaluated for all feasible combinations.

Braun gives two methods for estimating the parameters used in the quadratic system model. The first is to apply regression methods to measured data of total power consumption and controlled and uncontrolled variables. A set of experiments could be made to exercise the system over the expected range of operating conditions. If the quadratic cost function can be accurately fit only in a region near the optimum, it is suggested that experimental runs be made in the vicinity of the predicted optimal control. However, the predicted optimal control is dependent upon external forcing variables such as load and wet bulb temperature. Determining the quadratic model parameters for all expected ranges of wet bulb and load would constitute an extensive task.

Another approach to estimating the parameters is to construct a (computer) simulated system comprised of mechanistic models for each component. The determination of parameters used in the mechanistic models can be found from data taken over a limited range of conditions. Here, it is assumed that the mechanistic models are accurate representations of the real components and the parameters fit from data taken over any region of operation should be nearly constant over all operating regions. The simulation is then exercised over all ranges of operation and the parameters used in the system based optimization are fit from simulation data.

The near optimal control methodologies given earlier by Braun [Bra89] are applied in finding the optimum control for cooling towers in a chilled water system. [Bra90] Linear models of optimum air flow in terms of fractional chiller load are derived. It is shown that optimal tower air flow is strongly dependent upon chilled water load and only weakly dependent upon wet bulb temperature. Further assuming that the chilled water load may depend somewhat on ambient air wet bulb temperature, Braun makes a case for determining an approximate optimum tower air flow rate in terms of chiller load only. A number of simulations were run showing the approximate optimum system power consumption was within 1% of the actual optimum. However, because of the relatively “flat” dependence of total system power upon air flow near the optimum, the

approximate optimal airflows differed from the true optimum by up to 10%. Braun recommends the model parameters be fit from design data or determined from experimental data. For the case of multiple chillers, different optimal control models must be made for every possible combination of operating chillers.

Ulleberg used the second methodology of Braun's [Bra89] described above to determine optimal values of controlled variables in an emulated HVAC system. [Ull93] A quadratic model of total system power in terms of controlled and uncontrolled variables is proposed. The strategy used was to first operate the emulator over a learning period during which data was taken to fit the quadratic model parameters. During the learning period, the controlled variables were varied over a range of values in order to improve the fit of the parametric model. However, it was demonstrated that the resulting parametric model did not adequately predict the optimal control variables over all ranges of operation. Parameters fit from data taken mostly at intermediate loads resulted in significant model error when used to predict optimal controls at high loads. For the particular emulated system, the quadratic model was inadequate for approximating optimal control values.

The problem of optimizing a multiple chiller, multiple cooling tower chilled water plant was cast in terms of a mixed-integer nonlinear programming problem (MINLP) by Olson. [Ols90] The integer variables were the status (e.g. on/off, off/low/high) of the chillers and cooling tower fans, while others, such as chilled water and condenser water temperatures, were assumed to be continuous variables. Sequential quadratic programming (SQP) was used to solve the nonlinear problem in terms of the continuous variables and a heuristic algorithm was used to determine the integer variables. Empirical models relating chiller and fan power were used to link the dependency of the controlled variables to the total system power (the objective function.) The SQP approach sometimes drove the empirical models to be evaluated beyond their intended region of applicability. In order to keep the optimization algorithm from examining these infeasible areas, artificially high objective function values were returned to the optimization algorithm if the inputs to the models were outside reasonable ranges.

The possible integer combinations of cooling tower fans are arranged by Olson in a sequential order of increasing fan power and corresponding increase in air flow, in the same manner as Braun. [Bra90] A similar ordered sequence of chiller combinations is set up based upon the sum of maximum power consumption of the chiller combination. The solution method is to evaluate the nonlinear problem (given in terms of the continuous variables) by SQP for a given integer combination of cooling tower fans and chillers. However, the heuristic approach used is to compare total system power while searching up or down the integer sequences. The authors implicitly assume that their ordering of sequenced fans or chillers would yield a convex objective function if the integers were relaxed to continuous variables. This is likely in the case of the ordered cooling tower fans, but may not be true for the order of chiller combinations. The fans can only move air at the discrete increments given in the sequential ordering. The chillers, however, can operate at less than the full power draw that was used in ordering the sequence of chiller operation.

Olson used the optimization algorithm in a number of simulations, and the dependence of optimized total system power as a function of load was studied. It was demonstrated that the optimal power could be closely approximated by a linear model in terms of cooling load.

MacArthur presented a method for determining and implementing the optimal values of control variables using dynamic predictive models. [Mac93] A multivariable predictive controller is developed and tested by simulation. The predictive controller uses dynamic models relating the change in process output to changes in controller inputs. Parameters for the dynamic models are obtained by auto-regressive methods (ARMA). A receding horizon control (RHC) algorithm is presented which minimizes control action in keeping the subject system near the requested set points. Another optimization problem is formulated in which total system cost is to be minimized. The system cost is given in terms of process outputs and the dependence of system cost upon control variables is then determined using the predictive capabilities of the controller. It is shown that directly implementing a set of control variables that give optimal costs at steady state does not minimize energy use integrated over the transient response. The dependence of the cost function upon the state variables changes as the state changes. Rather than minimizing the control action, the resulting costs are minimized by applying the receding horizon control method.

Essentially, dynamic information on the subject system gathered and used by the predictive controller is used to determine minimum steady state operating conditions. The dynamic capabilities of RHC to minimize controller action is then extended to minimizing a cost function given in terms of measured outputs. It is not clear whether the dynamic model is adequate for determining the steady state minimum over a wide range of operating conditions. If the model is only valid near the current operating range, the resulting behavior would be similar to direct search methods where approximate local gradients tend to drive the system downhill in terms of the cost function.

The method was applied to a simulated residential building with a variable speed heat pump. The multivariable controller manipulated heat pump rpm and air flow to the residential space. Personal comfort, as quantized by a statistically based model given in terms of temperature and air velocity as well as other environmental factors, is the controlled variable. Heat pump COP is the objective to be minimized. The simulations demonstrated a 20% decrease in integrated energy consumption over a 24 hour period. However, costs for the air handler fan were not included in the objective function.

Austin developed optimal control strategies for a chilled water plant serving a pharmaceutical manufacturing plant. [Aus93] The chilled water plant has six chillers and a six cell cooling tower. The plant serves both process cooling requirements and comfort cooling requirements. Condenser water from the cooling tower serves the chillers and other process heat rejection requirements. A collection of constant speed and variable speed pumps are used in the condenser water loop and the chilled water loop.

The plant's six indivual chillers were each modeled using a polynomial with power as a quadratic function of load and entering condenser temperature. Cooling tower fan power was modeled as a quadratic function of cooling tower exit water temperature and total heat rejected. Individual equations of cooling tower fan power were fit for a series of wet bulb temperatures. The collection of models were used to determine optimal loading and optimal condenser water temperature as a function of total plant load and outdoor wet bulb temperature. The models were fit using manufacturer's data.

Several simplifications and assumptions were made in the analysis. The chiller operation was limited to sequentially loading each chillers. Beginning with a single chiller, as plant chilled water load increased, another chiller was not added until the first chiller was at maximum load. The analysis did not consider partially loading multiple chillers. In earlier work, Braun [Bra88] demonstrated that optimal loading of like multiple chillers occurs when the chillers are evenly loaded. With sequential loading, no two chillers ever have equal fractional loading (with respect to nominal chiller load). Chilled water supply temperature from each chiller was essentially fixed at 5.6 °C (42 °F). Combinations having chillers supplying different chilled water supply temperature that, when mixed, resulted in the required 5.6 °C were not explored.

2.3 Summary

The work to date which addresses optimized control of HVAC systems demonstrates a common objective pursued by different methodologies. Some employ mathematical optimization techniques while others use global searches through a range of operating conditions. The systems subject to optimization varied as well, from specific to more general arrangements. The value of the existing literature to current work lies mainly in its demonstration of the potential savings in using optimal control and in the recognition of difficulties in solving the problem. One pervasive problem is that of solving the optimization problem with integer or discrete variables such as on/off status of chillers or cooling tower fans.

The foundation of knowledge for building a structure in which to solve any generally posed chilled water system optimization problem is present in the systems science and process control literature. The means of solving the problem are addressed in mathematical science literature. Literature from these areas will be reviewed as appropriate when used in support of the work.

CHAPTER 3

Parameter Estimation

In this work, a system model is created for use as a predictive tool in optimization studies. The model must predict system performance with some measure of accuracy in order for the optimization results to be valid. The parameter estimation problem for the multicomponent chilled water system can be viewed in general terms as a nonlinear, multivariate minimization problem in which a set of parameters that minimize the difference between model predictions and observed system measurements is sought. In this chapter, methods of estimating model parameters are presented and compared by solving an example problem having known parameter values.

3.1 Model Choice Considerations

For optimization studies, a model need only predict variables that contribute to the objective function, such as those having energy costs. Consider a general model of a multivariate system,

$$y = f(x, c) \tag{3.1.1}$$

where y is a vector of dependent variables associated with costs, c is a vector of controlled variables and x a vector of independent or forcing variables. The equation could represent any given functional forms such as a set of polynomial equations or a neural network. Alternately, the equation

could represent a set of mechanistic equations, such as conservation laws and transport equations derived from theory. If the different model types were equally accurate in predicting the system responses over the widest possible range of values of independent and control variables, then relative computational speed may suggest the best model type. However, there are distinct advantages in using mechanistic models for the HVAC (chilled water) systems addressed in this work.

Fitting parameters to arbitrarily selected equations or arbitrarily configured neural networks falls under a general classification of *curve fitting*. [Bar74] Due to the arbitrary nature of the equations, curve fitting can only be used for summarizing data and interpolation between data values. The results cannot in general be used for extrapolation and do not generally provide any insight into the nature of the process. For example, derivatives ($\partial f / \partial x$) from an arbitrary function which fit the data may not be representative of the true nature of the process. Results of Ulleberg's [Ull93] implementation of Braun's method [Bra89a] for optimizing an HVAC system demonstrate problems associated with predicting a minimum using derivatives of a curve fit to discrete data. Ulleberg's curve fit was made with data taken largely over a limited region of system operation. Not only did the curve fit provide an inaccurate model in regions where only a small number of points were taken, but the derivatives of the curve in these regions were of opposite sign compared to that given by theory. Similar problems were encountered by Curtiss et al. in a study of adaptive control using an artificial neural network (ANN) transient model of a hot water coil. [Cur93] The ANN coil model response to an increase in hot water flow rate wrongly predicted an immediate decrease in outlet air temperature. This decrease lasted only a relatively short period before the coil responded as expected with an increase in air temperature. But, because a predictive controller responds to the rate and direction of predicted change in air temperature (derivative control), the actuator's initial response would be in the wrong direction. To correct this, certain weights in the neural network (neural network weights are analogous to parameters in a model composed of a system of nonlinear equations) were constrained to be either less than or greater than zero, which effectively forced the correct direction in the short term response and resulted in a realistic process model. In this case, knowledge of the process physics was required to make a usable process model.

Fitting data to equations derived from mechanistic theory is termed *model fitting*. Models derived from theory can be extremely useful for predicting system behavior in regions of operation lacking data. The derivatives of a well fit mechanistic model should closely represent real system behavior. Theoretical models are useful in optimization applications since the optimum may not occur in a region rich in experimental data points. The advantage of model fitting over curve fitting may be diminished if many data are available for system operation near the optimum for given values of independent variables.

In engineering practice, there is no distinct division between models derived from theory and arbitrary curve fits. Parametric models that closely approximate "true" behavior, yet are not derived from theory, may be postulated for a given process. For example, the asymptotic behavior of the fluid temperature exiting a heat exchanger as a function of flow rate may be captured with a variety of exponential functions. There is some measure of arbitrariness in the choice of the parametric function, but the behavior of the process may be well matched.

3.2 Parametric Models

3.2.1 Multivariate Model Representation

A system model can be defined as a system of interconnected components. Figure 3.2.1 shows a system model consisting of five generic components. For an individual component with multiple inputs and outputs, the relationships are more compactly shown in terms of vectors rather than a series of scalar variables. For example, the dependence between inputs, outputs and parameters for the first component can be described in terms of either scalar variables or vector variables:

$$\begin{aligned} y_1 &= f\left(x_1, x_2, \beta_1, \beta_2\right) \\ y_2 &= f\left(x_2, \beta_1\right) \end{aligned} \qquad \text{or equivalently} \qquad \mathrm{y} = \mathrm{f}(\mathrm{x}, \boldsymbol{\beta}) \tag{3.2.1}$$

In the above vector equation, y has elements y_1 and y_2, and similarly $\mathrm{x} = [x_1, x_2]^{\mathrm{T}}$ and $\boldsymbol{\beta} = [\beta_1, \beta_2]^{\mathrm{T}}$. Keeping with convention, vectors are column vectors, and the transpose is denoted when written in row format. The vector form of Equation 3.2.1 can be used to describe the input/

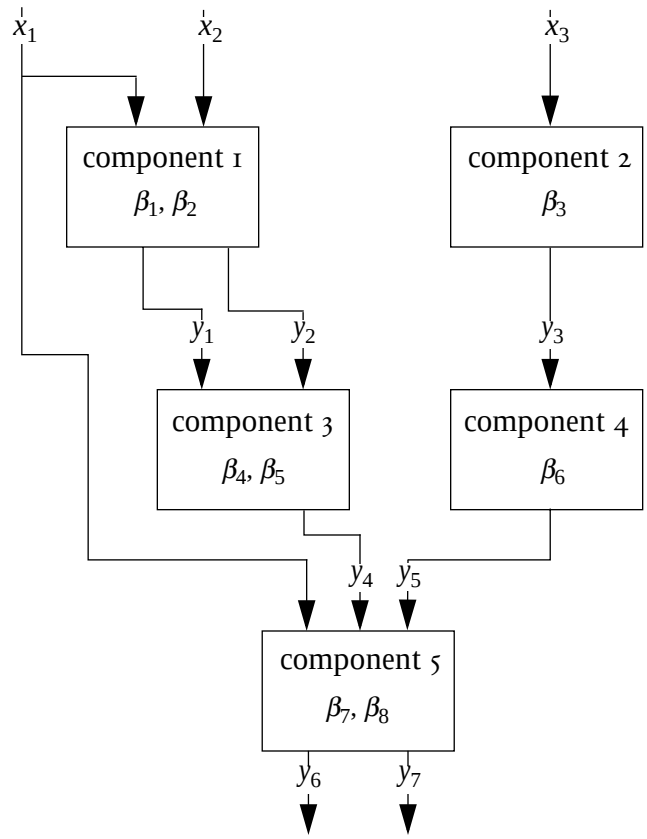

FIGURE 3.2.1: Block diagram showing interconnections of a multicomponent system.

output relationship of a group or system of components as well as that of a single component. For example, the composite system in Figure 3.2.1 can be represented by

$$[y_1, y_2, \ldots, y_7]^{\mathrm{T}} = \mathrm{f}\left([x_1, x_2, x_3]^{\mathrm{T}}, [\beta_1, \beta_2, \ldots, \beta_8]^{\mathrm{T}}\right) \qquad \text{or} \quad \mathrm{y} = \mathrm{f}(\mathrm{x}, \boldsymbol{\beta}) \qquad 3.2.2$$

The more compact vector notation for model input/output relationships will be used throughout this work.

3.2.2 Multiresponse Regression Models

In regression analysis, the system model is altered to account for the differences between model predictions and measured data. The differences between the observed dependent or *response* variables, $\tilde{\mathrm{y}} = [\tilde{y}_1, \ldots, \tilde{y}_j, \ldots \tilde{y}_m]^{\mathrm{T}}$, and the model predicted values, $\mathrm{y} = [y_1, \ldots, y_j, \ldots y_m]^{\mathrm{T}}$

are defined as the *residuals*, $\mathrm{r} = [\tilde{y}_1 - y_1, \ldots, \tilde{y}_j - y_j, \ldots, \tilde{y}_m - y_m]^{\mathrm{T}}$. A multiresponse regression model takes the form

$$y_j = f_j\left(x_1, \ldots, x_q; \beta_1, \ldots, \beta_p\right) + r_j \qquad \text{or} \qquad \mathrm{y} = \mathrm{f}(\mathrm{x}, \boldsymbol{\beta}) + \mathrm{r} \tag{3.2.3}$$

where $\mathrm{x} = [x_1, \ldots, x_k, \ldots, x_q]^{\mathrm{T}}$ is a vector of q independent input or predictor variables (also called regressor variables), and $\boldsymbol{\beta} = [\beta_1, \ldots, \beta_l, \ldots, \beta_p]^{\mathrm{T}}$ is a vector of p parameters. Equation 3.2.3 describes the relationship between a single observation of y and x for a given $\boldsymbol{\beta}$. The relationship between an entire data set of $i = 1,...,n$ observations is described in index or matrix notation as

$$y_{ij} = f_{ij}\left(x_{i1}, \ldots, x_{iq}; \beta_1, \ldots, \beta_p\right) + r_{ij} \qquad \text{or} \qquad Y = F(X, \boldsymbol{\beta}) + R \tag{3.2.4}$$

where Y and R are $n \times m$ matrices and X is an $n \times q$ matrix of independent input variables. For a set of fixed and known Y responses and X independent variables, the residuals can be considered a function of the parameter estimates,

$$R = R(\boldsymbol{\beta}) \tag{3.2.5}$$

It is useful to note that residuals are distinguished from errors in that error is defined as the difference between the measured value, $\tilde{y}$, and the *true* (although usually unknown) value, $\hat{y}$, of a variable,

$$\varepsilon = \tilde{y} - \hat{y} \tag{3.2.6}$$

and residuals are defined as the difference between the measured and predicted value, y:

$$r = \tilde{y} - y \tag{3.2.7}$$

In theory, for an exact model of the process, there is a set of true parameters and a corresponding set of true response values. Much of the underlying statistical theory of parameter estimation includes certain assumptions about the statistical properties of the errors. However, since the exact model and true parameter values for most problems are unknown, the errors are unknown. In the practice of parameter *estimation*, the residuals represent estimates of the errors where the statistical properties of the residuals are estimates of corresponding properties of the errors. For example, the unknown errors may be assumed to follow a certain distribution before applying a parameter esti-

mation technique. The distribution of the resulting residuals can be used to assess the validity of the error distribution assumption.

3.3 Parameter Estimation Methods

The quality of fit given by any parameter estimation method depends upon the statistical nature of the data. If a correct model and error free data were available, then only a few data points would be needed to determine the parameters. For example, to fit an nth order polynomial, only $n+1$ different data points are needed to precisely determine the $n+1$ coefficients. However, error free data is rarely available and consequently the quality of a fit is influenced by the nature of errors present in the data. In this section, the methods of least squares and maximum likelihood estimation are discussed after a brief review of a few probability concepts.

3.3.1 Probability Review

A brief review of certain probability concepts is useful before considering the statistical ideals associated with parameter estimation. Given a random variable ξ able to take on any value in a continuous distribution, a cumulative probability density function (pdf) of ξ can be defined.

$$F(x) = \Pr(\xi \leq x) \tag{3.3.1}$$

The curve shown in Figure 3.3.1 is an example of a cumulative probability density function. For

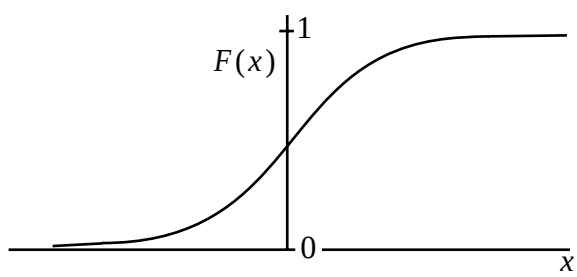

FIGURE 3.3.1: Example cumulative probability density function.

some given value of x, $F(x)$ denotes the probability that the random variable ξ is less than or equal to x. The probability is bound between zero and one, tending toward zero as x decreases and increasing toward one as x increases.

For a differentiable F(x), a probability density function (pdf) can be defined:

$$p(x) = \frac{dF}{dx} \tag{3.3.2}$$

The relationship between the pdf, $p(x)$, and the random variable ξ is illustrated by considering the graph of an example pdf in Figure 3.3.2 and the following equation:

$$\Pr(a \le \xi \le b) = F(b) - F(a) = \int_a^b p(x)\, dx \tag{3.3.3}$$

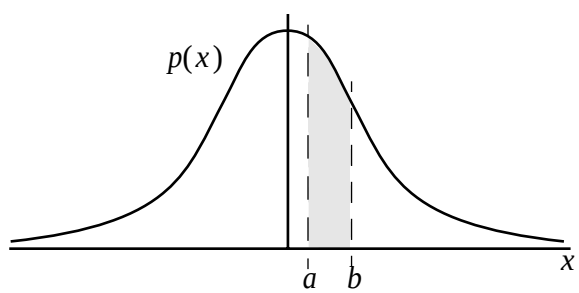

FIGURE 3.3.2: Example probability density function (pdf).

The probability that ξ is between values a and b is equivalent to the area beneath the curve between a and b.

Probability density functions are used to define an expected value or *expectation* of functions of the random variable.

$$E\Big(f(\xi)\Big) = \int_{-\infty}^{\infty} f(x)\, p(x)\, dx \tag{3.3.4}$$

The expectation of the random variable ξ is the mean of the variable,

$$\mu_\xi = E\Big(\xi\Big) = \int_{-\infty}^{\infty} x\, p(x)\, dx \tag{3.3.5}$$

and the variance (square of the standard deviation from the mean) is

$$\sigma_\xi^2 = E\left[\left(\xi - \mu_\xi\right)^2\right] = \int_{-\infty}^{\infty} \left(x - \mu_\xi\right)^2 \, p(x)\, dx \qquad 3.3.6$$

The approach for the univariate probability density function can be extended to the multivariate case, and joint probability density functions can be defined. However, the definitions above suffice to illustrate parameter estimation concepts. Although the probability distribution $p(x)$ can take on any functional form, a normal distribution, described below, is often assumed in parameter estimation analysis.

In many applied regression techniques the validity of the results is conditional upon the distribution of the errors. For example, it is shown that estimates by least squares will yield the "best" parameter estimates if the errors follow a normal (Gaussian) distribution. A normal distribution of a random variable x (univariate) is given by the function

$$p(x) = \frac{1}{\sigma\sqrt{2\pi}} \exp\left[\frac{-(x-\mu)^2}{2\sigma^2}\right] \qquad 3.3.7$$

with mean μ and variance σ^2. A multivariate normal distribution of an n dimensional random vector x has the form

$$p(\mathrm{x}) = \left(2\pi\right)^{-n/2} \det{}^{-1/2} V \exp\left[-\tfrac{1}{2}(\mathrm{x} - \boldsymbol{\mu})^{\mathrm{T}} V^{-1} (\mathrm{x} - \boldsymbol{\mu})\right] \qquad 3.3.8$$

with a mean $\boldsymbol{\mu}$ and covariance matrix V.

3.3.2 Parameter Estimation by Least Squares

The true values of the parameters are unknown and must be estimated using the data. The most common estimation procedure is that of least squares (LS). For a system with a single response variable, y, a set of parameter estimates is found which minimizes (finds the "least" value

of) a sum of squares of the residuals. The least squares minimization problem for a single response model can be stated as

$$\min_{\beta_1,\ldots,\beta_p} \sum_{i=1}^{n} \left[y_i - f\left(x_1,\ldots,x_q;\beta_1,\ldots,\beta_p\right)\right]^2 \qquad 3.3.9$$

For a multiresponse model, the least squares problem above can be extended to include a sum of squared residuals for all m responses

$$\min_{\beta_1,\ldots,\beta_p} \sum_{j=1}^{m}\sum_{i=1}^{n} \left[y_{ij} - f\left(x_{i1},\ldots,x_{iq};\beta_1,\ldots,\beta_p\right)\right]^2 \quad \text{or} \quad \min_{\boldsymbol{\beta}} \sum_{i=1}^{n} \left(\mathrm{y}_i - \mathrm{f}(\mathrm{x}_i,\boldsymbol{\beta})\right)^{\mathrm{T}} \left(\mathrm{y}_i - \mathrm{f}(\mathrm{x}_i,\boldsymbol{\beta})\right) \qquad 3.3.10$$

or, equivalently in matrix notation, the trace (sum of the diagonal elements) of the product of the residual matrix and its transpose

$$\min_{\boldsymbol{\beta}} \operatorname{tr}\left[R(\boldsymbol{\beta})^{\mathrm{T}} R(\boldsymbol{\beta})\right] \qquad 3.3.11$$

Equations 3.3.10 and 3.3.11 represent an *unweighted* or evenly weighted least squares criterion. Each vector of residuals influences the fit equally. However, in many applications, not all of the measurements are made with equal accuracy. Some responses may be a more precise measurement than others. For example, steam flow rate measurements may exhibit more variance than measurements of cooling tower water temperature.

The relative influence of individual vectors of residuals upon the least squares solution can be affected by incorporating weighting factors. A *weighted* least squared problem is formed by incorporating an $m \times m$ matrix of weighting factors W into Equation 3.3.10.

$$\min_{\boldsymbol{\beta}} \sum_{i=1}^{n} \left(\mathrm{y}_i - \mathrm{f}(\mathrm{x}_i,\boldsymbol{\beta})\right)^{\mathrm{T}} W \left(\mathrm{y}_i - \mathrm{f}(\mathrm{x}_i,\boldsymbol{\beta})\right) \qquad 3.3.12$$

The weighting matrix W may be a diagonal matrix (off diagonal entries are 0) of positive diagonal elements where the w_{ii} entry weights the sum of squares of residuals corresponding to the ith response. Alternatively, W can be a symmetric positive definite matrix where the off diagonal entries (w_{ij}, $\mathrm{i} \neq \mathrm{j}$) contribute by weighting the product of residuals from the ith and j^{th} responses.

Using statistical theory, it can be shown that if the model is correct and the errors follow a normal (Gaussian) distribution, then the solution of the least squares problem will yield the "best" parameter estimates. [Sen90] Solving the single response least squares problem in Equation 3.3.9 with data from a normal distribution will yield a best set of parameter estimates. However, the extended formulation for the multivariate case given in Equation 3.3.10 (unweighted least squares) will not result in the best set of parameter estimates unless the errors in each of the m response variables demonstrate exactly the same variance (the covariance matrix V would be diagonal with all diagonal elements equal). If the response variables have unequal variances, a weighted least squares formulation (Equation 3.3.12) must be used where the weighting matrix W is given by the inverse covariance matrix, V^{-1}.

In general, the errors and consequently the covariance matrix are unknown. However, the weighted least squares problem may be solved with an estimate of the covariance matrix. A two-stage procedure can be employed where the unweighted least squares problem is first solved. [Kan90] Then the weighted least squares problem is solved with an estimate of the covariance matrix $\tilde{V}$ generated from the residuals of the unweighted problem. The approximate covariance matrix is given in terms of the residuals as follows:

$$\tilde{V} = n^{-1} R^{\mathrm{T}} R \qquad 3.3.13$$

3.3.3 Other Estimation Methods

There are a number of methods for quantifying the difference between model predictions and observations other than using sum of squares. Some methods such as maximum likelihood estimation (MLE) consider the distribution of the residuals. For example, consider a single response model, where the residuals follow a probability density function, $p(r)$. For a given set of data, the residuals are dependent upon the parameter values, $r = r(\boldsymbol{\beta})$. The most probable or *likely* parameter values are those that result in residuals which maximize the pdf, $p(r)$. If the residuals are assumed to follow a normal distribution, the results of maximum likelihood estimation are the same as weighted least squares where weighting matrix is the inverse of the covariance matrix. The

maximization of probability density function is also used in Bayesian estimation, where a prior probability density function is assumed for the parameters and the residuals.

3.3.4 The Determinant Criterion

Box and Draper approached the multiresponse estimation problem using probabilistic arguments (Bayesian estimation). [Box65] It was demonstrated that given a data set *Y*, the probability that a set of parameter estimates, $\boldsymbol{\beta}$, is the set of true parameter values is inversely proportional to a measure of the residuals as follows:

$$p\left(\boldsymbol{\beta}\middle|Y\right) \propto \left|R^{\mathrm{T}}R\right|^{-n/2} \qquad 3.3.14$$

The probability is maximized when the determinant of $R^{\mathrm{T}}R$ is minimized. Bates and Watts derive the same criterion using a maximum likelihood argument. [Bat88] Also, Bates and Watts point out that geometrically, $R^{\mathrm{T}}R$ corresponds to the square of the volume of the *m* dimensional parallelepiped spanned by the residual vectors and minimizing the determinant corresponds to minimizing this volume.

3.3.5 Linear Dependencies in $R^{\mathrm{T}}R$

While the determinant criterion provides a means for weighing residuals according to variance, its computation can sometimes be problematic. For example, if one vector of residuals (a column of *R*) happens to be linearly dependent (or nearly linearly dependent) with another residual vector, then $R^{\mathrm{T}}R$ will not be full rank and the determinant will be zero (or a very small number). Any minimization algorithm will either fail or halt at this apparent minimum. Similar problems are faced when using the two step weighted least squares method where the covariance matrix is estimated from the inverse of $R^{\mathrm{T}}R$. If not of full rank, the inverse of $R^{\mathrm{T}}R$ is not defined.

Linear dependencies among residuals can be caused by linear dependencies in the responses. Such dependencies among the measured variables can occur in many HVAC system components. For example, consider the counterflow heat exchanger in Figure 3.3.3. The inlet and outlet temperatures are measured and an estimate of the overall heat transfer parameter, *UA*, is to be deter-

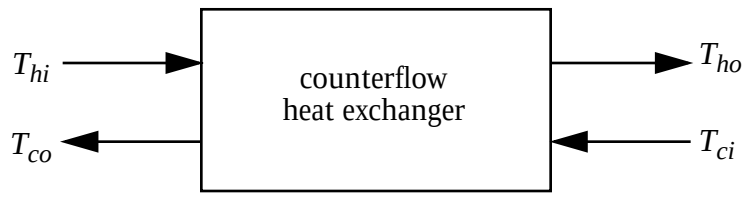

FIGURE 3.3.3: Inlet and outlet temperatures for a counter flow heat exchanger.

mined from the temperature measurements. The mass flow rates and fluid specific heats are known and assumed to be constant. An *Ntu*-effectiveness model can be used to represent the heat exchanger and an estimate of the heat exchanger's overall heat transfer coefficient, *UA*, is desired. The cold stream outlet temperature is given in terms of the inlet temperatures,

$$T_{ho} = T_{hi} - \varepsilon \frac{(\dot{m}c_p)_{\min}}{(\dot{m}c_p)_h}\left(T_{hi} - T_{ci}\right) \qquad 3.3.15$$

and similarly, the hot stream outlet temperature is given by

$$T_{co} = T_{ci} + \varepsilon \frac{(\dot{m}c_p)_{\min}}{(\dot{m}c_p)_c}\left(T_{hi} - T_{ci}\right) \qquad 3.3.16$$

where $(\dot{m}c_p)_{\min}$ is the minimum capacitance rate and the effectiveness, ε, is given in terms of the ratio of capacitance rates, *Ntu* and *UA*:

$$\varepsilon = \frac{1 - \exp\left[-Ntu\left(1 - C_r\right)\right]}{1 - C_r \exp\left[-Ntu\left(1 - C_r\right)\right]} \qquad 3.3.17$$

$$C_r = \frac{(\dot{m}c_p)_{\min}}{(\dot{m}c_p)_{\max}} \qquad 3.3.18$$

$$Ntu = \frac{UA}{(\dot{m}c_p)_{\min}} \qquad 3.3.19$$

The overall heat transfer coefficient *UA* can be estimated using either measurements of T_{ho} and Equation 3.3.15 or measurements of T_{co} and Equation 3.3.16 (along with Equations 3.3.17 and 3.3.19). Qualitatively, one might expect that using both measured outlet temperatures with Equations 3.3.15 and 3.3.16 in a multiresponse regression technique would result in a better estimate of *UA*. However, assuming that the overall heat transfer coefficient, *UA*, does not significantly vary with temperature, the residuals associated with T_{co} and T_{ho} are linearly dependent. The dependency arises from the energy balance about the heat exchanger,

$$(\dot{m}c_p)_h \left(T_{hi} - T_{ho}\right) = (\dot{m}c_p)_c \left(T_{co} - T_{ci}\right) \qquad 3.3.20$$

or, solving for T_{ho} in terms of T_{co}

$$T_{ho} = T_{hi} - \frac{(\dot{m}c_p)_c}{(\dot{m}c_p)_h}\left(T_{co} - T_{ci}\right) \qquad 3.3.21$$

Using Equation 3.3.21, the residual or difference between a measured value ($\tilde{T}_{hi}$) and predicted value ($\hat{T}_{hi}$) of T_{ho} is a linear function of the residual in T_{co}

$$\tilde{T}_{ho} - \hat{T}_{ho} = \frac{(\dot{m}c_p)_c}{(\dot{m}c_p)_h}\left(\hat{T}_{co} - \tilde{T}_{co}\right) \qquad 3.3.22$$

Consequently, the $R^{n\times 2}$ residual matrix for this example will only have rank=1 and the determinant of $R^{\mathrm{T}}R$ will be zero for any value of *UA* used to predict the outlet temperatures.

Energy and mass balances are often used in HVAC component models to predict dependent variables. Care must be used to find and remove any linear dependent responses from the residual matrix when using multiresponse regression techniques to determine system parameters. Box *et al.* [Box73] discuss the problems associated with linear dependencies among responses and suggest procedures for determining the dependencies. McLean *et al.* [McL79] extend the work of Box *et al.* in the detection of linear relationships in the residuals.

3.4 Parameter Identifiability Problems

3.4.1 Overparameterization

In some cases of nonlinear estimation, the parameter values at a problem solution are not unique. This problem will occur if the model function is specified with too many parameters (overparameterized). An example of a non unique solution can be demonstrated with the simple model below, a nonlinear function in terms of the parameters β_1 and β_2:

$$y = \beta_1 \beta_2 x \tag{3.4.1}$$

While there may only be a single value of the product $\beta_1 \beta_2$ that minimizes the residuals, there is a continuum of possible values of β_1 and β_2. The minimization algorithm will show no preference for one combination over another. Equation 3.4.1 explicitly demonstrates how problems of parameter identifiability can arise. However, in a general system of nonlinear model equations, potential problems with parameter identification may not be so obvious.

Overparameterization is not always the result of a bad model. Parameter identification problems can occur in exact models when a fit is made with limited data. For example, consider the model below with a single response y and two independent (regressor) variables x_1 and x_2, and three parameters, β_1, β_2 and β_3:

$$y = \beta_1 x_1 + \beta_2 x_2^{\beta_3} \tag{3.4.2}$$

If the independent variable x_2 varied little or not at all in the data set used for the regression analysis, good estimates for β_2 and β_3 cannot be determined. Use of a model with these parameters to extrapolate predictions over different values of the independent variable would yield questionable results.

Even if an independent variable is measured over a broad range, a nonlinear model may still suffer from parameter identifiability problems. For example, the two curves shown in Figure 3.4.1 are generated from the following equation:

$$y = \beta_1 \exp(1 - x^{\beta_3}) + \exp(\beta_2 x) \tag{3.4.3}$$

The only difference between the curves is that the value of β_3 in the solid curve is 8.75 and in the dashed curve is 1.25. Clearly, data taken anywhere in the range of $3 < x < \infty$ will not allow a close estimate of β_3. Overparameterization problems are exhibited in the example problem and discussed in Section 3.5.4 below.

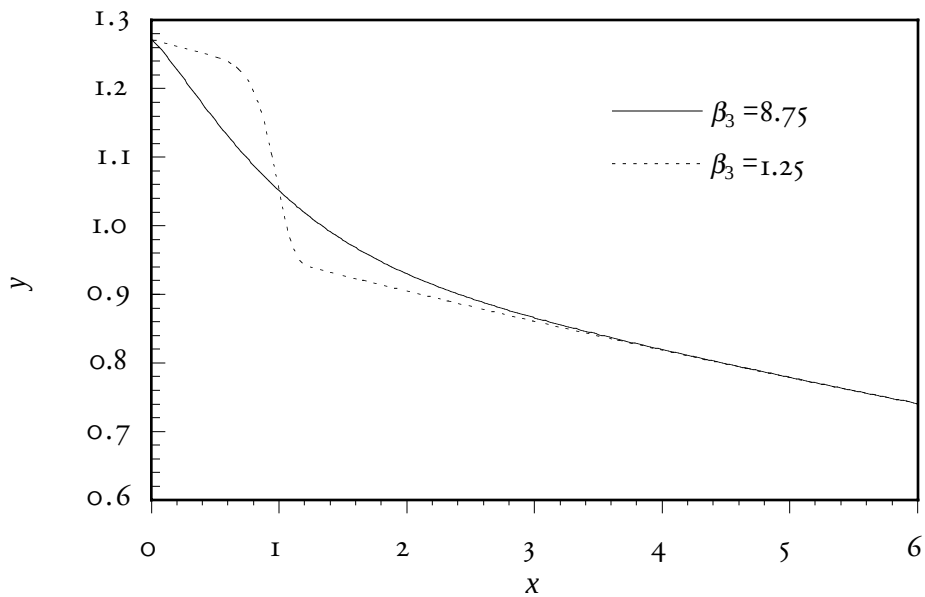

FIGURE 3.4.1: Plot of Equation 3.4.3 for β_3=8.75 (solid line) and β_3=1.25 (dashed line).

The TRNSYS cooling tower model used in this work includes a type of effectiveness/number of transfer units (*Ntu*) relationship used in the mass transfer rate equation. The outlet water temperature depends upon the inlet air wet bulb temperature, the inlet water temperature and an effectiveness defined in terms of *Ntu*. The *Ntu* is dependent upon the mass flow rates of air and water through the tower and upon two parameters, *c* and *n*:

$$Ntu = c\left(\frac{\dot{m}_{\mathrm{w}}}{\dot{m}_{\mathrm{a}}}\right)^{1+n} \qquad 3.4.4$$

If the data available for estimating the cooling tower parameters have constant or near constant water and air flow rates, then the effect of either *c* or *n* upon the tower outlet water temperature could not be discerned independently. Thus *c* and *n* cannot be uniquely identified.

Even if multiplicative parameters such as in Equation 3.4.1 were not present in any individual model equation, the same redundancy in parameters can occur in estimation using a composite model. For example, one output of a component modeled as $y_1 = \beta_1 x_1$ is used as an input to another component ($x_2 = y_1$) having an output $y_2 = \beta_2 x_2$. If the output of the first component, y_1, is not measured, the residuals corresponding to the output of the second component are effectively used to determine both parameters β_1 and β_2 during the regression. The two components are equivalent to a single component where $y_2 = \beta_1 \beta_2 x_1$, just as in Equation 3.4.1

Seber and Wild describe a measure indicative of parameter identifiability problems. [Seb89] For a univariate response model, $y = f(x, \boldsymbol{\beta})$, and a data set of n observations of x and y, a vector representation of the predicted n responses as a function of $\boldsymbol{\beta}$ is formed

$$\mathrm{f}(\boldsymbol{\beta}) = \left[f_1(\boldsymbol{\beta}),\ f_2(\boldsymbol{\beta}),\ \ldots, f_n(\boldsymbol{\beta}) \right]^{\mathrm{T}} \qquad 3.4.5$$

The derivative of the vector f($\boldsymbol{\beta}$) with respect to p parameters ($\boldsymbol{\beta} = [\beta_1, \beta_2, \ldots, \beta_p]$) is the matrix

$$F'(\boldsymbol{\beta}) = \begin{bmatrix} \frac{\partial f_1(\boldsymbol{\beta})}{\partial \beta_1} & \frac{\partial f_1(\boldsymbol{\beta})}{\partial \beta_2} & \cdots & \frac{\partial f_1(\boldsymbol{\beta})}{\partial \beta_p} \\ \frac{\partial f_2(\boldsymbol{\beta})}{\partial \beta_1} & \frac{\partial f_2(\boldsymbol{\beta})}{\partial \beta_2} & \cdots & \frac{\partial f_2(\boldsymbol{\beta})}{\partial \beta_p} \\ \vdots & \vdots & \ddots & \vdots \\ \frac{\partial f_n(\boldsymbol{\beta})}{\partial \beta_1} & \frac{\partial f_n(\boldsymbol{\beta})}{\partial \beta_2} & \cdots & \frac{\partial f_n(\boldsymbol{\beta})}{\partial \beta_p} \end{bmatrix} \qquad 3.4.6$$

The matrix elements correspond to the first order terms of a linear approximation to f($\boldsymbol{\beta}$) about $\boldsymbol{\beta}$ (truncated Taylor Series). Linear dependencies within the matrix product $F'^{\mathrm{T}} F'$ are indicative of parameter identifiability problems. Unless the data are error free and the model exact, the matrix $F'^{\mathrm{T}} F'$ will not be identically singular (det $F'^{\mathrm{T}} F' = 0$). However, the determinant may be very close to 0 and the matrix is then described as ill-conditioned.

3.4.2 Parameter Variance

Another indication of parameter identifiability problems is large variances in the parameter estimates. Parameter estimates are functions of random variables and possess a certain distribu-

tion. The distribution of the estimates depends both upon the model and upon the distribution of the random variables. For models with multiple parameters, a variance-covariance matrix, $V_{\boldsymbol{\beta}}$, of the parameter estimates can be defined. If multiple sets of data taken at equivalent values of independent or regressor variables are available, the parameter estimation problem can be solved with each data set. The set of resulting parameter estimates from the multiple (replicated) data will not be equal, but will demonstrate some random error and an associated variance. For m sets of replicated data, m parameter estimates can be found. The estimated mean of the distribution of parameter estimates is

$$\bar{\boldsymbol{\beta}} = \frac{1}{m} \sum_{k=1}^{m} \boldsymbol{\beta}_k \qquad 3.4.7$$

and the covariance matrix is estimated as

$$V_{\boldsymbol{\beta}} = \frac{1}{m-1} \sum_{k=1}^{m} \left(\boldsymbol{\beta}_k - \bar{\boldsymbol{\beta}}\right)\left(\boldsymbol{\beta}_k - \bar{\boldsymbol{\beta}}\right)^{\mathrm{T}} \quad . \qquad 3.4.8$$

In cases where replicated data are not available, statistical properties of model parameters may be estimated by simulating a set of experiments. [Bar74] Given a model, a set of “true” response data can be calculated with a given set of input variable values. Computer generated pseudorandom numbers can be used to add random error to the responses values, creating sets of “noisy” data. The sets of contaminated data can be used to determine multiple estimates of parameters. Mean values, a covariance matrix, and parameter bias can then be calculated. These methods are applied to the example problem and discussed in Section 3.5.9.

A parameter covariance matrix can also be estimated from geometric features of the minimized objective function (e.g. a sum of squares). Rather than examining the changes in parameter estimates due to small changes in the data over multiplicative data sets, expressions are derived for parameter variance based upon the effect of small differential changes in a given data set. A small change in measured values will cause some change in the objective function. The change in the objective function would cause its minimum location (i.e. the parameter estimates) to change as well. From these ideas of small differential changes, expressions for an estimated covariance matrix

in terms of the curvature of the objective function can be derived. [Bar74] The derivations usually include assumptions about the distribution of errors in the data and how well a linearized model approximates the nonlinear model at the objective function minimum. Bard states that for a wide class of maximum likelihood estimates with normal distributions, the covariance matrix is approximately equal to the inverse of the objective function Hessian matrix. The Hessian matrix is a second order measure of curvature in multidimensional functions. For an objective function ϕ dependent upon parameters $\boldsymbol{\beta} = [\beta_1, \ldots, \beta_l, \ldots, \beta_p]^{\mathrm{T}}$, the Hessian is defined as

$$H(\beta) = \frac{\partial^2 \phi}{\partial \beta^{\mathrm{T}} \partial \beta} = \begin{bmatrix} \frac{\partial^2 \phi(\beta)}{\partial \beta_1 \partial \beta_1} & \frac{\partial^2 \phi(\beta)}{\partial \beta_1 \partial \beta_2} & \cdots & \frac{\partial^2 \phi(\beta)}{\partial \beta_1 \partial \beta_p} \\ \frac{\partial^2 \phi(\beta)}{\partial \beta_2 \partial \beta_1} & \frac{\partial^2 \phi(\beta)}{\partial \beta_2 \partial \beta_2} & \cdots & \frac{\partial^2 \phi(\beta)}{\partial \beta_2 \partial \beta_p} \\ \vdots & \vdots & \ddots & \vdots \\ \frac{\partial^2 \phi(\beta)}{\partial \beta_p \partial \beta_1} & \frac{\partial^2 \phi(\beta)}{\partial \beta_p \partial \beta_2} & \cdots & \frac{\partial^2 \phi(\beta)}{\partial \beta_p \partial \beta_p} \end{bmatrix} \qquad 3.4.9$$

Elements of the Hessian matrix for a quadratic function (e.g. a sum of squared residuals objective function associated with a linear parametric model) would be constant. A “good” fit for the parameter estimates is essential for a reasonable estimate of the parameter covariance matrix via the inverse Hessian. An overparameterized model will result in an objective function surface having an ill conditioned Hessian matrix at the minimum with a meaningless inverse.

3.4.3 Parameter Identification Problems Summary

The occurrence of parameter identifiability problems does not necessarily negate the use of the parameter estimates. Whether or not the parameter estimates result in a model that can predict the measured data with good accuracy can be judged by evaluating the residuals associated with each response. The estimated parameters may still yield a model with adequate predictive capabilities. However, the individual component parameters possessing identifiability problems should be limited to use with the original composite system model with which the regression was made. If nearly “true” parameter estimates are required for use with individual component models in different composite systems, parameter variance should be examined. Large variance in param-

eters may also bring into question the relative advantage of mechanistic models over curve fits for predicting responses outside the range of the measured data used in the fit (extrapolation). For example, the variance in parameter β_3 in Equation 3.4.3 (plotted in Figure 3.4.1) would be large if fit with the regressor data (x) greater than three and would not be suitable for predictions when x is between zero and two.

3.5 Example Chilled Water Plant

3.5.1 Chilled Water System Simulation with TRNSYS

Before addressing the problem of parameter estimation, a means of modeling a multicomponent system will be discussed. A transient system simulation program, TRNSYS [Kle84], was developed at the University of Wisconsin Solar Energy Laboratory for investigating the performance and behavior of thermal energy systems. The program is modular so that a number of individual component models may be linked to form a system. The modular feature of TRNSYS allows any general chilled water system to be simulated. Numerous HVAC system component models such as chillers, cooling towers, pumps, fans and heat exchangers have been written for use with TRNSYS. Component models can be modified or new ones written to suit individual applications. Dynamic or state equations are incorporated into components that model thermal storage elements, such as chilled water storage tanks and building structures. Many TRNSYS component models incorporate mechanistic design equations derived from first principles of heat or mass transfer and thermodynamics. Component outputs, y, are given as a function of the inputs, x, and a set of parameters, β (i.e. $y = f(x;\beta)$).

3.5.2 Example System Description

The use of multiresponse regression techniques are illustrated here with an example chilled water system model. The model consists of four components as shown in Figure 3.5.1.This example system represents a steam driven chiller, a cooling tower and a surface condenser. Separate chiller and steam turbine components represent the steam driven chiller. The system function is to cool a flow of water, $\dot{m}_{\text{chw}}$, from some relatively warm chilled water return temperature, T_{chwr}, to a prescribed chilled water supply temperature, T_{chws}. The chiller compressor is driven by a steam turbine that exhausts to a surface condenser. A cooling tower is used to reject heat from the

chiller's refrigerant condenser and the steam condenser to the environment. For this example, five variables are categorized as independent and eight variables as dependent. Independent variables include ambient air wet bulb and dry bulb temperatures, T_{wb} and T_{db}, steam inlet pressure for the turbine, p_{in}, and chilled water supply and return temperatures, T_{chws} and T_{chwr}. Dependent variables include steam flow rate, $\dot{m}_{steam}$, turbine exhaust enthalpy and pressure, h_{exh} and p_{exh}, cooling tower outlet temperature, T_{cws}, chiller condenser water outlet temperature, T_{cdwo}, chiller power, P_{comp}, surface condenser hot well and water outlet temperatures, T_{hw} and T_{cwr} .

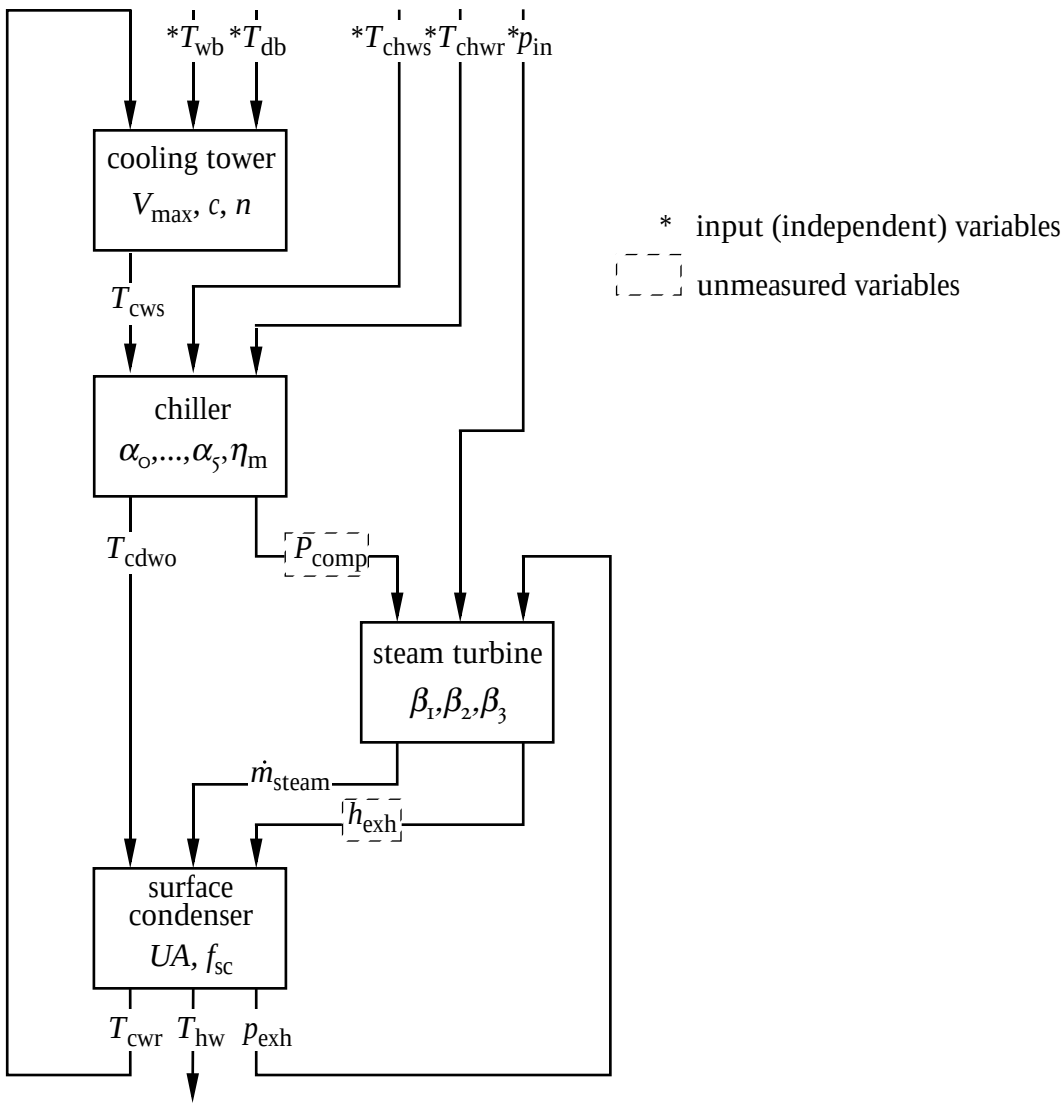

FIGURE 3.5.1: Block diagram showing interconnections in the example chilled water system.

The models for the turbine, chiller, cooling tower and surface condenser used to model an actual plant are described in Chapter 4. All but the chiller model use mechanistic equations. Chiller power is modeled by a second order parametric equation in terms of entering water temperatures and the chiller load. The equation has been shown to closely match the predictions of a detailed mechanistic model. [Bra88]

A total of 15 parameters are used in the four component models. The objective in this example regression problem is to determine estimates for the parameters from a set of simulated measured data. Desirable parameter estimates will result in a composite system model that can closely predict the dependent variables over a range of independent variable (regressor) values. Both unweighted and weighted least squares methods as well as the determinant criterion will be used to estimate the parameters. The data set used in the example was generated by the composite model with a set of selected parameter values. The "true" data were then "contaminated" with noise following a multivariate normal distribution (Equation 3.3.8) with a zero mean and selected covariance matrix V.

Measurements for all dependent variables would rarely be available in an actual plant. Of the eight dependent variables defined for this example, it is assumed that two are not measurable: the compressor power and the enthalpy of the turbine exhaust. The multivariate regression is performed with the remaining six dependent variables. The set of test data consists of 240 (hourly) responses. All independent variables were varied with periodic functions to simulate periodic weather changes. A separate data set (not used in the regression analysis) is used to evaluate the predictive capabilities. The independent variables in the separate set were varied over ranges not encountered in the data set used for the fit.

3.5.3 Minimization Algorithms Used

Solution of the parameter estimation problem involves minimizing some quantity such as a sum of squares or the determinant of the $R^{\mathrm{T}}R$ matrix. There are numerous algorithms available for finding minima, each with its own advantages depending upon the attributes of the function to be minimized. For this example study, three different algorithms were used to minimize either a sum of squares objective function or the determinant objective function.

A sequential quadratic programming (SQP) minimization algorithm included in the Numerical Algorithms Group (NAG) Library was used on both the sum of squares and determinant formulations. [NAG91] Sequential quadratic programming is an often used method for solving nonlinear constrained optimization problems. Quadratic programming refers to a method of finding the minimum of a quadratic function with linear constraints, for example

$$\begin{aligned} &\min_{\mathrm{x}} \quad \phi(\mathrm{x}) = \mathrm{c}^{\mathrm{T}}\mathrm{x} + \tfrac{1}{2}\mathrm{x}^{\mathrm{T}} G\,\mathrm{x} \\ &\text{such that} \\ &\qquad A\mathrm{x} = b \end{aligned} \tag{3.5.1}$$

where G is a symmetric and positive definite matrix. Sequential quadratic programming attempts to solve a general nonlinear minimization problem (with linear or nonlinear constraints) by solving a sequence of quadratic programming subproblems that approximate the original problem. Various algorithms exist for implementing the general strategy of sequential quadratic programming. Boggs and Tolle present a review of the basic SQP method and some of its popular implementations. [Bog95]

A software package that uses the Levenburg-Marquart algorithm was also used on the sum of squares problem formulation. The package, ODRPACK, was developed explicitly for regression problems by the Applied and Computational Mathematics Division of the National Institute of Standards and Technology. Since the computation of a least squares objective function is internal to the software package, this method was not used with the determinant formulation of the regression problem.

The Levenberg-Marquardt algorithm uses elements of two other minimization algorithms, linearization and steepest descent. If the model outputs were linear in terms of the parameters, as in linear regression problems, the objective function surface (a sum of squares of residuals) would be second order with respect to the parameters. For example, the surface of the sum of squares objective function, ϕ, for a two parameter (β_1 and β_2) linear regression problem would be a paraboloid in the three dimensional space spanned by $\{\beta_1,\beta_2,\phi\}$. In a linearization algorithm, the nonlinear model responses are approximated by a Taylor series truncated after the first derivative term.

The resulting approximate sum of squares surface at a given point is an *n* dimensional paraboloid cotangent with the original objective function surface. Just as a point and first derivative of a parabola in two dimensions, $y = \beta_2 x^2 + \beta_1 x + \beta_0$, uniquely define the value of *x* at the parabola minimum (assuming a convex parabola, $\beta_2 > 0$), the function value and derivatives with respect to the parameters uniquely define the minimum point of a strictly convex quadratic function in higher dimensions. After the function is evaluated at the initial parameter guess, $\boldsymbol{\beta}_0$, and derivatives calculated at this initial point, the value of $\boldsymbol{\beta}$ at the minimum of the approximating paraboloid is calculated. Derivatives and the function value can then be calculated at this new point and another estimated minimum point found. This process is continued until a minimum is reached.

Steepest descent methods require computation of derivatives of the objective function at the initial guess and use the gradient at that point to determine a direction of steepest descent. The function is minimized along this line of steepest gradient until a minimum (on the line) is found. Another gradient is calculated from the minimum and the line minimization performed again iteratively until the minimum is found.

In a sense, the linearization method provides a direction away from a current point to the minimum point of the approximating quadratic surface. The steepest descent method also provides a direction toward a new point. Briefly, the Levenberg-Marquardt method makes use of both sources of directional information to select a “best” direction, and also determines an appropriate step size in that direction. The algorithm has been found to work well in solving many nonlinear parameter estimation problems. A detailed description of the Levenberg-Marquardt method can be found in the text by Gill, *et al*. [Gil81]

A derivative free method of optimization, the Nelder-Mead algorithm, was also used to solve both the sum of squares and determinant formulations. The particular algorithm used is available in the public domain and coded in FORTRAN90. [Mil95] The Nelder-Mead algorithm uses only function evaluations to “fall downhill” on a multidimensional function surface. For an *n* dimensional function, *n*+1 points on the function surface form the vertices of a geometrical simplex. For example, four points on the surface of a three dimensional bowl shaped surface form the vertices of a tetrahedral simplex. The simplex falls downhill, shrinking or expanding its shape as new ver-

tices (function values) are computed according to the algorithm rules. The algorithm is advantageous where the function surface may be nonsmooth because computation of derivatives or estimates of derivatives are not required. The Nelder-Mead is a well known algorithm and descriptions can be found in most texts on numerical minimization methods. [Gil81]

3.5.4 Parameter Identifiability Problems with the Cooling Tower Model

In the effectiveness-*Ntu* model used in the TRNSYS cooling tower model (a detailed description of the cooling tower model is given in Section 4.4.4), *Ntu* is defined as

$$Ntu = c\left(\frac{\dot{m}_{\mathrm{w}}}{\rho_{\mathrm{air}} V_{\mathrm{max}} f_{\mathrm{air}}}\right)^{n+1} \tag{3.5.2}$$

where V_{max} is a maximum volumetric flow rate, ρ_{air} is the air density and f_{air} indicates the fraction of maximum volumetric flow rate. It is common to describe relative air flow rate in cooling towers by fractional fan speed (roughly equivalent to fractional volumetric flow rate) rather than explicitly by air mass flow rate, hence f_{air} is used as a component model input variable. Initially, it could be assumed that these three parameters, c, n and V_{max} are to be determined by parameter estimation. However, examining Equation 3.5.2, the parameter V_{max} could be factored out and combined with c,

$$Ntu = \left(\frac{c}{V_{\mathrm{max}}^{n+1}}\right)\left(\frac{\dot{m}_{\mathrm{w}}}{\rho_{\mathrm{air}} f_{\mathrm{air}}}\right)^{n+1} \tag{3.5.3}$$

and thus unique values of c and V_{max} cannot be determined from regression. This parameter identifiability problem does not limit the utilization of the predictive model as V_{max} can be fixed and a value of c estimated.

The particular configuration of the cooling tower model used in the example is a four cell tower where the overall leaving water temperature is the mixed temperature of the individual cells. It is assumed that the entering water flow is uniformly distributed over all cells at a constant rate. Individual cell leaving water temperatures are found with individual *Ntu* calculations since not all

cells may have the same air flow rates (e.g. two cells with fans fully on and two others with their fans turning at half speed). However, the same c, n and $V_{\max}$ are assumed for each Ntu calculation.

To identify unique estimates of c and n, measurements at differing air flow rates must be available. The exponent n quantifies how cooling tower performance depends upon the ratio of water to air mass flow rates. If the ratio is constant in the data used with the parameter estimation procedure, the exponent n cannot be estimated independent of the coefficient c. Again, one of the parameters, for example n, could be fixed and the remaining parameter estimated in the regression problem. In this example, the air and water flow rates are constant over all data used in the fit, but of the four individual cells, two operate at full fan speed and two at half fan speed. Ideally, with error free measurements of input or output variables, a unique value of n could be determined.

A parameter estimation analysis was performed on just the cooling tower component (rather than the composite system), where the sum of squared differences between measured and model predicted values of cooling tower water outlet temperature were minimized. Two estimation runs were performed to find estimates of c and n, one using error-free or "noiseless" measured data and the other using the noisy data. The sequential quadratic programming (SQP) minimization routine arrived at the "true" parameter values of c = 1.7 and n = -0.7 when the problem was solved with the error-free data. However, when the cooling tower outlet water temperature measurements containing the normally distributed noise (with a standard deviation of 0.3°C) were used, the algorithm arrived at c = 1.7 and n = -1.1 . Examining the sum of squares objective function in terms of c and n plotted in Figure 3.5.2, it is evident that the surface is relatively flat with respect to n. The enlarged view of the surface near the minimum in Figure 3.5.3 shows a very shallow convex depression. When the noisy data were included in the analysis, the shallow depression of the "true" minimum (with respect to n) was not discernible to the minimization algorithm. Typically with overparameterization, the minimum of the objective function (e.g. a sum of squares) occurs on a curve or higher dimensional surface rather than at a point. For example, in Figure 3.5.2 the minimum appears to occur along a curve on the floor of the surface. The higher dimensional surface corresponds to ill-conditioning in the $F'^{\mathrm{T}}F'$ matrix given in Equation 3.4.6.

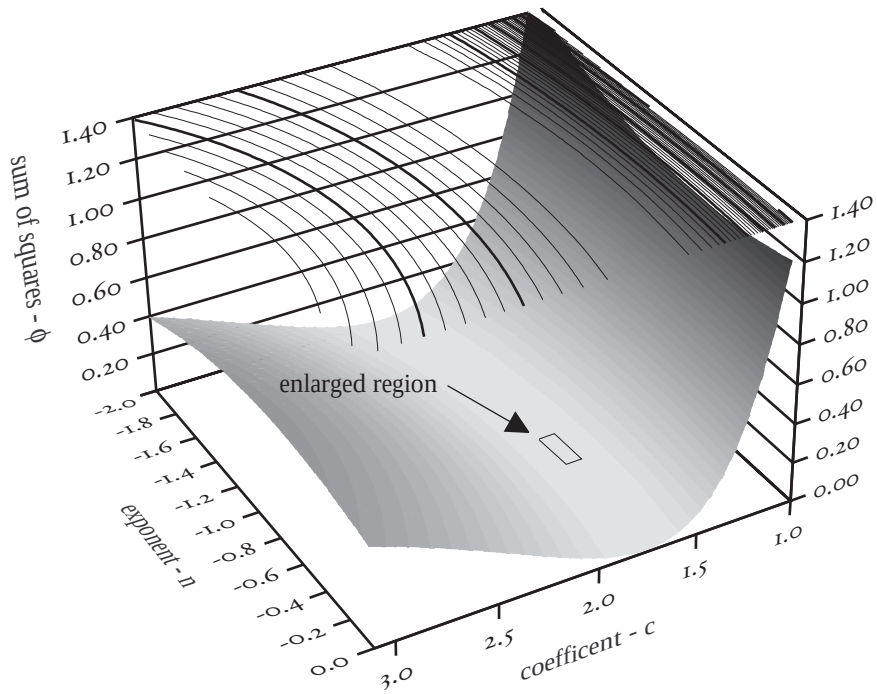

FIGURE 3.5.2: Objective function surface in terms of parameters *c* and *n* for the cooling tower parameter estimation example.

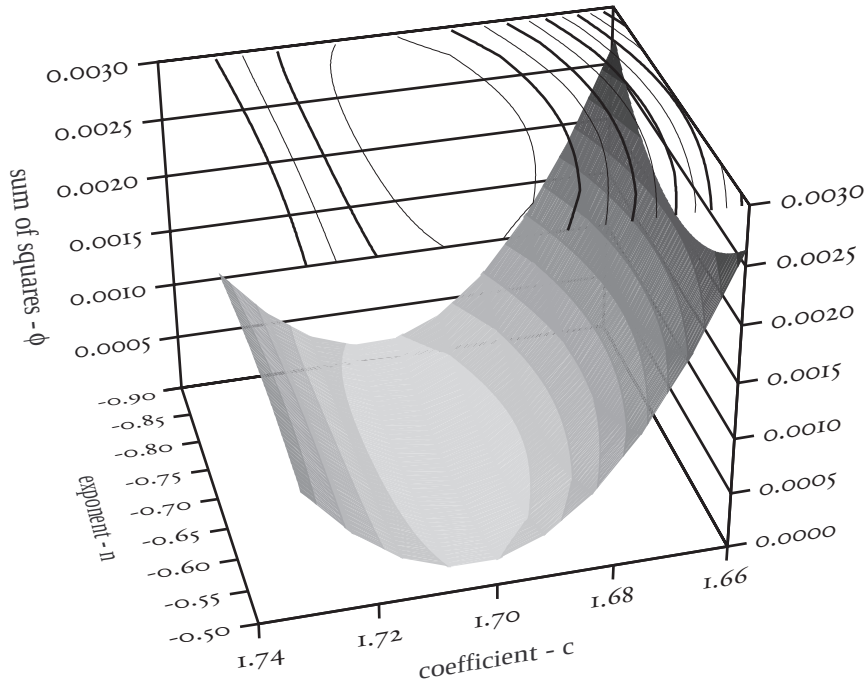

FIGURE 3.5.3: Enlargement of objective function surface in Figure 3.5.2.

In the comparative parameter estimation runs made with the example composite chilled water system, only thirteen parameters were estimated, the values of V_{max} and n fixed to reduce parameter identifiability problems discussed above.

3.5.5 Starting Values

The general regression problem is a multivariate nonlinear minimization problem which requires initial guesses for the unknown parameters. Many minimization algorithms used on nonlinear functions can at most only guarantee a local minima in a convex region that includes the starting point. A global minimum corresponding to the best parameter estimates will only be found if the initial guess is in a convex region containing the global minimum.

Reasonable values for initial parameter estimates may be obtained for mechanistic component models derived from theory. For example, an estimate of the overall heat transfer coefficient used in the condenser model could be calculated using the known size, geometry (number of tubes and passes) and flow rates of the condenser. Frequently, for modeling purposes, a curve fit rather than a mechanistic model can provide for a more computationally simple model, able to closely match the mechanistic model's predictive capability. For example, Braun [Bra88] demonstrated how a simpler quadratic model can closely match a more detailed mechanistic chiller model. Braun's chiller model includes a curve fit of chiller power as a quadratic function of inlet temperature difference and evaporator heat load and is used in the TRNSYS chiller component. However, starting values for parameters in component models which use curve fits cannot be explicitly calculated. The starting values used for the six coefficients (α_0-α_5) in the example problem are parameters known to be good estimates for a different chiller. [Bra88] Guess values for the other components were taken from nominal values found for similar type equipment. Starting values for all variables along with inclusive limits are given in Table 3.5.1.

3.5.6 Explanation of Tables of Regression Results

Results from applying ordinary (unweighted) least squares, weighted least squares and the determinant criterion methods with the various minimization algorithms are tabulated in Tables 3.5.2 through Tables 3.5.5 and discussed in Section 3.5.7 below. The parameter estimation problem is solved for twenty four different combinations of estimation method, response set and

TABLE 3.5.1: Parameter Starting Values and Bounds

parameter	starting value	lower limit	upper limit
β_1	0.700	-2.0	2.0
β_2	0.100	-1.0	1.0
β_3	0.100	-1.0	1.0
α_0	0.1107	-25.0	25.0
α_1	0.3198	-25.0	25.0
α_2	0.4662	0.0	25.0
α_3	-0.0956	-25.0	25.0
α_4	0.2152	0.0	25.0
α_5	-0.0656	-25.0	25.0
η_m	0.720	0.10	1.10
UA	16.000	1.0e-5	500.0
f_{hw}	0.100	0.0	1.0
c	1.100	0.01	10.0

minimization algorithm. Results from the twenty four separate runs are tabulated, with the runs grouped according to three different categories: the estimation method, the number of responses used in the objective function and the minimization algorithm. These categories are indicated in the three left columns.

Four tables of results are presented in Section 3.5.7. Table 3.5.2 lists the results from runs using the ordinary least squares objective function including sums of squared residuals over all six responses. Table 3.5.3 lists results for ordinary least squares using four and three responses in the sums of squared residuals. Table 3.5.4 lists results from runs using a weighted least squares objective function and sums of squared residuals over six, four and three responses. Table 3.5.5 lists results from runs using the determinant criterion with six, four and three responses.

Four residual quantities are given for comparison. The first column of results is a scaled sum of squared residuals for all six responses which is a relative indication of how well the regression fits all the measured data. For the example problem considered, steam mass flow rate is the only variable associated with energy costs and its residuals are considered separately. Three measures of

steam mass flow rate residuals tabulated in the next three columns are the sum of squared residuals, standard deviation of residuals and mean of the residuals.

For each run, two different sets of residuals quantities are tabulated. An “F” in the left column indicates the residuals (measured value minus predicted) are from the data (240 observations) used in the solving the parameter estimation problem. A “P” in the left column indicates the presented results are from comparing predicted values with true values (differences between predicted values and true values are termed *errors* rather than *residuals*) over another 240 observations not used in the fit. A broader range of independent variable values were used to generate these additional observations, and the tabulated error quantities give a relative indication of how well the model can predict responses that must be extrapolated beyond the region of the data used in the fit.

Also, for each run, the thirteen parameter estimates determined in the regression are tabulated in the right columns. The parameter entries span two rows, the corresponding variable names (β_1, β_2, etc.) are indicated in the table heading.

The top two lines of entries in each table are residual (and error) quantities that would correspond to a perfect fit of model to data. The parameter values in the top two lines are those used to generate the data set used in the fit and the additional 240 observations used for the predictive comparisons (“P” results). The data used in the fit (the first 240 observations) were “contaminated” with noise from a multivariate normal distribution to produce a set of simulated data measurements. The residuals with quantities tabulated for the *fit* set, “F”, are the differences between the predicted response values using the true parameters and the simulated measurements. For the steam flow rate, the added noise came from a distribution having a zero mean and a standard deviation of 100. These values are evidenced in the tabulated standard deviation of 101.2 and mean of -8.3 (0.06% of the mean steam flow rate) over the 240 observations of simulated steam flow rate.

Model predictions over the additional 240 observations, data set “P”, are compared with true response values (without noise) rather than with noisy simulated measured data as is done for predictions over the fit period, data set “F”. Errors from a regression producing a perfect fit would all

be zero over data set “P”, hence the entries of ~0 for comparison at the top of the tables.

3.5.7 Method Comparisons

The ordinary least squares method was used with three different minimization algorithms and three different sets of responses for comparison. Regression results using six responses in the sum of squared residuals objective function are given in Table 3.5.2 and results using four and three responses are given in Table 3.5.3. The reduced number of responses is used to evaluate the effect of possible collinearity among the responses upon the regression results.

Collinearity among the responses will cause degeneracy in the $R^{\mathrm{T}}R$ matrix used in the weighted least squares and determinant criterion methods and subsequently will result in an unsuccessful regression. While ordinary least squares is not as accurate as weighted least squares in multiresponse estimation problems, collinear responses with ordinary least squares will not result in failure during solution. Ideally, in a least squares formulation, responses should be weighted according to their variance, but disproportionate weighting caused by collinearity may not strongly influence the regression results.

The two responses removed for the four-response runs were the temperature leaving the hot well, T_{hw}, and the temperature of the chiller condenser leaving water, T_{cwo}. Considering small heat losses from the hot well to the ambient environment, the hot well temperature can be estimated with an energy balance about the surface condenser and will vary near linearly with the surface condenser outlet water temperature, T_{cdwo}, which is already used as a response. Leaving water temperature from the chiller condenser, T_{cwo}, can also be determined from an energy balance about the chiller, and will vary linearly with chiller compressor power. Although chiller power is not a measured response in the example system, steam mass flow (a measured response) rate can vary near linearly with chiller power and as a result demonstrate the same linearity with the chiller condenser outlet water temperature. The exhaust pressure was additionally removed in the three response runs, leaving one response each from the cooling tower, the surface condenser and the combined chiller/steam turbine components.

Using the ordinary least squares method (results given in Tables 3.5.2 and Table 3.5.3), both the Levenburg-Marquardt (ODRPACK) and sequential quadratic programming (SQP) algorithms performed successfully using the set of six, four or three responses. The Nelder-Mead simplex algorithm did not perform as well, arriving at parameter estimates which yielded a sum of squared residuals (scaled) over fifteen times greater than those resulting from the Levenburg-Marquardt algorithm (5659.0 vs. 364.6). Over the data used in the fit (data set "F"), the Levenburg-Marquardt algorithm using four responses resulted in both the smallest total sum of squared residuals over all responses (3240.2) and the smallest sum of squared residuals for steam flow rate (4.53×10^6). Using the same algorithm but with three responses yielded the smallest standard deviation of steam flow residuals (2.72). Considering the predictive performance over parameter set "P", the sequential quadratic programming method with three and six responses gave the best results.

Considering all 24 runs, using the weighted least squares method with the Levenburg-Marquardt method and four responses (p_{exh}, $\dot{m}_{\mathrm{steam}}$,T_{cdwo}, T_{cwi}) resulted in the lowest sum of squares (4.47×10^6) for the steam flow rate over the fit data set "F". Results for all the weighted least squares runs are given in Table 3.5.4. The results from the weighted analysis showed only slight improvement over the results of the unweighted least squares using the same method and same four responses. The least steam flow sum of squares residuals over the predicted period came from using the ordinary least squares analysis with the SQP algorithm and the same four responses mentioned above (139.0).

In the weighted least squares category, using the Levenburg-Marquardt algorithm, using four responses showed a very slight improvement over using six. However, using three responses resulted in larger residuals. The SQP method did not result in a good fit for the six and four response cases, but did arrive at a reasonable result for the three response case. The poorer fit is due to unreasonable weights in the weighting matrix. The weighting matrix is the inverse of the $R^{\mathrm{T}}R$ matrix at the solution to the ordinary least squares problem for the same number of responses. The $R^{\mathrm{T}}R$ matrices at the solution to the six and four response SQP runs were ill condi-

TABLE 3.5.2: Example System Regression Results - Ordinary Least Squares, Six Responses

estimation method[1]	number of responses used[2]	minimization algorithm[3]	data set compared[4]	scaled sum of squared residuals or errors over all responses	sum of squared residuals or errors for steam flow rate (kg/hr x10^6)	standard deviation of steam flow residuals or errors (kg/hr)	mean of steam flow residuals or errors (kg/hr)	β_1 / α_0	β_2 / α_1	β_3 / α_2	UA / α_3	f_{hw} / α_4	c / α_5	η_m
residual and parameter "true" values			F	184.4	2.46	101.2	-8.28	0.50	0.15	0.10	11.00	0.50	1.70	
			P	~0	~0	~0	~0	7.336e-2	-0.3259	0.5744	-3.888e-2	0.3321	0.3684	0.850
ordinary least squares	six responses	SQP	F	888.3	12.30	210.7	83.76	0.6962	5.228e-2	4.210e-2	16.1915	0.1056	1.2820	
			P	814.1[b]	11.35[b]	217.7	8.89	-7.360e-2	1.819e-2	0.4425	2.831e-2	0.4674	0.1993	0.6942
		SQP*	F	329.6	4.61	138.7	6.63	0.7288	4.640e-2	-5.329e-2	10.1154	0.6055	1.2430	
			P	971.3	13.59	202.6	-125.46	-0.1235	0.1321	0.3984	0.1808	0.3807	-4.337e-4	0.4623
		LM	F	364.6[d]	4.83[d]	142.0	-7.11[c]	0.7350	9.881e-3	5.173e-3	7.6104	0.1000	1.4264	
			P	1,055.2	14.61	234.9	-76.84	3.344e-2	-0.2055	0.7258	-5.869e-2	0.5868	-2.299e-2	0.9390
		NM	F	5659.0	79.10	539.2	-200.13	0.7580	0.2281	3.525e-2	10.379	8.746e-2	1.4366	
			P	3713.0	51.97	412.2	-217.65	-4.190e-2	-0.2095	0.5722	0.2053	0.1567	0.7078	0.730

[1] Estimation Method: Ordinary least squares (OLS), weighted least squares (WLS) or determinant criterion (DET)

[2] Number of responses used in objective function:
Six – p_{exh}, m_{steam}, T_{cdwo}, T_{hw}, T_{cwi}, T_{cwo}
Four – p_{exh}, m_{steam}, T_{cdwo}, T_{cwi}
Three – m_{steam}, T_{cdwo}, T_{cwi}

[3] Minimization algorithm used: Sequential quadratic programming (SQP), Levenburg-Marquardt with ODRPACK (LM), Nelder-Mead (NM).
An asterisk (*) indicates error free data were used in the fit.

[4] Predictions were compared either set "F" – the 240 noisy data points use in the fit, or set "P" – another 240 data points (true values) not used in the fit.

[a, b, c, d] indicate the "best" four results in each category of residuals. Error free data sets (*) were not included in the ranking.

TABLE 3.5.3: Example System Regression Results - Ordinary Least Squares, Four and Three Responses

estimation method[1]	number of responses used[2]	minimization algorithm[3]	data set compared[4]	scaled sum of squared residuals or errors over all responses	sum of squared residuals or errors for steam flow rate (kg/hr x10^6)	standard deviation of steam flow residuals or errors (kg/hr)	mean of steam flow residuals or errors (kg/hr)	β_1 / α_0	β_2 / α_1	β_3 / α_2	UA / α_3	f_{hw} / α_4	c / α_5	η_m
residual and parameter "true" values			F	184.4	2.46	101.2	-8.28	0.50	0.15	0.10	11.00	0.50	1.70	
			P	~0	~0	~0	~0	7.336e-2	-0.3259	0.5744	-3.888e-2	0.3321	0.3684	0.850
ordinary least squares	four	SQP	F	887.6	12.30	226.2	-17.17	0.6554	0.2558	9.871e-2	11.5903	9.434e-2	1.4056	
			P	1054.8	14.76	160.6	-189.21	-4.068e-2	0.1412	0.4471	-8.409e-2	0.5062	0.3234	0.8947
		SQP*	F	2728.8	38.09	397.0	41.20	0.7201	2.532e-2	2.318e-2	15.837	9.952e-2	1.108	
			P	2447.3	34.13	361.1	-111.24	-0.2172	0.3540	0.4733	0.1204	0.5987	-0.3096	0.7207
		LM	F	340.2[a]	4.53[b]	137.5[c]	-8.34	0.7458	1.717e-2	7.749e-3	7.5287	0.1000	1.5319	
			P	900.8[c]	12.49[c]	218.3	-67.78	3.109e-2	-2.175	0.7495	-4.555e-2	0.5932	1.176e-3	0.6452
		LM*	F	648.8	8.93	192.9	-12.4	0.65624	1.210e-2	8.147e-3	11.099	0.1000	1.3057	
			P	1766.6[c]	24.67	281.5	-154.9	-3.159e-4	-7.592e-3	0.5335	-0.1199	0.5846	-4.093e-2	0.8804
	three	SQP	F	503.0	6.86	168.9	-12.85	0.5513	0.1126	6.359e-2	19.1319	0.1350	1.1295	
			P	443.2[a]	6.11[a]	139.0	-78.87	0.1563	-0.3790	0.4691	-0.2389	0.4089	0.5889	0.1000
		SQP*	F	2883.9	40.33	410.7	-7.11	0.8081	0.1929	-5.428e-2	14.702	2.154e-2	1.1122	
			P	12127.4	169.72	726.7	-425.81	0.3585	-5.208e-2	0.5870	-0.8235	0.9859	0.1424	0.2760
		LM	F	424.7	5.77	131.9[a]	2.72[a]	0.7386	1.255e-2	7.298e-3	9.8109	0.1000	1.2906	
			P	1122.7	15.66	236.9	-96.90	1.442e-3	-0.1194	0.6680	-5.876e-2	0.6015	-2.976e-2	0.8063

tioned (determinant approximately equal to zero) and the matrix inversion resulted in a meaningless weighting matrix.

The determinant criterion may not be well suited for a general multivariate, multiparameter nonlinear regression problem as evidenced in the results given in Table 3.5.5. The volume of an n dimensional parallelpiped which represents the objective function (see Section 3.3.4) could prematurely "collapse" along an edge if two or more responses approached collinearity. For example, during the minimum search, one or more parameters could possibly take on values which cause one response to be nearly collinear with another. Any region in the parameter space which may give rise to collinearity in the responses will correspond to a local minimum of the determinant objective function. The Nelder-Mead minimization algorithm (a derivative free downhill search technique) performed much better than the SQP algorithm when using the determinant criterion. The resulting residual measures were on the same order as using the Nelder-Mead algorithm and the ordinary least squares objective function. However, the SQP algorithm outperformed the Nelder-Mead algorithm when using the sum of squares objective function. This difference gives some indication that the multidimensional objective function surface of the determinant criterion is more troublesome to minimization algorithms which evaluate derivatives than the corresponding sum of squares surface.

Overall, the ordinary least squares method and either the Levenburg-Marquardt or sequential quadratic programming methods yielded the best results for the example regression problem. Weighted least squares did not demonstrate any significant improvement over ordinary least squares. The determinant criterion was comparatively unsuccessful in solving the example problem.

For comparison purposes, the ordinary least squares regression runs were also performed with error-free measured data (runs marked with an asterisk were made with error-free data). Using the SQP algorithm, the six response case with error-free data resulted in very small residuals, (standard deviation of steam flow residuals was 138.7) but the four and three response cases were relatively unsuccessful (standard deviations of steam flow residuals of about 400). Also, using the Levenburg-Marquardt algorithm (ODRPACK) and four response variables, smaller residuals

TABLE 3.5.4: Example System Regression Results - Weighted Least Squares

estimation method[1]	number of responses used[2]	minimization algorithm[3]	data set compared[4]	scaled sum of squared residuals or errors over all responses	sum of squared residuals or errors for steam flow rate (kg/hr x10^6)	standard deviation of steam flow residuals or errors (kg/hr)	mean of steam flow residuals or errors (kg/hr)	β_1	β_2	β_3	UA	f_{hw}	c	
								α_0	α_1	α_2	α_3	α_4	α_5	η_m
residual and parameter "true" values			F	184.4	2.46	101.2	-8.28	0.50	0.15	0.10	11.00	0.50	1.70	
			P	~0	~0	~0	~0	7.336e-2	-0.3259	0.5744	-3.888e-2	0.3321	0.3684	0.850
weighted least squares	six	SQP	F	30590.8	427.99	1316.7	238.33	0.6746	4.319e-2	3.035e-2	16.0585	0.1058	1.1332	
			P	43492.3	608.72	1517.17	492.55	1.413e-2	0.1189	0.5672	-0.2123	0.3945	0.1824	0.7128
		LM	F	358.9[c]	4.72[c]	140.31[d]	-8.29	0.6504	1.296e-2	4.233e-3	6.9875	0.3480	1.4943	
			P	1049.2	14.47	232.66	-80.04	2.727e-2	-0.1732	0.6322	-4.154e-2	0.5066	-1.608e-2	1.0840
	four	SQP	F	6219.8	86.89	589.8	-125.24	0.6746	4.319e-2	3.035e-2	16.0585	0.1058	1.1332	
			P	8513.0	119.07	669.8	-222.25	1.141e-2	0.1189	0.5672	-0.2127	0.3945	0.1824	0.7128
		LM	F	353.4[b]	4.47[a]	136.5[b]	-7.75[d]	0.7135	2.056e-2	6.828e-3	6.3299	0.1000	1.3643	
			P	973.7[d]	13.22[d]	222.2	-77.26	3.110e-2	-0.2000	0.6896	-4.2628	0.5492	1.178e-3	0.8264
	three	SQP	F	430.8	5.81	155.4	12.78	0.7504	5.794e-3	2.829e-2	29.5745	0.1136	1.3538	
			P	965.1	13.35	215.2	-97.53	6.116e-2	-0.1743	0.5526	-0.2221	0.6313	0.2979	0.7104
		LM	F	403.9	5.45	150.9	-5.26[b]	0.7646	1.324e-2	7.264e-3	8.5527	0.1000	1.3433	
			P	1071.3	14.91	232.0	-92.26	1.438e-3	-0.1313	0.6970	-4.736e-2	0.6100	-2.844e-2	0.8293

TABLE 3.5.5: Example System Regression Results - Determinant Criterion

estimation method[1]	number of responses used[2]	minimization algorithm[3]	data set compared[4]	scaled sum of squared residuals or errors over all responses	sum of squared residuals or errors for steam flow rate (kg/hr x10^6)	standard deviation of steam flow residuals or errors (kg/hr)	mean of steam flow residuals or errors (kg/hr)	β_1 / α_0	β_2 / α_1	β_3 / α_2	UA / α_3	f_{hw} / α_4	c / α_5	η_m
residual and parameter "true" values			F	184.4	2.46	101.2	-8.28	0.50	0.15	0.10	11.00	0.50	1.70	
			P	~0	~0	~0	~0	7.336e-2	-0.3259	0.5744	-3.888e-2	0.3321	0.3684	0.850
determinant criterion	six	SQP	F	21837.5	305.54	838.6	756.87	0.6498	7.171e-2	-7.537e-2	15.8981	0.1640	1.3980	
			P	26320.4	368.39	1020.2	706.05	-1.621e-2	0.2495	0.3549	-4.729e-2	0.4588	-0.2095	0.8997
	four	SQP	F	71032.1	993.92	1864.1	-825.12	0.6712	2.056e-2	1.525e-2	15.8295	0.1081	1.1150	
			P	112512.3	1574.72	2532.6	-417.2	0.1147	4.997e-2	0.5289	7.979e-2	0.2797	-0.1696	0.7134
		SQP*	F	666016.4	9322.51	1004.1	-6151.41	0.7024	3.655e-2	2.671e-2	15.9853	0.1039	1.1291	
			P	630616.5	8827.01	1307.2	-5922.62	0.1485	0.2386	0.5661	-7.426e-3	0.3292	-8.863e-2	0.7188
		NM	F	2153.4	30.02	299.0	-189.86	0.7710	0.1322	0.1341	11.9100	0.1009	1.4172	
			P	4230.0	59.20	334.0	-368.26	0.1417	-0.1279	0.2462	-0.4925	0.6938	1.0023	0.7022
	three	SQP	F	317793.2	4447.89	1625.84	-3987.55	0.7052	1.557e-2	4.046e-4	16.7804	0.1030	1.1164	
			P	301312.1	4217.32	2204.87	-3568.04	0.1410	0.3420	0.4731	-5.321e-2	0.2642	-3.113e-2	0.7186
		SQP*	F	300897.4	4211.42	1280.47	-3989.3	0.7024	3.655e-2	2.671e-2	15.9853	0.1039	1.1291	
			P	281882.0	3945.4	1772.86	-3648.2	0.1485	0.2386	0.5661	-7.426e-3	0.3292	-8.863e-2	0.7188
		NM	F	1582.4	22.02	297.64	-59.49	0.7705	0.1881	0.1286	11.7419	0.1023	1.3994	
			P	5672.8	79.40	481.67	-315.91	0.1874	-0.1639	0.5500	-0.5695	0.9577	0.4867	0.6909

resulted from the data set which included error. Although not proven here, the added noise in the responses may result in more accurate gradients of the objective function. For example, consider a single response case where β^* represents the true value of β and $\hat{y}$ represents the true response values over $i = 1,...n$ observations of independent and response variables x and y.

$$\hat{y}_i = f\left(x_i;\beta_i^*\right) \tag{3.5.4}$$

The measured response variable y includes a random error ε from a normal distribution with a zero mean.

$$y_i + \varepsilon_i = f\left(x_i;\beta_i^*\right) \tag{3.5.5}$$

The sum of squares objective function for the error free case is

$$\phi(\beta) = \sum_i^n \left(y_i - f(x_i;\beta)\right)^2 \tag{3.5.6}$$

and the corresponding objective function for the responses measured with error is

$$\phi_\varepsilon(\beta) = \sum_i^n \left(y_i + \varepsilon_i - f(x_i;\beta)\right)^2 \tag{3.5.7}$$

The first derivatives of the respective objective functions are

$$\frac{\partial\phi}{\partial\beta} = \sum_i^n -2\left(y_i - f(x_i;\beta)\right)\frac{\partial f(x_i;\beta)}{\partial\beta} \tag{3.5.8}$$

and

$$\frac{\partial\phi_\varepsilon}{\partial\beta} = \sum_i^n -2\left(y_i + \varepsilon_i - f(x_i;\beta)\right)\frac{\partial f(x_i;\beta)}{\partial\beta} \tag{3.5.9}$$

At the minima, where $\beta = \beta^*$, the first derivatives are zero. However, for the error-free case, the $y_i - f\left(x_i;\beta_i\right)$ term approaches zero toward the minima, and can cause the sum in Equation 3.5.8 to fall below the minimization algorithm tolerance at a value of β further from the minima than the value of β that results in Equation 3.5.9 falling below the same tolerance. There is some small

calculated error between the true data set containing $\hat{y}$ and the TRNSYS calculated values of y at β^* because a slightly looser convergence tolerance is used in the regression runs than is used in generating the true data set. This may have contributed to the success of the six response run using error-free data, as more of the error due to the looser tolerance is accumulated for six responses than for four.

3.5.8 Residual Plots

One measure of success in parameter estimation is to compare the estimated values with their true values. However, the ultimate objective of the regression procedure is to obtain parameters that result in a composite model with good predictive qualities. Some individual parameter estimates can have significant error due to overparameterization (see Section 3.4), but the combination of parameters found in the regression can still produce a composite model with good fit. The model predictive capabilities resulting from the various parametric estimation methods can be better judged by evaluating the residuals associated with the dependent variables. If the example system model were to be used in a cost optimization algorithm, the model would be judged solely by how well it could predict the one variable associated with energy costs, the steam mass flow rate. The total sum of squares of residuals for steam flow rate gives one relative indication of how well a particular model fits the data; however, the distribution of the residuals should also be considered. The standard deviation and mean values of steam flow residuals are adequate for describing a normal distribution; however, without assuming normality, the distribution can be conveniently judged by examination of residual plots.

Residuals resulting from a successful regression should support the assumptions made in the analysis. For example, if the minimized sum of squares or minimized $R^{\mathrm{T}}R$ determinant is to result in the best fit, the residuals should possess a normal distribution with a zero mean. Calculated steam flow rate values “contaminated” with normally distributed errors to simumlate instrument noise are plotted against the true values in Figure 3.5.4. The distribution of residuals from a successful regression should be similar to that of the errors. The steam flow residuals from the regression run having the smallest sum of squares demonstrate very good results and are plotted in Figure 3.5.5. The residuals have a standard deviation of 136.5, very close to the standard deviation

in the error (100), and a mean of -7.8 corresponding to distribution centered close to zero.

A plot of steam flow residuals from the regression run having the smallest sum of squares of residuals over the predictive period "P" is shown in Figure 3.5.6. A "perfect" fit would arrive at the true parameter values and the model predictions would be equivalent to the true values (error values would be zero). The plot of steam flow rate errors shows a tight band, but with a deterministic curvature. While the regression run found a reasonable minimum of squared residuals over the fit period (the standard deviation of residuals for this run was 139), all thirteen estimated parameters did not approach their true values. The curvature is indicative of a failure in the model to account for some nonlinear dependence. For a linear model with a single regressor (independent variable), the curvature would indicate that a quadratic term with respect to the regressor should be added to the model. For the multiresponse nonlinear example at hand, any set of parameters not identical to the true values can result in some amount of curvature, and the curvature present in Figure 3.5.6 does not necessarily indicate a quadratic term should be added to one of the model equations. For example, another regression run which demonstrated the best fit over the initial 240 observations ("F" data set) yielded a different curvature over the predictive "P" data set. The periodic shape to the band of points in Figure 3.5.7 is due to the forced periodic variation in the regressor variables.

Qualitatively, this multiresponse, nonlinear parameter estimation problem is almost certain to have some level of parameter identification problems. It is difficult for any minimization algorithm to arrive at precisely a local minima when the objective function surface exhibits "flat" regions in all of the thirteen dimensions. Some statistical measures of parameter variance for the model and minimization method are presented in Section 3.5.9 below.

Plots of measured and predicted values versus time of steam flow rate or other response variables would also aid in comparing the regression results. However, for most of the runs showing relatively small standard deviation in steam mass flow rates, curves of predicted and measured values overlap each other and are indistinguishable in a plot scaled over the range of steam flow rate. For example, a comparatively large steam flow rate residual of 250 is only 2% of the mean steam

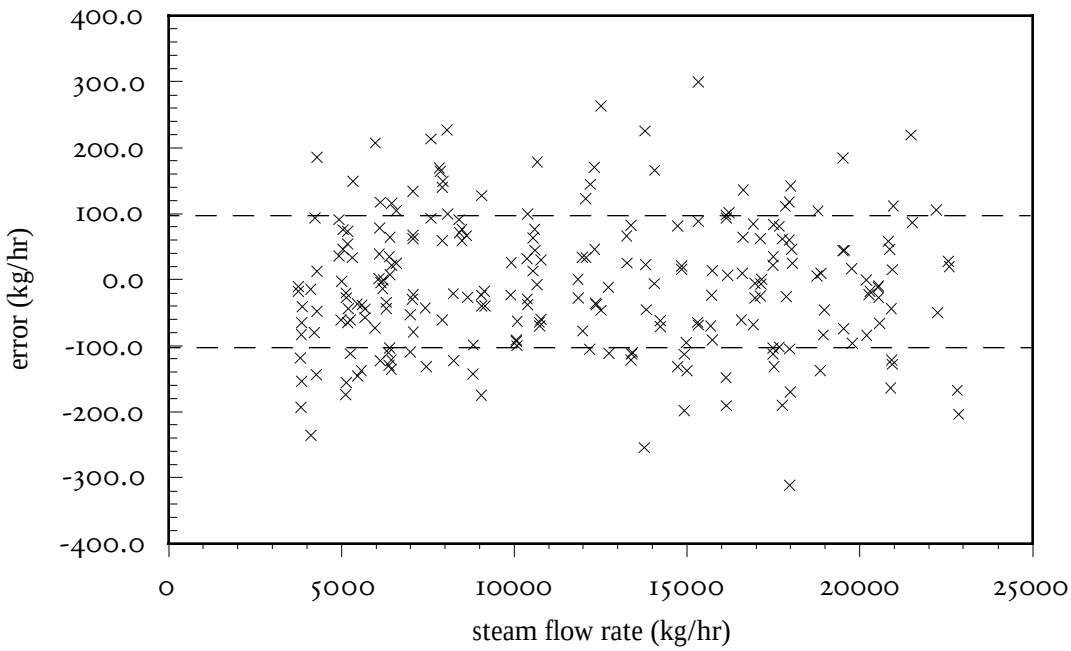

FIGURE 3.5.4: Error vs. "true" steam flow rate values over the initial 240 points of simulated measured data. The random error has a standard deviation of 100.

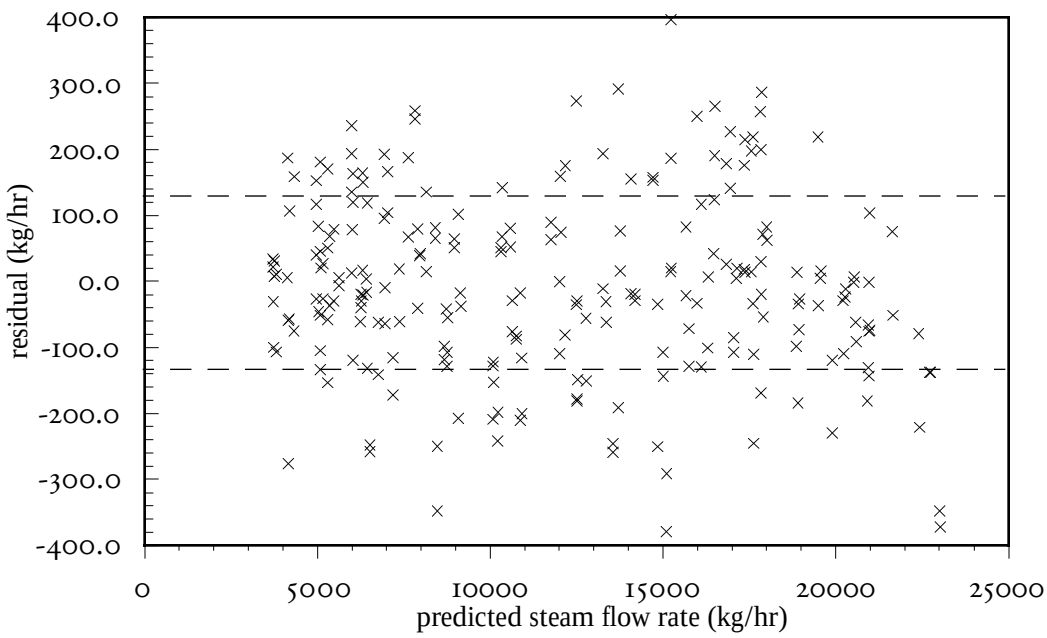

FIGURE 3.5.5: Residuals (measured - predicted values) of steam flow rate for the initial 240 data points. Estimation method used weighted least squares with the Levenberg-Marquardt minimization algorithm and four responses in the objective function. The residuals have a standard deviation of 136.5.

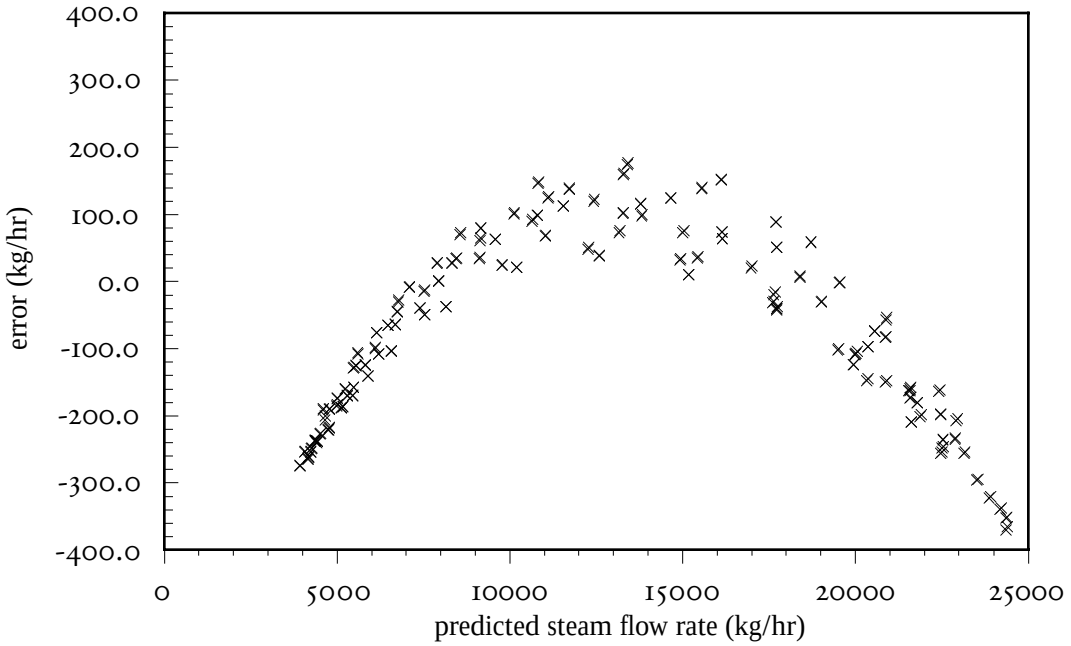

FIGURE 3.5.6: Steam flow rate errors vs. predicted values over the second set of 240 observations. Parameter estimates used in generating these data are from the application of ordinary least squares and the SQP algorithm.

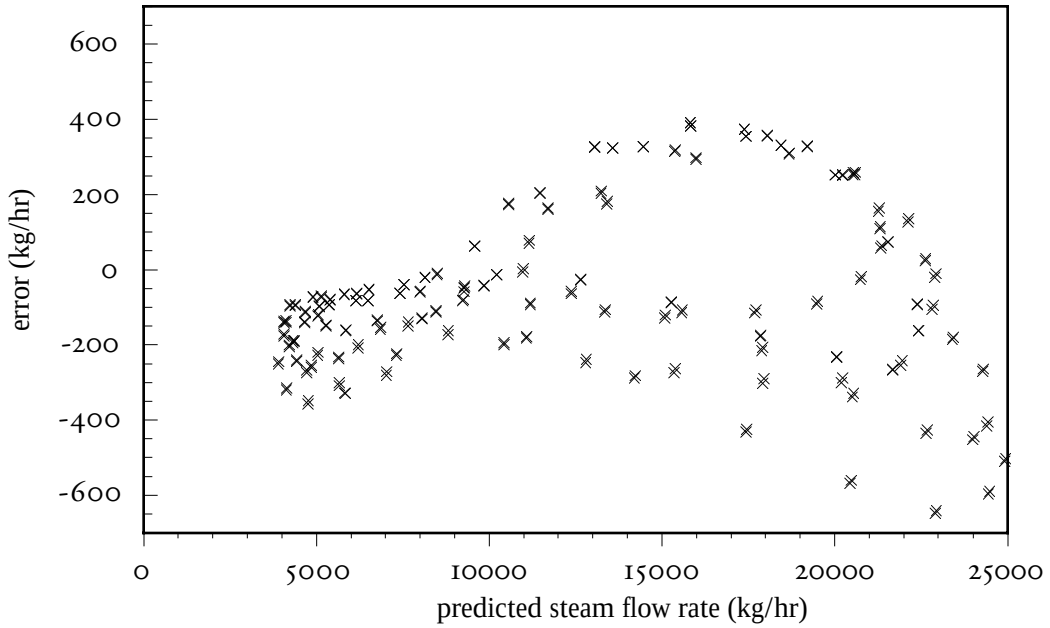

FIGURE 3.5.7: Steam flow rate errors vs. predicted values over the second set of 240 observations. Parameter estimates used to generate these residuals are the result of using four regressor variables in a weighted least squares objective function and the Levenburg-Marquardt algorithm (ODRPACK).

flow rate. Any run resulting in a standard deviation of steam flow residuals less than about 300 could be considered successful, yielding reasonably accurate steam flow rate predictions.

3.5.9 Example Problem Parameter Variance Estimates

In addition to the data used in the earlier example problem, one hundred sets of simulated replicated data were used to obtain one hundred sets of parameter estimates. The same ordinary least squares method with six responses using the SQP algorithm was used in each case with the same starting values for the parameters. Each data set contains errors drawn from a multivariate pseudorandom number generator where the errors follow a multivariate normal distribution with a given covariance matrix. Parameter bias and variance were then computed as outlined in Section 3.4.2. The resulting statistical properties are a function of both the model and the estimation procedure. It has been demonstrated that, in general, nonlinear estimation problems will nearly always have biased parameters. [Box70] The mean, bias, and standard deviation (square root of variance) of the example problem parameter estimates are given in Table 3.5.6.

All parameter means demonstrate significant bias, and most demonstrate significant standard deviation. The two parameters showing relatively small standard deviation are the overall heat transfer coefficient, *UA*, and the coefficient *c* used in the cooling tower *Ntu* (Equation 3.5.2). These two parameters can be estimated with a single observation and cannot contribute to overparameterization (see Section 3.4.1). For example, the coefficient *c* is the only parameter estimated for the cooling tower component model and could be calculated from a single observation of inlet and outlet cooling water temperature measurements.

Overparameterization is possible with the multiple parameters used in the steam turbine and chilled water plant models and, to some extent, is demonstrated by the relatively large values of standard deviation for these variables. The steam turbine and chiller component models are mechanistic models in part, but both make some use of curve fits and the α and β parameters in Table 3.5.7 are coefficients in those curve fits. To reduce the variance, some parameters could be fixed or the models rewritten to use different curves. However, the application of the resulting models may be limited to the regression problem at hand and not apply to other cases where the plant is operated over different ranges of independent variables.

TABLE 3.5.6: Parameter Variance and Bias Estimates for the Example Problem

parameter	mean value	true value	bias	bias as a percent of true value	standard deviation	standard deviation as a percent of true value
β_1	0.6680	0.5000	0.1680	33.61	0.0669	13.37
β_2	5.072e-2	0.1500	-0.0993	-66.18	0.0557	37.10
β_3	2.425e-2	0.1000	-0.0758	-75.75	0.0243	24.33
α_0	9.807e-2	0.0734	0.0247	33.68	0.0518	70.59
α_1	-0.1869	-0.3259	0.1390	-42.64	0.0999	-30.66
α_2	0.5140	0.5744	-0.0604	-10.52	0.1078	18.77
α_3	-0.2460	-0.0389	-0.2072	532.81	0.1044	-268.40
α_4	0.5656	0.3321	0.2335	70.30	0.0830	24.99
α_5	0.2973	0.3684	-0.0711	-19.31	0.1032	28.01
η_{m}	0.7158	0.8500	-0.1342	-15.78	0.1423	16.74
UA	16.4295	11.0000	5.4295	49.36	0.2729	2.48
f_{hw}	0.1626	0.5000	-0.3374	-67.47	0.1256	25.19
c	1.3301	1.7000	-0.3699	-21.76	0.0760	4.47

3.5.10 Outliers

To examine the influence of "bad" data points, approximately five percent of the data was replaced with data with very large error. These large error data points were random values taken from a normal distribution having an extremely large variance. In some cases, the values were physically impossible, such as cooling tower water temperatures above 100°C or subzero chilled water temperature values. Data demonstrating very large error are called "outliers," since on plots comparing regression predictions to measured data, they would lie noticeably far removed from the regression results. Six runs were made to compare the relative influence of outliers in each of the six response variables. Results of the runs are given in Table 3.5.7. Steam flow rate residuals during the predictive period were shown to be most sensitive to outliers within hot well temperature measurements, T_{hw} , and least sensitive to outliers in chiller condenser leaving water temperature, T_{cwo} . Hot well temperature is strongly dependent with the saturation temperature (and

therefore steam exhaust pressure) in the surface condenser. The large error introduced into the hot well measurements resulted in steam flow rate residuals even larger than those added to the steam flow rate data in a separate run. During the fit period, steam flow rate residuals were most affected by the large errors in the surface condenser leaving water temperature, T_{cond}, which again is strongly dependent on turbine exhaust pressure. As an example of the variance of the parameter estimates, the run with large errors in chiller condenser leaving water temperature, T_{cwo} , resulted in smaller residuals than the identical run without large errors in any of the variables.

Overall, the outliers did influence steam flow rate predictions to varying extent for five of the six responses. However, the magnitude of the outliers was large enough that they could have been identified and removed by examining a plot of residuals. For example, in Figure 3.5.8 residuals for the hot well temperature are plotted against their predicted values. Ten of the twelve outliers are immediately apparent and the remaining two can be picked out upon closer examination. In an actual application, the observations which include these outliers could be removed and the regression run again. One robust regression method for the single response case includes only the smallest m out of n residuals used in the sum of squares computation where m is greater than half of n. For the multidimensional case, however, an observation that includes an outlier for one response may have good data for other responses and the decision to remove the observation from the regression is not as straightforward.

Missing data values could be considered to be additional parameters and their values estimated by solution of the regression problem. This may be impractical for a large amount of missing data. Stewart *et al.* describe a slightly more complicated approach derived from Bayesian theory. [Ste92]

Problems with missing data are minimal with chilled water plants as numerous observations are generally available. Most measured variables are recorded at a constant rate (e.g. hourly data) as an aid in monitoring plant operation. Where partial observations represent a small fraction of the available data, their removal will not significantly affect regression results. Making use of incomplete observations takes on a greater importance when they comprise a significant portion

TABLE 3.5.7: Example System Regression Results - Outliers Included in Data

estimation method[1]	number of responses used[2]	minimization algorithm[3]	data set compared[4]	scaled sum of squared residuals or errors over all responses	sum of squared residuals or errors for steam flow rate (kg/hr x10^6)	standard deviation of steam flow residuals or errors (kg/hr)	mean of steam flow residuals or errors (kg/hr)	β_1 / α_0	β_2 / α_1	β_3 / α_2	UA / α_3	f_{hw} / α_4	c / α_5	η_m
residual and parameter "true" values			F	184.4	2.46	101.2	-8.28	0.50	0.15	0.10	11.00	0.50	1.70	
			P	~0	~0	~0	~0	7.336e-2	-0.3259	0.5744	-3.888e-2	0.3321	0.3684	0.850
ordinary least squares	SQP	p_{exp}	F	2475.8	34.52	373.8	68.26	0.6988	0.1141	4.311e-2	16.007	9.869e-2	1.3081	
			P	2400.2	33.56	341.0	-155.12	-0.1210	0.4214	0.5424	-0.1533	0.7907	-0.3493	0.7049
		m_{steam}	F	2143.1	29.86	335.3	-111.46	0.8380	0.1622	-0.1005	15.1615	8.365e-2	1.4016	
			P	7780.9	108.91	501.8	-450.57	-3.545e-2	0.3673	0.3706	-3.991e-2	0.6039	-0.1738	0.7483
		T_{cond}	F	6410.3	89.57	612.1	-4.77	0.9184	2.553e-2	3.637e-2	16.1731	0.1288	1.3723	
			P	6779.5	94.8	614.9	-136.10	0.1202	0.1956	0.4282	-0.6520	0.8598	0.4838	0.6896
		T_{hw}	F	2309.1	32.19	364.7	-41.10	0.5230	0.2476	-9.174e-2	15.9828	0.0000	1.3680	
			P	11599.8	162.38	700.4	-433.63	0.1350	0.1801	0.4546	-0.3017	0.5875	-0.2575	0.7899
		T_{cwi}	F	3228.7	45.08	434.3	-4.19	0.7809	-2.060e-2	2.605e-2	10.5890	0.4978	1.4693	
			P	6248.0	87.46	500.6	-338.91	-6.196e-2	0.4361	0.4631	-0.3726	0.9671	-0.3266	0.9241
		T_{cwo}	F	495.4	6.81	168.2	14.35	0.5245	8.208e-2	7.287e-3	15.8837	9.698e-5	1.3520	
			P	742.9	10.38	171.9	-177.56	-2.054e-2	3.674e-2	0.3288	-2.229e-2	0.3565	0.1357	0.7556

of the data set and when the data are rare or expensive to remeasure, for example, data taken in an experimental setting.

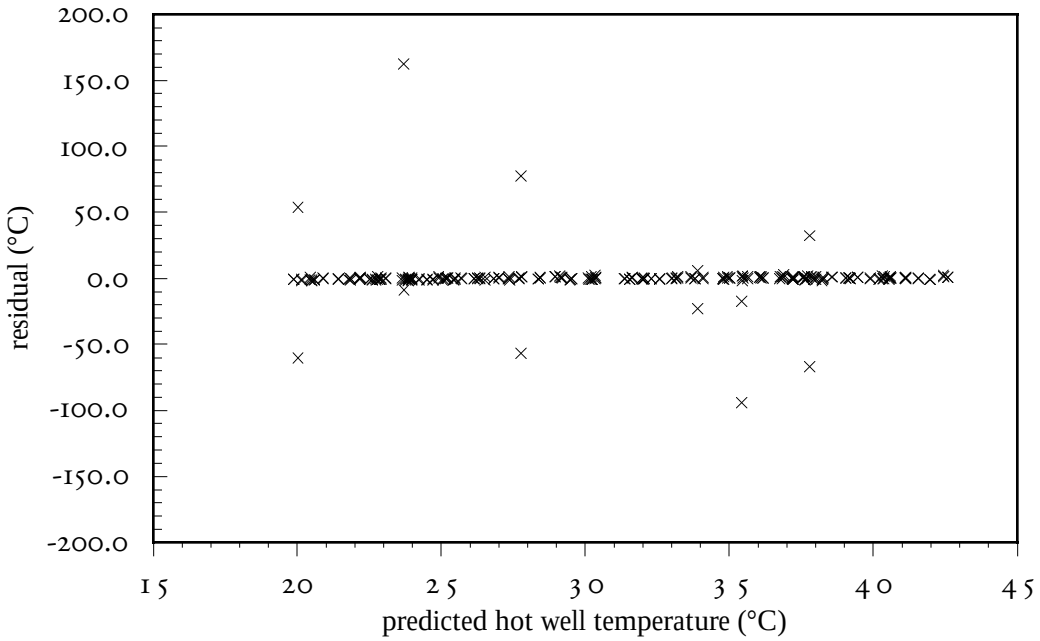

FIGURE 3.5.8: Plot of residuals of hot well temperatures resulting from regression. Twelve outliers, evident in the plot, were included in the measured data.

3.6 Summary

This chapter presents an approach for creating and evaluating a predictive model of a chilled water plant. The plant model was constructed using the TRNSYS simulation program and mechanistic component models. Various multiresponse regression techniques were used to solve the parameter estimation problem for an example system.

The different approaches and solution methods were applied to the chilled water plant model using simulated measured data. The simulated data was created using the model and a known set of parameters. A given series of independent variable data was input to the model to generate a series of responses. The model computed responses were then contaminated with noise to simulate observations of actual measured data.

The influence of using different sets of response variables in the estimation problem was investigated. Using more responses than just those for which predictions are needed (e.g. cost associated responses) can result in a better predictive model. However, adding responses that can be collinear with other responses is detrimental.

Methods including ordinary and weighted least squares and a residual matrix determinant criterion were used to frame the problem. Different minimization algorithms for solving the estimation problem were applied and the results compared. For the example system studied, using ordinary least squares with sequential quadratic programming minimization is an effective method for solving the parameter estimation problem. Using weighted least squares or the determinant criterion did not demonstrate any significant improvement in fit compared to ordinary least squares.

CHAPTER 4

Parameter Estimation - Walnut Street Plant

In this chapter, methods presented in Chapter 3 are applied to data taken from an operating chilled water plant. A plant model is created and the various parameter estimation approaches discussed in Chapter 3 are applied and compared. A set of model parameters that result in the best fit of measured data is found for use in subsequent plant optimization studies (Chapter 5).

4.1 Central Plant Description

A chilled water plant on the University of Wisconsin-Madison campus serves as a model for applying the methods of parametric estimation and optimal supervisory control. A schematic representation of the plant is shown in Figure 4.1.1. The plant includes four large centrifugal compressors, three driven by steam turbine and one by electric motor. Design loads for the chillers are 3,500 tons for each of the two smaller steam driven compressors and 5,500 tons for the remaining steam and electrically driven compressors. Five two-cell cooling towers are used to reject heat to the environment. Chilled water pumps (CHP) draw from the chilled water return (chwr) header,

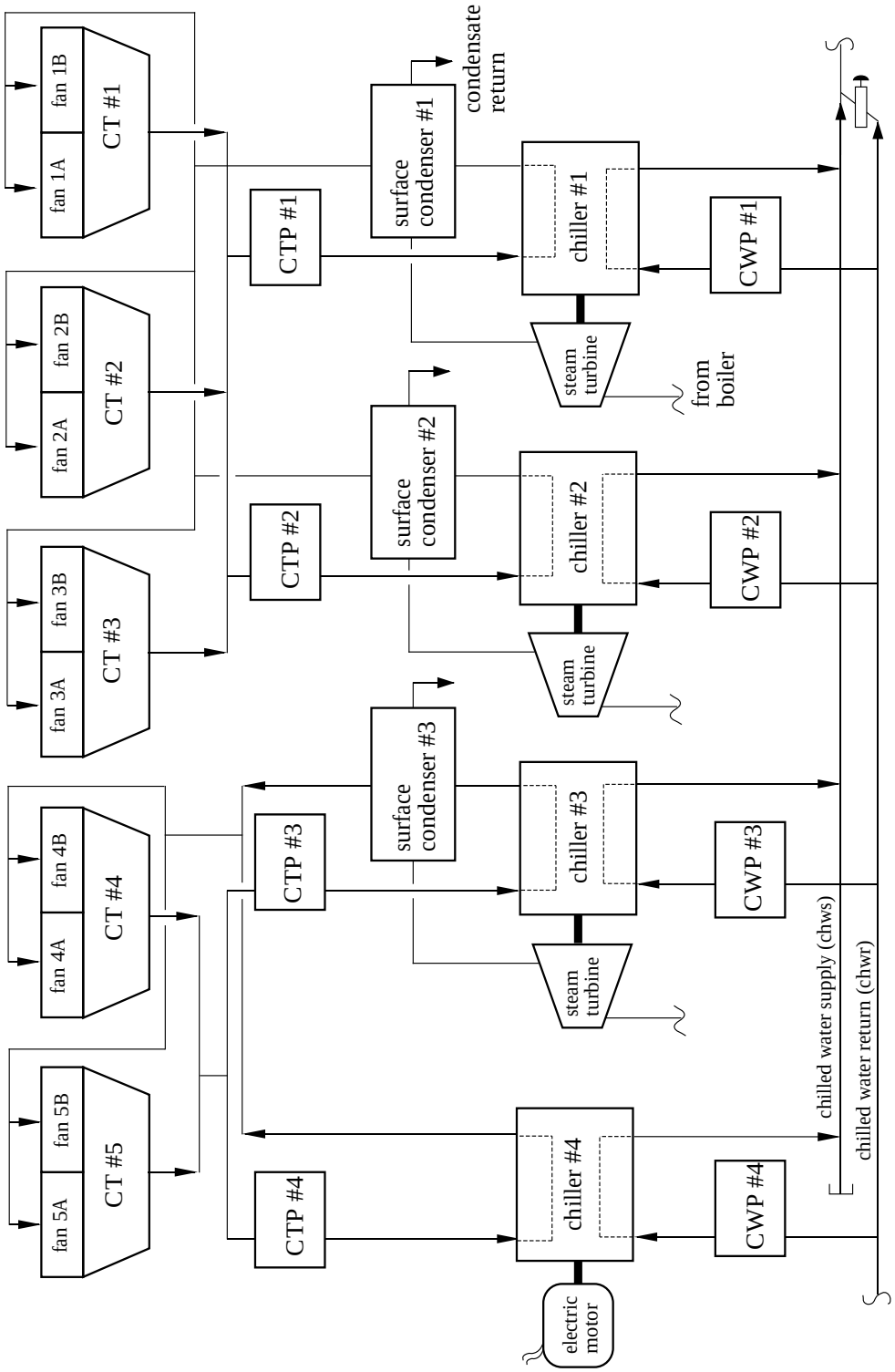

FIGURE 4.1.1: Walnut Street chilled water plant schematic.

pumping the water though the evaporative heat exchanger and into the chilled water supply (chws) header. The chilled water pumps are designed primarily to meet the pressure drop through the evaporator rather than provide a pressure differential between the main distribution supply and return chilled water line. Large main distribution pumps (not shown on the schematic) maintain pressure between the supply and return lines sufficient for distribution throughout the campus.

Condenser water pumps (CWP) circulate water between the refrigerant condenser and the cooling towers. For the steam driven turbines, a "surface condenser" is placed between the refrigerant condenser and the cooling tower. This heat exchanger is used to condense the steam turbine exhaust before returning the condensate to the boilers. Turbine exhaust pressures are normally subatmospheric with a saturated steam temperature around 37°C.

The five cooling towers (CT) are grouped into two sets. Cooling towers #1, #2 and #3 normally serve chiller #1 and chiller #2. Cooling towers #4 and #5 normally serve chillers #3 and #4. However, piping connections allow for condenser water from one group to be cooled by cooling towers in the other group. It is not possible to connect any given chiller condenser to any cooling tower as multiple towers receive flow from a common header. For example, condenser water from chillers #1 and #2 flows into a common pipe before being split between cooling towers #1, #2 and #3. If chillers #1 and #2 are both operating, the flow is normally split such that ⅔ of the condenser water from each chiller flows to cooling towers #1 and #3 respectively. The other ⅓ from each chiller is mixed and enters cooling tower #2. Cooling towers #1, #2 and #3 have individual sumps while cooling towers #4 and #5 share a common sump. All cooling towers have two cells each and one fan per cell. Four towers have two speed (off/low/high) fans and one tower (CT #3) has a set of single speed (on/off) fans.

Chillers #3 and #4 and cooling towers #4 and #5 are recent additions to the Walnut Street plant and are better instrumented than the older components. Also, design data such as pump curves and cooling tower performance data are available for the newer components. Due to the greater availability and confidence in data, the parametric estimation studies and optimization studies in this work only consider these newer components of the Walnut Street Plant.

4.2 Data Measurements

Various system measurements are recorded at two hour intervals by plant personnel. The procedure includes reading a gauge or digital display and recording the measurement by hand on a log sheet. A representative copy of a log sheet recording observations for the electric chiller on July 11, 1994 is shown in Figure 4.2.1. The resulting data are subject not only to measurement error but also to human error in reading and transcription. All of the recorded measurements are not observed at the same moment in time. The operator walks through the plant, recording necessary measurements along the way. This walking tour is done over a 15 to 20 minute period, depending upon the operator's duties during the tour and number of data points read. Only some of the measurements entered into the log are used in the model. Many measurements significant to plant maintenance requirements are recorded, such as bearing oil temperatures and cooling tower water pH.

For the electric chiller, measured electric power is approximated from the recorded "motor amps." Power draw for a three phase electric motor can be estimated from

$$P = \sqrt{3}\, E\, I\ \ pf \qquad 4.2.1$$

where E is the line to line voltage potential (volts) and I is the line current (amps) and pf is the power factor, which is dependent upon the phase difference between voltage and current in alternating current (AC) devices. Measurements of line voltage at the motor are not recorded, but remain fairly constant at the rated line voltage of 4160 volts. A constant power factor of 0.75 is assumed.

Inlet and outlet pressures at the pumps are used along with manufacturer's pump curves to estimate chilled and condenser water flow rates. Chilled water supply and return temperatures as well as chiller condenser entering and leaving water temperatures are directly recorded. Measurements of steam mass flow rate and inlet and exhaust pressures at the turbine are recorded on a steam chiller log similar to the electric chiller log. Also, the condenser water temperature at the inlet and outlet to the surface condenser as well as the condensate temperature in the hot well are recorded.

WEST CAMPUS HEATING & CHILLING
505 NORTH WALNUT

CHILLER NO. 4 DATE JUL 11 '94

	MID	2	4	6	8	10	NOON	2	4	6	8	10
COMPRESSOR												
Cooler Refg Temp	44	44	45	45	45	44	44	43	43	42	43	44
Cond Refg Temp	93	89	90	90	97	103	116	128	132	136	128	122
Comp Brg Oil PSI	19	19	19	19	19.1	19.1	19	19	19.1	19.2	19.1	19.4
Cooler Oil Temp	99	95	95	93	—	—	—	—	98	98	96	94
Comp Brg Temp	111	110	109	109	125	125	125	125	128	130	128	126
Brg Oil Temp Inboard	113	112	112	112	122	122	124	124	124	125	123	122
Brg Oil Temp Outboard	108	107	107	107	126	126	126	126	127	128	126	125
Oil Filter PSID	20	22	22	22	21	21	21	21	20.7	19.1	19.0	19.0
Resv Oil Level	✓	✓	✓	✓	✓	✓	✓	✓	✓	✓	✓	✓
Vane Position	11	8	9	9	26	30	38	50	73	86	30	76
Mtr Gear Sup Oil Tmp	115	112	108	108	108	110	113	128	119	120	116	111
MOTOR ELECTRIC DRIVE												
Motor Amps	312	289	280	282	322	354	416	476	536	550	470	428
Lo Spd Brg Comp End	132	131	131	131	130	128	127	129	129	129	130	131
Lo Spd Brg Mtr End (F5)	131	126	126	126	126	127	132	138	138	138	137	136
Hi Spd Brg Comp End (F5)	159	158	158	158	157	154	153	151	150	150	150	150
Hi Spd Brg Mtr End (F5)	177	176	176	176	176	176	177	181	184	189	186	181
Mtr Brg Drive End (F6)	142	140	139	139	139	138	140	143	145	148	148	148
Mtr Brg Non Drive End (F6)	142	138	138	138	139	140	141	142	143	144	141	141
MAIN BREAKER AMPS												
"AA"												
"AB"												
"AC"												
"BA"												
"BB"												
"BC"												
COOLER/CONDENSOR												
Chilled Water PSID	5	5	5	5	5	5	5	5	5	6	5	5
Chilled Water Inlet Temp	46	46	46	46	46	47	49	50	52.4	52.4	51.1	49.8
Chilled Water Outlet Temp	40	40	40	40	40	40	40	41	40.7	40.5	40.3	40.0
Tower Water PSID	4	4	4	4	4	4	4	4	4	4	4	4
Tower Water Inlet Temp	69	69	69	70	69	72	76	80	81	82	80	78
Tower Water Outlet Temp	74	74	73	74	74	76	82	86	87	88	86	84
TOWER PUMP												
Strainer Inlet PSI	19.5	19.5	19.5	19.5	19.5	19.5	19.5	19.5	2	2	2	2
Pump Suction PSI	19.5	19.5	19.5	19.5	19.5	19.5	19.5	19.5	19	19	19	19
Pump Discharge PSI	68	68	68	64	68	68	68	68	68	68	68	68
CHILLED WATER PUMP												
Strainer Inlet PSI	97	97	96	96	96	97	97	97	2	2	2	2
Pump Suction PSI	94	94	94	94	85	85	86	85	86	88	87	86
Pump Discharge PSI	134	134	134	134	133	133	133	133	133	134	133	133
PLANT PSIG												
Chilled Water Supply					120	117	116	116	118	118	119	119
Chilled Water Return					95	94	94	95	96	96	97	97
Chilled Water PSID					25	23	22	21	22	22	22	22
SAND FILTER'S PSID	17	18	18	18	18	17	17	18	18	18	18	19
TOWER WATER												
TDS Actual	2200	2250	2200	2200	2200	2200	2100	2100	2100	2100	2200	2200
Tower Pac	2150	2150	2150	2100	2150	2150	2100	2200	2150	2150	2150	2100
PH Actual	8.4											
Tower Pac	8.5	8.5	8.5	8.5	8.5	8.5	8.5	8.5	8.5	8.5	8.4	8.3
PH Adj Up or Down										✓		
"M" Alkalinity	368	352	352	360	364	384	392	388	420	500	420	360
Odd # Fan Speed Hi-Lo	H L					H L	H L	H L	H H	H H	H H	H H
Even # Fan Speed Hi-Lo	H L					H L	H L	H L	H H	H H	H H	H H
Wet Bulb Temperature	55	56	57	57	59	63	68	72	73	75	73	70
Dry Bulb Temperature	62	60	60	60	62	68	76	82	83	85	80	75
Security Check In												

FIGURE 4.2.1: Log sheet for chiller #4 (electric motor driven) on July 11, 1994.

Outdoor wet and dry bulb temperature measurements and the fan speeds for the individual cooling tower fans are recorded near the bottom of the log. The outdoor air wet bulb temperature is measured with a fixed alcohol in glass thermometer outside the facility, shaded from the sun. Since outdoor air is not forced over the bulb, the measured wet bulb temperatures will likely be in error with high readings during light winds. Overall, the accuracy and precision of the measured data are far from what is desired in a laboratory setting, but typical of operating chilled water plants.

Data taken over July and August of 1994 were used for this study. A few observations were unrecorded or incomplete, and were removed from the data set. The data set represents approximately 54 days of operating data. There are 643 observations, made at two hour intervals. The data set was partitioned into three parts, which will be referred to as Periods I, II and III. The first 240 observations (Period I) are used in the regression analysis to determine parameter estimates. The next 272 observations (Period II) are used to compare the predictive capabilities over data not used in the fit. During these first 512 observations, both the steam electric chillers are operating. But during the final 131 observations (Period III), only the steam turbine is operating. Condenser water flow rate increases for the steam turbine when it is operated alone, and the predictive capabilities can be further compared for this change in operating conditions.

4.3 TRNSYS Walnut Street Plant Model

Individual TRNSYS component models of chillers, heat exchangers and a cooling tower are combined in a TRNSYS "deck" of the Walnut Street Plant, where the connections between outputs of one component and inputs of others are defined. A wiring diagram showing the connections defined in the deck is given in Figure 4.3.1. Independent (regressor) variables include wet and dry bulb temperatures, T_{wb} and T_{db}, chilled water return temperatures entering the chiller evaporators, $T_{\mathrm{chws\,\#3}}$ and $T_{\mathrm{chws\,\#4}}$, the chilled and condenser water mass flow rates $\dot{m}_{\mathrm{chw\,\#3}}$, $\dot{m}_{\mathrm{chw\,\#4}}$, $\dot{m}_{\mathrm{cw\,\#3}}$ and $\dot{m}_{\mathrm{cw\,\#4}}$ and the turbine inlet steam pressure, p_{in}. The independent variables are indicated by a bold line and the dependent variables by a thin line. The dashed lines indicate control variables, defined separately from independent and dependent variables when used in optimal supervisory control analysis. However, for the purposes of parameter estimation, the control vari-

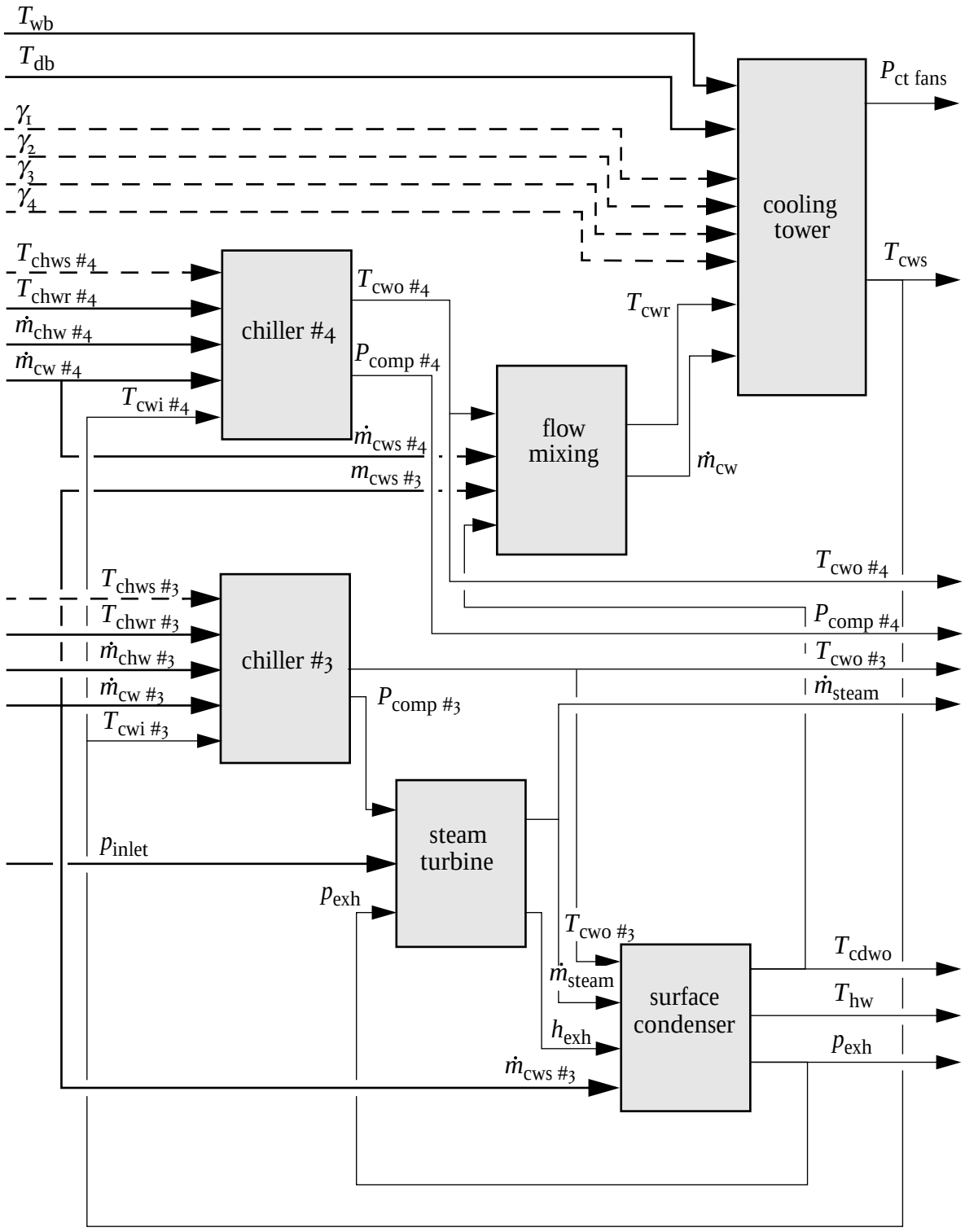

FIGURE 4.3.1: Walnut Street TRNSYS model wiring diagram showing input and output connections of the component variables.

ables are considered independent variables. Control variables include the discrete fan speeds for the individual cooling tower fans γ_1, γ_2, γ_3 and γ_4 and the chilled water supply temperatures, $T_{\text{chws \#3}}$ and $T_{\text{chws \#4}}$.

All outputs of each component are dependent variables. Chiller output variables include compressor power, P_{comp}, and condenser water outlet temperature, T_{cwo}. Dependent variables from the steam turbine component include steam mass flow rate $\dot{m}_{\text{steam}}$ and steam exhaust enthalpy, h_{exh}. Surface condenser outputs include condenser water outlet temperature, T_{cdwo}, hot well water temperature, T_{hw}, and exhaust pressure, p_{exh}. The electric chiller condenser outlet flow and surface condenser outlet flow are mixed before entering the cooling tower and their mixed temperature is designated as the condenser water return temperature, T_{cwr} , and the combined condenser water flow rate is $\dot{m}_{\text{cw}}$. Cooling tower outputs include fan motor power $P_{\text{ct fans}}$ and the temperature of the cooling tower outlet water supplied to the chiller condensers, T_{cws}.

4.4 Component Models

4.4.1 Chiller Model

The TRNSYS chiller component model predicts compressor power consumption, P_{comp} , and leaving temperature of the condenser water, T_{cwr} . Input variables to the chiller model include entering chilled water temperature, T_{chwr} , a set point for the leaving chilled water temperature, T_{chws} , entering condenser water temperature, T_{cws} , and both chilled and condenser water flow rates, $\dot{m}_{\text{chw}}$ and $\dot{m}_{\text{cw}}$. A diagram of the chiller model is shown in Figure 4.4.1.

Mechanistic models of the compressor, evaporator, condenser and expansion device could be combined to represent the chiller model. However, Braun [Bra88] developed an empirical model of a centrifugal chiller that closely matches predictions of mechanistic models. This quadratic model, Equation 4.4.1, is used in the TRNSYS chiller component subroutine. Six parameters (α_{1-6}) are used to relate compressor power, P_{comp}, to a load $\dot{Q}_{\text{load}}$ and temperature difference between leaving condenser and chilled water flows (T_{cwr} - T_{chws}):

$$\frac{P_{\text{comp}}}{P_{\text{design}}} = \alpha_0 + \alpha_1 x + \alpha_2 x^2 + \alpha_3 y + \alpha_4 y^2 + \alpha_5 xy \qquad 4.4.1$$

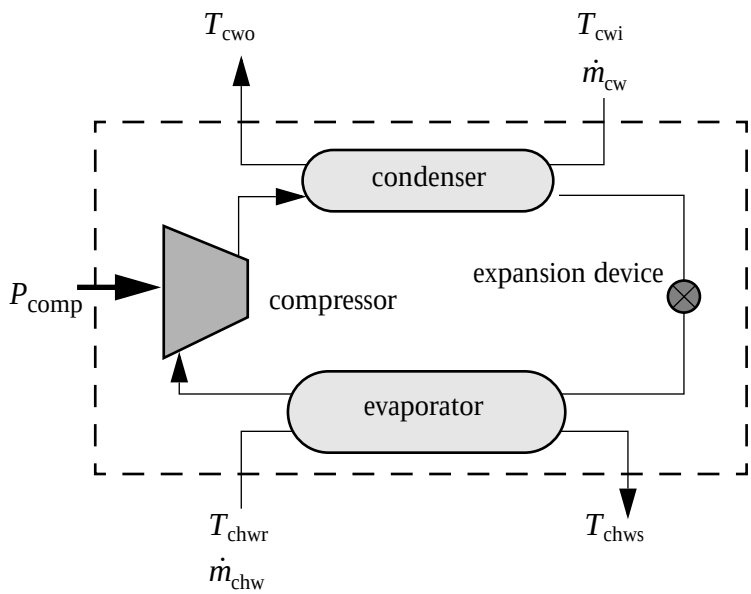

FIGURE 4.4.1: Diagram of TRNSYS chiller component model.

where x and y represent the load and temperature difference, scaled by their design values:

$$x = \frac{\dot{Q}_{load}}{\dot{Q}_{design}} \quad ; \qquad y = \frac{\left(T_{cwr} - T_{chws}\right)}{\left(T_{cwr} - T_{chws}\right)_{design}} \tag{4.4.2}$$

A mechanical efficiency parameter, η_m represents the fraction of energy input to the prime mover which is actually input to the refrigeration cycle. The sum of compressor energy and load is used along with condenser flow rate and specific heat to determine leaving condenser water temperature, T_{cwr}:

$$\dot{Q}_{condenser} = \dot{Q}_{load} + \eta_m P_{comp} = \dot{m}_{cws} c_{p,cws}\left(T_{cwo} - T_{cwi}\right) \tag{4.4.3}$$

For the electrically driven chiller, P_{comp} represents the electrical energy consumption of the motor. For the steam driven chiller, P_{comp} represents the energy input to the compressor provided by the steam turbine, modelled as a separate component.

4.4.2 Steam Turbine Model

The steam turbine component model uses input and exhaust pressures, along with required power from the chiller component, to determine steam flow rate and exhaust enthalpy. From an energy balance (assuming an adiabatic process), turbine power is the product of the steam mass flow rate and the enthalpy change across the turbine. Turbine power can also be expressed in terms of an isentropic efficiency and the isentropic change in enthalpy from the inlet to exhaust pressure,

$$P_{\text{turbine}} = \dot{m}_{\text{steam}}\ \eta_{\text{s}} \left(h_{\text{in}} - h_{\text{exh,s}}\right) \tag{4.4.4}$$

where the isentropic efficiency is given as the ratio of the actual change in enthalpy to the change if the exhaust steam left with the same entropy as the inlet steam conditions.

For the turbine model, isentropic efficiency is modeled as a linear function of pressure ratio and turbine power,

$$\eta_{\text{s}} = \beta_0 + \beta_1 \left(\frac{p_{\text{in}}}{p_{\text{exh}}} \frac{1}{p_{\text{r,scale}}} \right) + \beta_2 \left(\frac{P_{\text{turbine}}}{P_{\text{scale}}} \right) \tag{4.4.5}$$

where $p_{\text{r, scale}}$ and P_{scale} are used to scale the pressure ratio and power respectively. Although not a purely mechanistic model derived from theory, manufacturers' curves of turbine efficiency demonstrate a dependence upon the pressure across the turbine and the turbine power. [Hic87] These curves usually show a nonlinear (approximately quadratic) dependence; however, here it is assumed that a linear model will yield an adequate representation. Modeling isentropic efficiency with a quadratic model would require nine parameters versus three for the linear model. A nine parameter quadratic model used in some preliminary regression analyses was found to contribute to overparameterization problems as discussed in Section 3.4.2.

Given the power required, the inlet steam conditions and the exhaust pressure, Equation 4.4.4 is solved for steam mass flow rate,

$$\dot{m}_{\text{steam}} = \frac{P_{\text{turbine}}}{\left(h_{\text{in}} - h_{\text{exh,s}}\right)} \frac{1}{\eta_{\text{s}}} \tag{4.4.6}$$

and the exhaust enthalpy is then calculated from an energy balance, assuming an adiabatic process:

$$h_{\text{exh}} = h_{\text{in}} - \frac{P_{\text{turbine}}}{\dot{m}_{\text{steam}}} \tag{4.4.7}$$

4.4.3 Heat Exchanger (Surface Condenser) Model

The surface condenser was modeled with a TRNSYS heat exchanger component. A diagram of the turbine and surface condenser combination is shown in Figure 4.4.2. An effectiveness-NTU relationship is used to model the heat transfer. The following effectiveness expression for a condensing heat exchanger was used to model the condensing portion of the surface condenser:

$$\varepsilon = 1 - \exp\left(-\frac{UA}{\dot{m}_{\text{cw}} c_{\text{p}}}\right) \tag{4.4.8}$$

The overall heat transfer coefficient is assumed to be constant although it probably varies with flow rate and fluid temperatures. However, it is reasonable to assume a near constant *UA* in this application as the condenser water flow is nearly constant and the condensing temperature does not vary widely.

The effectiveness is the ratio of actual heat exchanged to the maximum possible heat exchange if the entering condenser water were heated to the saturated steam temperature. However, the steam exhaust enthalpy rather than the saturated steam temperature is available as an input from the steam turbine component. The steam saturation temperature, T_{sat}, is determined from an energy balance

$$\varepsilon \dot{m}_{\text{cw}} c_{\text{p}} \left(T_{\text{sat}} - T_{\text{cdwi}}\right) = \dot{m}_{\text{steam}} \left(h_{\text{exh}} - h_f\left(T_{\text{sat}}\right)\right). \tag{4.4.9}$$

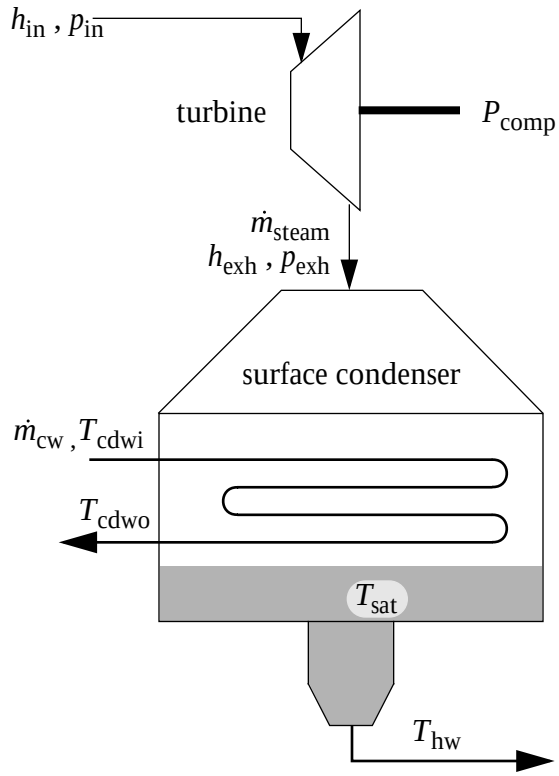

FIGURE 4.4.2: Diagram of steam turbine and surface condenser.

Thermodynamic model equations are then used to obtain the corresponding saturated pressure from the calculated saturated temperature. Although the entering steam may be superheated, it is assumed that the influence of the desuperheating portion of the condenser upon the effectiveness used in Equation 4.4.9 is negligible.

The condensate may be subcooled in the hot well by heat exchange through the vessel walls. This heat loss is usually unwanted as the lost heat must eventually be added at the boiler to change the condensate back into steam. Separate measurements of hot well temperatures are made at the Walnut Street Plant and a model quantifying the temperature drop due to subcooling as a function of water flow rate and condensing temperature is used:

$$T_{sat} - T_{hw} = f_{hw} \exp\left(-\frac{\dot{m}_{steam}}{\dot{m}_{steam,\ norm}}\right)\left(T_{sat} - T_{cwi}\right) \qquad 4.4.10$$

Although the condensate in the hot well will lose heat to the ambient environment, the ambient conditions are unknown. As an approximation, it is assumed that the subcooling in the hot well will be some fraction of the difference between the saturated temperature in the condenser, T_{sat} , and the entering condenser water, T_{cwi}. At high steam flow rates, the condensate leaving the hot well will approach the saturation temperature and will tend toward the entering condenser water temperature.

4.4.4 Cooling Tower Model

The TRNSYS cooling tower component model developed by Braun [Bra88] incorporates an effectiveness/Ntu relationship to model heat and mass transfer transport. The cooling tower effectiveness is defined as the ratio of change in air enthalpy to the maximum possible change in air enthalpy:

$$\varepsilon_{\text{a}} = \frac{h_{\text{a, out}} - h_{\text{a, in}}}{h_{\text{sat}}(T_{\text{cwr}}) - h_{\text{a, in}}} \tag{4.4.11}$$

The maximum possible change in enthalpy would occur if the air flow left the cooling tower saturated at the entering water temperature. For the crossflow cooling tower used in this work, the air side effectiveness is given in terms of the *Ntu* and a ratio of heat capacitance rates:

$$\varepsilon_{\text{a}} = C_{\text{r}}^{-1}\left(1 - \exp\left\{-C_{\text{r}}\left[1 - \exp\left(-Ntu\right)\right]\right\}\right) \tag{4.4.12}$$

The heat capacitance ratio C_{r} is given in terms of the air and entering water mass flow rates and specific heats:

$$C_{\text{r}} = \frac{\dot{m}_{\text{a}}\, c_{\text{sat}}}{\dot{m}_{\text{cw}}\, c_{\text{p,cw}}} \tag{4.4.13}$$

The specific heat associated with the moist air stream, c_{sat} , is given as the change in saturated air enthalpy with respect to temperature. An average value is used where

$$c_{\text{sat}} = \frac{h_{\text{sat}}(T_{\text{cwi}}) - h_{\text{sat}}(T_{\text{cwo}})}{T_{\text{cwi}} - T_{\text{cwo}}} \tag{4.4.14}$$

A general correlation is given for Ntu in terms of the flow rates:

$$Ntu = c\left(\frac{\dot{m}_{\mathrm{cw}}}{\dot{m}_{\mathrm{a}}}\right)^{1+n} \tag{4.4.15}$$

The coefficient c and exponent n depend upon the tower design and are usually determined with performance data from a specific tower.

Outlet water temperature is determined from an energy balance about the cooling tower,

$$\dot{m}_{\mathrm{cw}}\, c_{\mathrm{p,cw}}\left(T_{\mathrm{cwi}} - T_{\mathrm{cwo}}\right) = \dot{m}_{\mathrm{a}}\left(h_{\mathrm{a,\ out}} - h_{\mathrm{a,\ in}}\right) + \dot{m}_{\mathrm{a}}\left(\omega_{\mathrm{a,\ out}} - \omega_{\mathrm{a,\ in}}\right)h_{\mathrm{f,mw}} \tag{4.4.16}$$

where the difference in air enthalpy is determined from Equation 4.4.11 and the right most term in Equation 4.4.16 accounts for the energy associated with the tower makeup water flow, typically one to four percent of the entering water flow rate.

4.5 Parameter Estimation for the Walnut Street Plant Model

4.5.1 Parameter Estimation Methods

The sequential quadratic programming (SQP) minimization algorithm was used for parameter estimation studies with the Walnut Street Plant model. The SQP algorithm yielded some of the best results for the example system regression problem in Chapter 3 and required less computational time than the ODRPACK (Levenburg-Marquardt) algorithm. Ordinary least squares and the determinant criterion (both discussed in Section 3.3) were used to formulate the regression problem. Weighted least squares did not demonstrate any significant advantage over ordinary least squares in the example system regression problem or in preliminary trial runs with the Walnut Street Plant model. Consequently, the weighted least squares method was not used with the Walnut Street Plant model.

Residuals corresponding to various combinations of responses (measured dependent variables) were minimized in comparative parameter estimation runs. Ten measured responses are available: $\dot{m}_{\mathrm{steam}}$, p_{exh}, T_{cdwi}, T_{cdwo}, T_{hw}, $T_{\mathrm{cwi\ \#3}}$, $T_{\mathrm{cwo\ \#3}}$, $T_{\mathrm{cwi\ \#4}}$, $T_{\mathrm{cwo\ \#4}}$, $P_{\mathrm{chiller\ \#4}}$. However, two pairs of temperature measurements are of the same water flows at different points along the flow. The condenser entering water flows for both chillers are from the same common header (the

condenser water supply line from the cooling tower) and should be nearly equivalent in temperature ($T_{\text{cwi \#3}} \approx T_{\text{cwi \#4}}$). Also the water temperature leaving the condenser of chiller #3, $T_{\text{cwo \#3}}$, should be nearly equivalent to the water temperature entering the surface condenser, T_{cdwi}. Removing the two nearly identical responses leaves eight distinct response variables. Linear dependencies among these eight are still possible and comparative runs are made regressing against subsets of six, four, two and one variables.

Parameter estimates are needed for a total of 22 parameters. The parameters and associated equations and component models are listed below in Table 4.5.1.

TABLE 4.5.1: List of parameters used in the composite chilled water plant model.

Parameter	Referenced Equation	Component Model
$\alpha_{0,e}$ $\alpha_{1,e}$ $\alpha_{2,e}$ $\alpha_{3,e}$ $\alpha_{4,e}$ $\alpha_{5,e}$	Equation 4.4.1	electric motor driven chiller
$\eta_{m,s}$	Equation 4.4.3	
β_1 β_2 β_3	Equation 4.4.5	steam turbine
UA	Equation 4.4.8	steam "surface" condenser
f_{hw}	Equation 4.4.10	
$\alpha_{0,s}$ $\alpha_{1,s}$ $\alpha_{2,s}$ $\alpha_{3,s}$ $\alpha_{4,s}$ $\alpha_{5,s}$	Equation 4.4.1	steam turbine driven chiller
$\eta_{m,s}$	Equation 4.4.3	
c n V_{max}	Equation 4.5.2	cooling tower

Two modeling approaches were used to formulate parameter estimation problems. In one approach, a composite model of the interconnected components was used to find estimates for all twenty two parameters. Although this is a straight forward approach, it requires the solution of a large multidimensional nonlinear optimization problem that is potentially both difficult to solve and computationally expensive. In the other approach, the dimension of the optimization problem was reduced by formulating parameter estimation problems for individual components. For example, the cooling tower parameters can be estimated using only the cooling tower model and data for the inlet and outlet flows.

In cases where not all inputs of an individual component have measured data available, its model parameters cannot be estimated independent of other components. For example, the steam turbine model requires a power input to calculate steam mass flow rate requirements but the shaft power between the turbine and the chiller compressor is not measured. Although parameter estimates using an individual component may not be possible, a subsystem or collection of additional components in which all inputs are available may be identified. Combining the turbine component model with the chiller model allows the power input to the turbine to be calculated via the chiller model from other available measured data. In this application the surface condenser model requires an inlet steam enthalpy input which is also not measured. Therefore, the surface condenser is combined with the turbine and chiller components to form a subsystem for which all inputs have measured data. A diagram of the three component subsystem is shown in Figure 4.5.1.

Parameter estimation runs were made using both composite and subsystem models while two other aspects of problem formulation and solution were also varied: the scalar function of residuals minimized in the regression and the number of responses used. Problems were solved using ordinary least squares or the determinant criterion. As given in Chapter 3, the use of all available measured (independent) responses can contribute to a more accurate model. However, adding collinear responses is detrimental to the results. Different combinations of responses are used in the runs to compare the effects of using different responses. Table 4.5.2 summarizes the different variations used in the 21 parameter estimation runs.

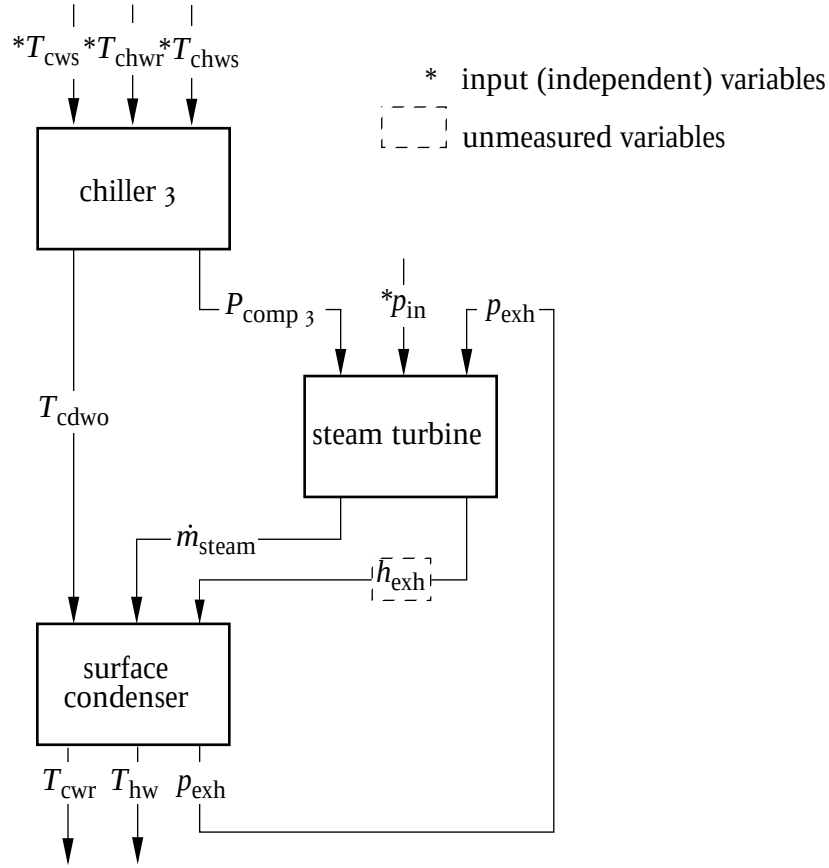

FIGURE 4.5.1: Diagram showing interconnections of the chiller/steam turbine/surface condenser subsystem.

The predictive capabilities were assessed by comparing model predictions to a subset of measured data not used in the fit. All regression runs minimize the residuals over the same 240 observations (Period I) and comparisons of predictive performance are made with model predictions and measured data over another set of 272 observations (Period II). Model accuracy can be assessed by examining plots of the residuals versus the predicted value of the associated response as in Figure 4.5.3. Since the intended use of this model is in optimization (cost minimization) studies, the relative success of each run can be evaluated by comparing the accuracy in predicting variables associated with costs. For optimization studies using the Walnut Street Plant model, steam flow rate and electric chiller power are the primary variables associated with energy costs. Examin-

TABLE 4.5.2: Problem configurations used in parameter estimation runs.

Model Configuration	Subsystem Component(s)	Objective Minimized	Responses Used
Composite		Least Squares	$\dot{m}_{\text{steam}}$, $P_{\text{comp \#4}}$
			$\dot{m}_{\text{steam}}$, $P_{\text{comp \#4}}$, T_{cdwo}, T_{cws}
			$\dot{m}_{\text{steam}}$, $P_{\text{comp \#4}}$, T_{cdwo}, T_{cws}, T_{cdwi}, $T_{\text{cwo \#4}}$
			$\dot{m}_{\text{steam}}$, $P_{\text{comp \#4}}$, T_{cdwo}, T_{cws}, T_{cdwi}, $T_{\text{cwo \#4}}$, T_{hw}, p_{exh}
		Determinant	$\dot{m}_{\text{steam}}$, $P_{\text{comp \#4}}$
			$\dot{m}_{\text{steam}}$, $P_{\text{comp \#4}}$, T_{cdwo}, T_{cws}
			$\dot{m}_{\text{steam}}$, $P_{\text{comp \#4}}$, T_{cdwo}, T_{cws}, T_{cdwi}, $T_{\text{cwo \#4}}$
			$\dot{m}_{\text{steam}}$, $P_{\text{comp \#4}}$, T_{cdwo}, T_{cws}, T_{cdwi}, $T_{\text{cwo \#4}}$, T_{hw}, p_{exh}
Subsystem	Steam Turbine-Surface Condenser-Chiller	Least Squares	$\dot{m}_{\text{steam}}$
			$\dot{m}_{\text{steam}}$, T_{cdwo}
			$\dot{m}_{\text{steam}}$, T_{cdwo}, p_{exh}
			$\dot{m}_{\text{steam}}$, T_{cdwo}, p_{exh}, T_{hw}
			$\dot{m}_{\text{steam}}$, T_{cdwo}, p_{exh}, T_{hw}, $T_{\text{cwo \#3}}$
		Determinant	$\dot{m}_{\text{steam}}$, T_{cdwo}
			$\dot{m}_{\text{steam}}$, T_{cdwo}, p_{exh}
			$\dot{m}_{\text{steam}}$, T_{cdwo}, p_{exh}, T_{hw}
			$\dot{m}_{\text{steam}}$, T_{cdwo}, p_{exh}, T_{hw}, $T_{\text{cwo \#3}}$
	Electric Chiller	Least Squares	$P_{\text{comp \#4}}$
			$P_{\text{comp \#4}}$, $T_{\text{cwo \#4}}$
		Determinant	$P_{\text{comp \#4}}$, $T_{\text{cwo \#4}}$
	Cooling Tower	Least Squares	T_{cws}

ing residuals associated with steam flow rate and electric power provides a good comparative measure of the fit.

4.5.2 Parameter Estimation Results - Composite Model

Ordinary least squares and the determinant criterion objective functions were both used and are discussed separately below. The number of responses used with the composite model varied between two and eight. The standard deviations of the steam flow residuals and electric power residuals resulting from the different applications are tabulated in Table 4.5.3. Standard deviations of residuals as a percentage of mean steam flow rate and mean power are plotted in Figure 4.5.2. Both methods produced similar results with neither method demonstrating any clear advantage in

producing a better fit. In this case, the determinant criterion did not demonstrate poor performance when compared to least squares as was shown in the example problem in Section 3.5. The only significant difference in the example problem of Chapter 3 is that simulated rather than real measured data were used in the parameter estimation runs. Measurement noise in the simulated data set was relatively small compared to estimated noise in the real data set. For example, steam flow rate residual standard deviation in the simulated data set is 100 kg/hr (0.95% of the mean steam flow rate) and is estimated to be 749 kg/hr (7.0% of the mean steam flow rate) in the real data set. In the limit, as errors in the data approach zero (and assuming an error free model), the determinant of the $R^{\mathrm{T}}R$ matrix at the solution becomes undefined. With small errors, as in the simulated data, the objective function surface given by the determinant criterion may represent a more difficult problem for the minimization algorithm. (See discussion in Section 3.5.7.)

Determinant Criterion

Use of the determinant criterion objective function and four responses yielded the smallest standard deviation in steam flow residuals (1089 kg/hr, 10.5% of mean flow rate) over Period II. The steam flow standard deviation increased using both fewer and more responses. The increase in standard deviation using six and eight responses (1123 [10.8%] and 1599 kg/hr [15.6%] respectively) indicates some amount of collinearity with the added responses. A trial run using all ten measured responses (with known collinearities) caused the run using the determinant criterion to fail, the minimization algorithm never moving from the starting point. Using only steam flow rate and electric chiller power responses to fit the parameters resulted in a steam flow residuals standard deviation of 1380 kg/hr (13.2%).

For electric chiller power predictions with the determinant criterion, using just two responses (steam flow rate and electric chiller power) yielded the smallest electric power residuals (standard deviation of 265 kW, 12.3% of mean power). Using the four, six and eight response sets increased the standard deviation to 364 (16.9%), 581 kW (27.0%) and 900.3 kW (41.8%), respectively.

Least Squares

The smallest steam flow residual standard deviation using ordinary least squares was obtained using only steam flow rate and electric chiller power responses (1161 kg/hr [11.1%]). Using four, six

TABLE 4.5.3: Walnut Street Regression Results

estimation method[1]	no. responses used[2]	data set[3]	sum of squared residuals, all responses (scaled)	standard deviation of steam flow residuals (kg/hr)	standard deviation of electric power residuals (kW)
ordinary least squares	two	F	19764[B]	1170.3[C]	219.0[B]
		P	29060[B]	1160.9	249.6B
	four	F	26960	1450.2	258.8
		P	31957[C]	1434.9	296.8
	six	F	31785	1576.7	278.7
		P	39226	1615.7	313.8
	eight	F	28144	1469.9	243.7
		P	36792	1568.7	264.2[C]
determinant criterion	two	F	22662[C]	1301.9	243.0[C]
		P	32994	1380.0	264.7
	four	F	30184	1154.9[B]	345.7
		P	38009	1089.2[B]	363.9
	six	F	27732	1319.7	353.2
		P	44282	1122.7[C]	581.0
	eight	F	195325	1831.7	608.7
		P	294856	1599.4	900.3
[4]sub-system		F	17558[A]	1129.0[A]	185.3[A]
		P	11063[A]	867.3[A]	127.3[A]

1 Estimation Method: Ordinary least squares or determinant criterion

2 Number of responses used in objective function:

Eight– p_{exh}, m_{steam}, T_{cdwi}, T_{cdwo}, T_{hw} , T_{cws}, $T_{cwo\ \#4}$,$P_{comp\ \#4}$

Six– $\dot{m}_{steam}$, T_{cdwi}, T_{cdwo}, T_{cws}, $T_{cwo\ \#4}$, $P_{comp\ \#4}$

Four– $\dot{m}_{steam}$, T_{cdwo}, T_{cws} , $P_{comp\ 4}$

Two– $\dot{m}_{steam}$, $P_{comp\ \#4}$ $\dot{m}_{steam}$

3 Data set: F – the set of data used in the fit (Period I). P - another series of data not used in the fit (Period II).

4 Subsystem - Results from using parameter estimates found in separate subsystem runs.

A, B, C, indicates "best" three results in category F or P over all eight runs and the separate subsystem results listed in the table.

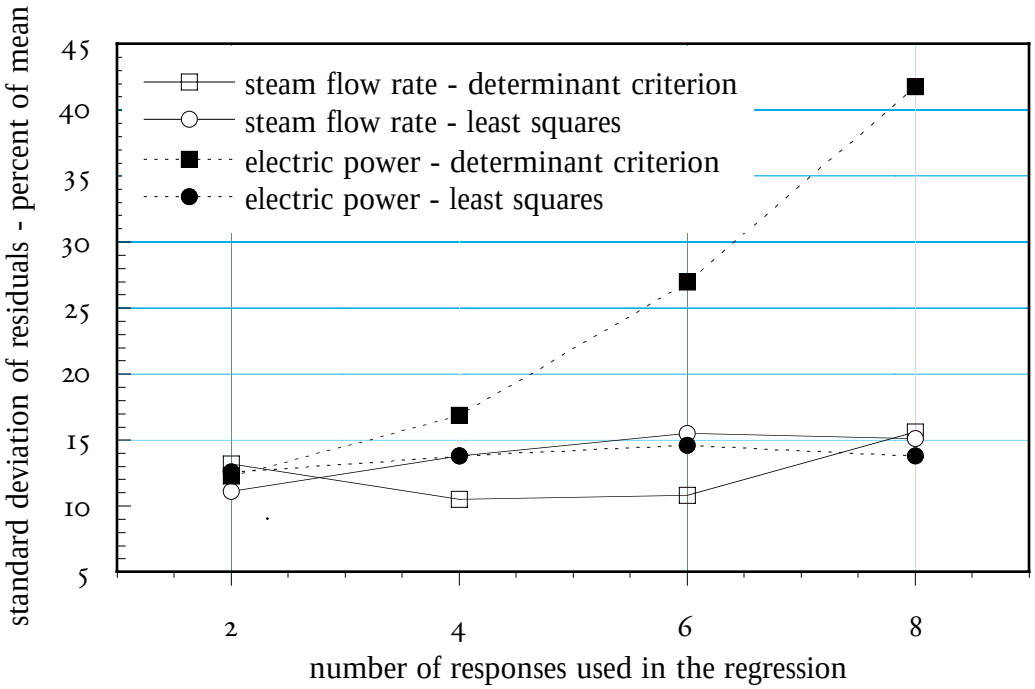

FIGURE 4.5.2: Steam flow rate and electric power residuals standard deviations resulting from applying the determinant criterion and least squares with various responses.

and eight responses yielded slightly increased standard deviations (1435 [13.8%], 1611 [15.5%] and 1569 kg/hr [15.1%] respectively). Although the best runs from both the determinant criterion and ordinary least squares appications had similar results, their parameter estimates were different, demonstrative of large variance and some amount of overparameterization in the model.

Using ordinary least squares with just the steam flow rate and electric chiller power responses produced the smallest standard deviation in electric chiller power residuals (250 kW [12.6%]). Using four, six and eight responses increased the standard deviation (297 [13.8%], 313 [14.6%] and 296 kW [13.8%] respectively).

The best number of responses using either the determinant criterion or least squares is different for the steam flow rate and electric chiller power predictions (two responses yield the best predictions in electric chiller power vs. four responses for steam flow rate.) The argument for improving the model by adding more independent responses appears to be contraindicated considering the electric power predictions. However, responses other than electric chiller power and

electric chiller leaving condenser water temperature are nearly independent of the electric chiller component model parameters. Adding any response other than these two essentially weakens the objective function's (e.g. sum of squared residuals) dependence upon electric chiller model parameters and consequently results in poorer predictions. As discussed in Section 4.5.3 below, breaking out the model components to use in separate regression runs significantly improves the fit.

4.5.3 Parameter Estimation Results - Individual Components and Subsystems

Steam Turbine/Surface Condenser/Chiller

Estimation runs for the separate subsystems were also made. The steam turbine/chiller/surface condenser subsystem parameters were estimated using both ordinary least squares and the determinant criterion formulations with various responses. The smallest residuals in steam flow rate predictions using the subsystem model were significantly lower than those using the composite system. Ordinary least squares with three responses (steam flow rate, surface condenser outlet water temperature and chiller condenser outlet water temperature) produced the smallest steam flow rate residual standard deviation of 749 kg/hr [7.2%]. The determinant criterion with an additional response (hot well temperature response) yielded similar results with a standard deviation of 778 kg/hr [7.5%]. For this subsystem, there was no clear advantage between ordinary least squares and the determinant criterion methods.

Electric Chiller

The electric chiller component model has two outputs: chiller power and leaving condenser water temperature. Solving the ordinary least squares problem using power as the only response resulted in an electric power residuals standard deviation of 133 kW [6.2%] while using both power and condenser water outlet temperature as responses resulted in a slightly improved standard deviation of 130 kW [6.0%]. Using power and condenser water outlet temperature with the determinant criterion resulted in an electric power residuals standard deviation of 145.7 kW [6.7%]

Cooling Tower

For the cooling tower, sump outlet temperature is the only output, which negates use of the determinant criterion. Applying ordinary least squares to this model resulted in a standard deviation of 0.5 °C for the outlet temperature residuals.

Composite Model Predictions Using Parameters from Subsystem Results

Compared to results using the composite model, residuals over the predictive period (Period II) were substantially smaller for all dependent variables using the separate subsystem component models. Since the composite model rather than separate subsystem models will be exercised by the optimization algorithm, predictions from the composite model using the better parameters found in subsystem regressions are examined. Predictions with these parameters resulted in a steam flow residual standard deviation of 867 kg/hr [8.3%] and electric power residual standard deviation of 127 kW [5.9%]. Both are substantially better than the best results obtained from using the composite model in solving the parameter estimation problem (1089.2 kg/hr and 249.6 kW, respectively).

Plots of steam flow rate and electric power residuals are shown in Figures 4.5.3 and 4.5.4 respectively. For comparison, the range of the vertical axis in Figure 4.5.3 is the same percentage of mean measured steam mass flow rate as the range of the vertical axis in Figure 4.5.4 is of mean measured electric chiller power. Comparatively, the electric chiller power residuals demonstrate a better fit with a smaller distribution about the zero axis. The electric chiller power residuals are also more uniformly distributed than the steam flow residuals. Underprediction is more likely at higher values of steam flow rate. The better fit of electric chiller power was possible due to the availability of measured data for all input and output variables of the chiller model. This allowed the seven parameters of the electric chiller model to be estimated separately from the rest of the composite plant model.

Because power measurements were not available for the steam chiller model, it was necessary to combine the chiller model with the steam turbine model and the surface condenser model. (A schematic of the subsystem is shown in Figure 4.5.1.) A total of twelve parameter estimates are needed for the subsystem model (seven for the chiller, three for the turbine and two for the con-

denser). The subsystem model represents a more difficult parameter estimation problem because of the greater number of parameters and the set of nonlinear functions used in the three model combination.

A few points demonstrate a significant difference between model predictions and measured data. Some of these large residuals can be attributed in part to having different plant personnel reading and recording measurements over different periods of time. The standard deviations of steam flow and electric power residuals are approximately eight and six percent respectively of the mean values over the predictive period.

4.5.4 Use of Manufacturer's Data for Parameter Estimates

Manufacturer's data for the cooling tower were used to estimate model parameters for comparison with the results derived from actual plant data. The comparison is made to illustrate use of manufacturer's data to predict plant performance in the absence of measured data. Identifying significant differences between manufacturer's predictions and actual performance could also be useful in identifying maintenance problems in the plant, such as excessive fouling of heat transfer surfaces or excessive restrictions in flow paths.

Graphs showing water outlet temperature as a function of inlet temperature and outdoor wet bulb temperature were provided by the manufacturer. Three graphs gave tower performance at 90, 100 and 110 percent of design water flow. For a given wet bulb temperature and difference in water temperature across the cooling tower, the tower leaving water temperature is read from the graph. All manufacturer's graphs assumed a constant air flow rate with all fans operating at full speed. The graphical data were digitized and translated to tabular data for use in the estimation runs.

In the cooling tower model, two parameters are required. *Ntu* is given in terms of the relative air and water flow rates and two parameters *c* and *n*.

$$Ntu = c\left(\frac{\dot{m}_{\mathrm{cw}}}{\dot{m}_{\mathrm{a}}}\right)^{1+n} \tag{4.5.1}$$

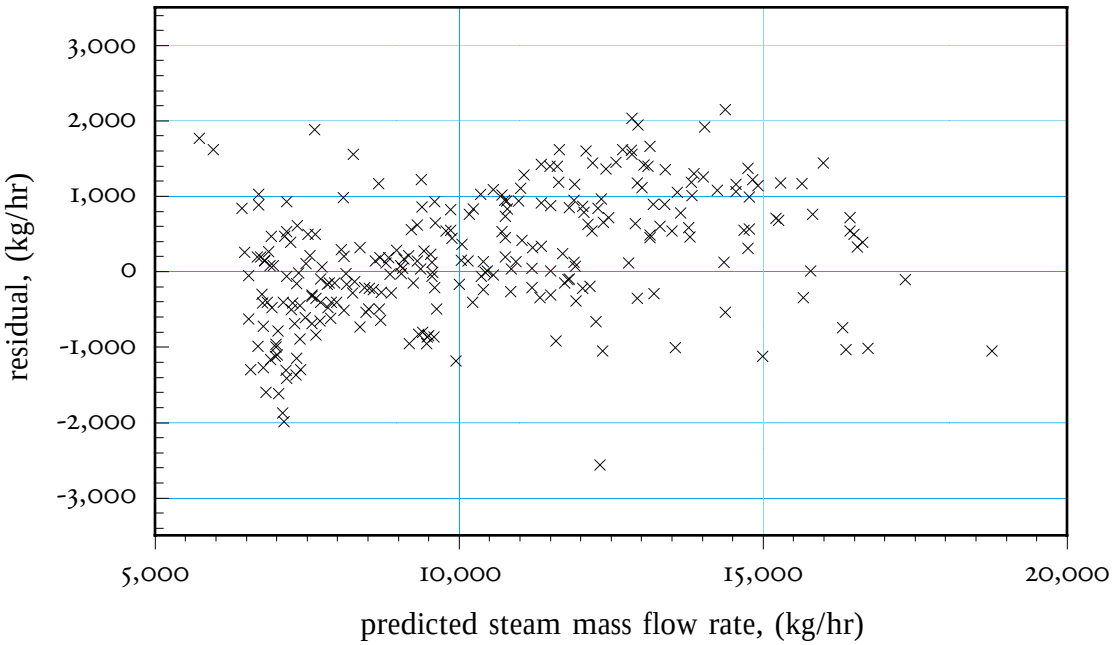

FIGURE 4.5.3: Steam mass flow rate residuals from composite model predictions using parameters estimated from subsystem component models.

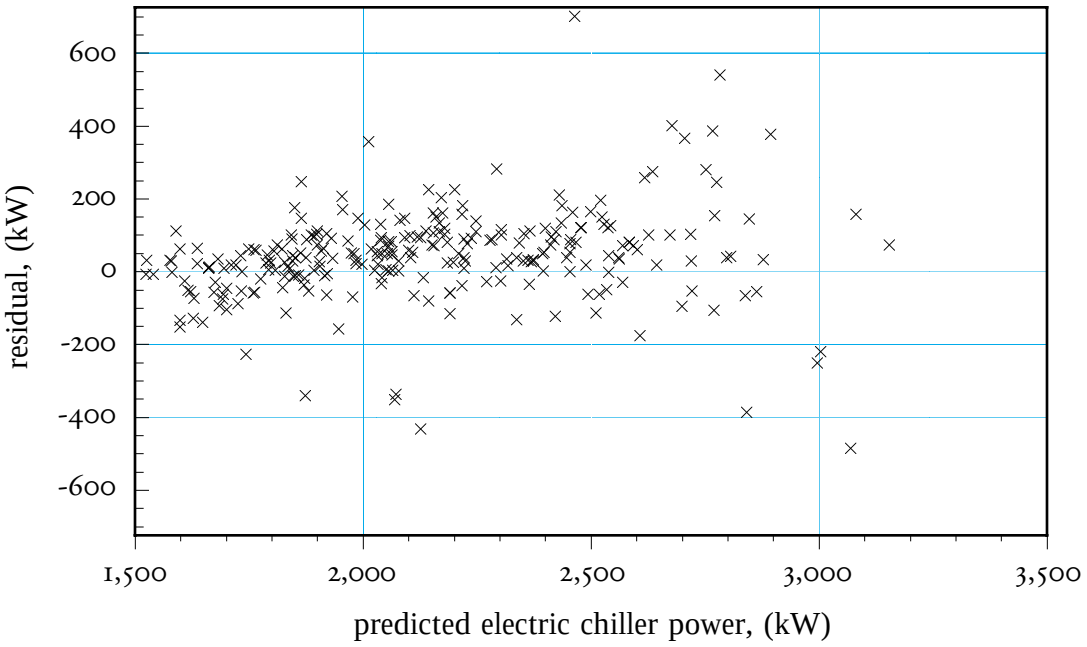

FIGURE 4.5.4: Electric chiller power residuals from composite model predictions using parameters estimated from subsystem component models.

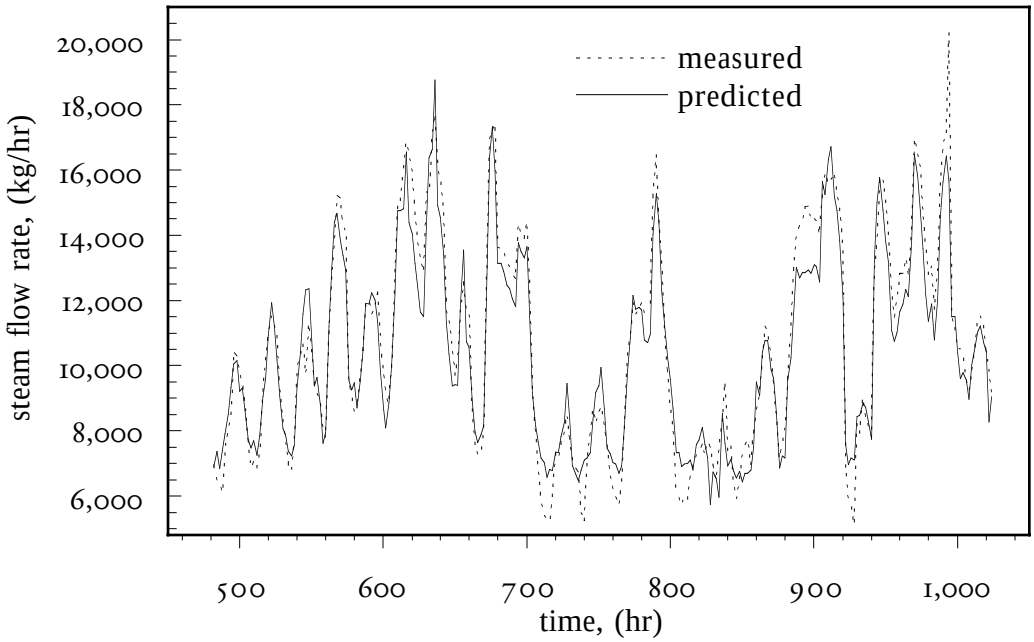

FIGURE 4.5.5: Measured and predicted steam mass flow rate with parameters estimated using subsystem component models.

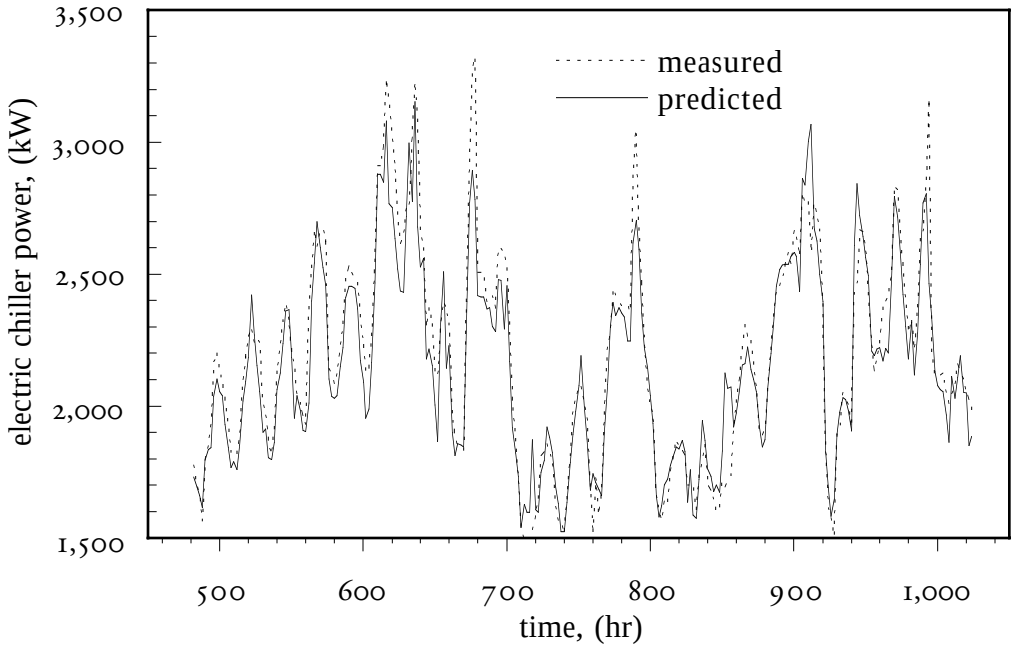

FIGURE 4.5.6: Measured and predicted electric chiller power with parameters estimated using subsystem component models.

However, three model parameters were estimated in the comparative runs. For both manufacturer's and measured data, the air flow rate is only given as a fraction of full flow, therefore the *Ntu* relationship was altered to be a function of fractional flow rate, f_{air} and a third parameter, maximum volumetric flow rate V_{max}.

$$Ntu = c\left(\frac{\dot{m}_{\text{w}}}{\rho_{\text{air}} V_{\text{max}}\ f_{\text{air}}}\right)^{n+1} \tag{4.5.2}$$

For accurate predictions of *Ntu* under varying air and water flow rates, the data used in estimating the two parameters should also include a range of flow rates. Flow rate data available from the manufacturer varies over a smaller range than that recorded at the plant. In the plant data, tower air flow rate is varied as the fans are sequenced on and off, but in the manufacturer's data, air flow rate was assumed to be constant at the maximum possible rate.

The cooling tower model has only one dependent variable, water outlet temperature; therefore the ordinary least squares formulation of the parameter estimation problem was applied. Independent (input) variables include air and water flow rates, water inlet temperature and outdoor dry and wet bulb temperatures. Parameter estimates resulting from both manufacturer's and measured data are given in Table 4.5.4.

TABLE 4.5.4: Estimated Cooling Tower Parameters

parameter	Manufacturer's Data	Measured Data
c	2.423	1.355
n	-3.191	-0.658
V_{max}	14.573	12.895

A comparison of residuals over the Period II data is shown in Figures 4.5.7 and 4.5.8. Residuals resulting from parameter estimates using measured data have a standard deviation of 0.497 °C and mean of 0.17 °C, while those from using manufacturer's data have a standard deviation of 0.661 °C and mean of 0.72 °C. Temperature predictions versus measured data are compared in Figures 4.5.9 and 4.5.10. As can be expected, the parameters estimated from the measured data

result in smaller residuals than those resulting from regression with the manufacturer's data. Predictions resulting from manufacturer's data show better tower performance (lower outlet temperatures) than demonstrated in the measured data. The differences between predictions resulting from the two data sets appear relatively small. However, using the parameters from manufacturer's data with the composite model introduced greater error in both steam and electric power predictions. Comparative results are given in Table 4.5.5. The positive mean values of residuals correspond to underpredicting steam flow rate and power.

TABLE 4.5.5: Estimation Results Using Manufacturer's and Measured Data

Predicted Variable	Using Cooling Tower Parameters from Manufacturer's Data		Using Cooling Tower Parameters from Measured Data	
	standard deviation	mean	standard deviation	mean
steam flow rate (kg/hr)	1231.4 (11.6%)	592.3 (5.6%)	867.3 (8.3%)	210.4 (2.0%)
electric power (kW)	209.2 (9.5%)	111.9 (5.1%)	127.3 (5.8%)	43.9 (2.0%)

4.5.5 Parameter Estimation Summary

This chapter presents an approach for creating and evaluating predictive models of chilled water plants for use in optimization studies. A chilled water plant model was constructed using the TRNSYS simulation program and mechanistic component models. Various multiresponse regression techniques were explored in solving the parameter estimation problem. The influence of using different sets of response variables in the estimation problem was also investigated. Using more responses than just those for which predictions are needed (e.g. cost associated responses) can result in a better predictive model. However, adding all measured responses can be detrimental if collinearity among the responses is present.

For a multiresponse plant model, it is beneficial to separate the system into the smallest subsystems possible before estimating parameters. The subsystem models can be treated as independent parameter estimation problems if measured data are available for all subsystem input variables. Subsystem models may be individual components where all input variables are available as measurements, or a group of interconnected component models when some input measure-

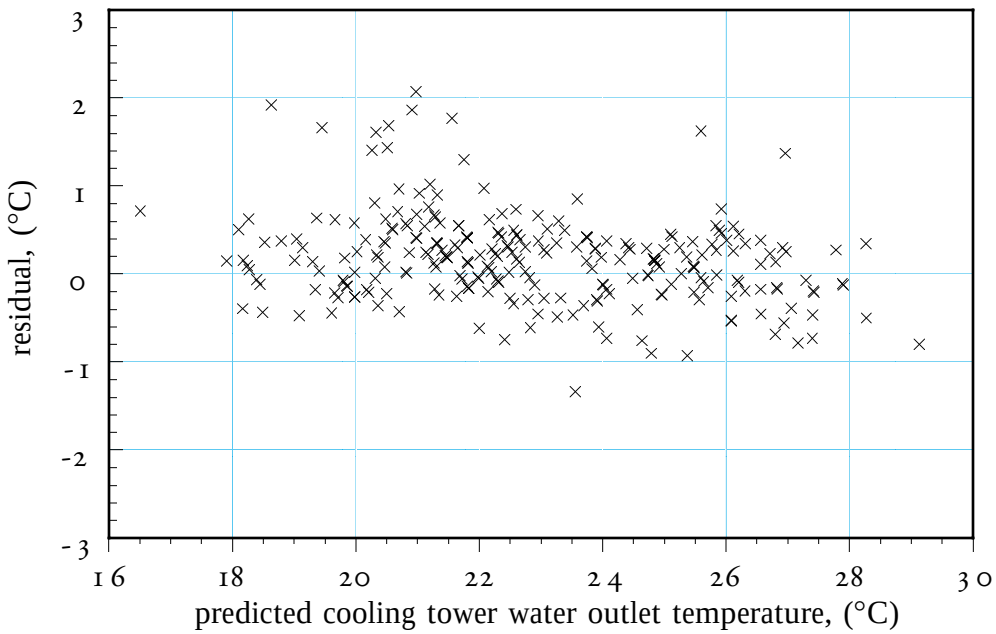

FIGURE 4.5.7: Residual plot for cooling tower water outlet temperature with parameters estimated from measured data.

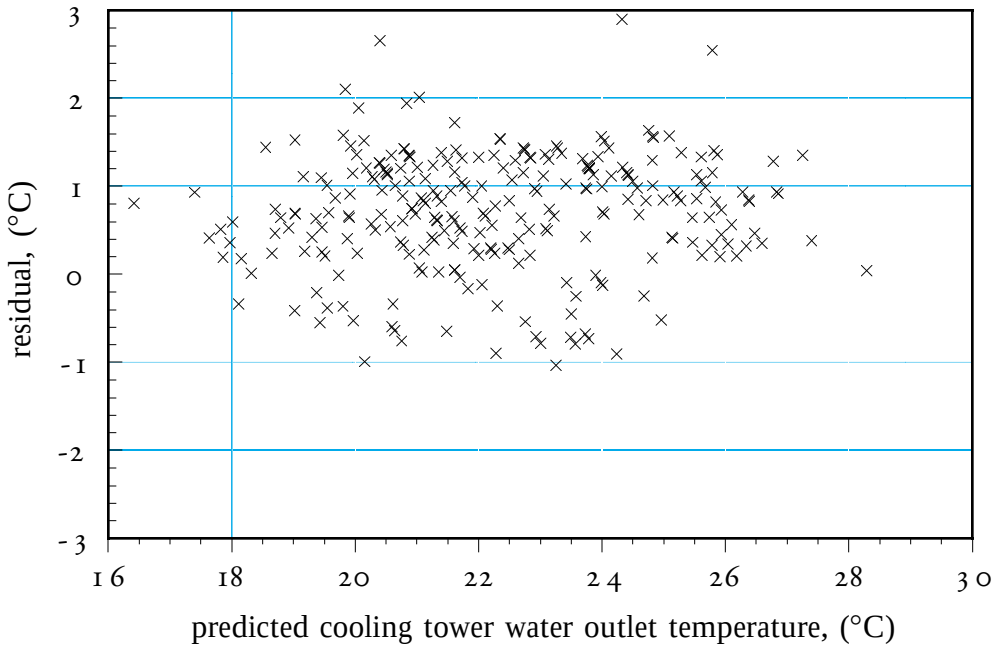

FIGURE 4.5.8: Residual plot for cooling tower water outlet temperature with parameters estimated from manufacturer's data.

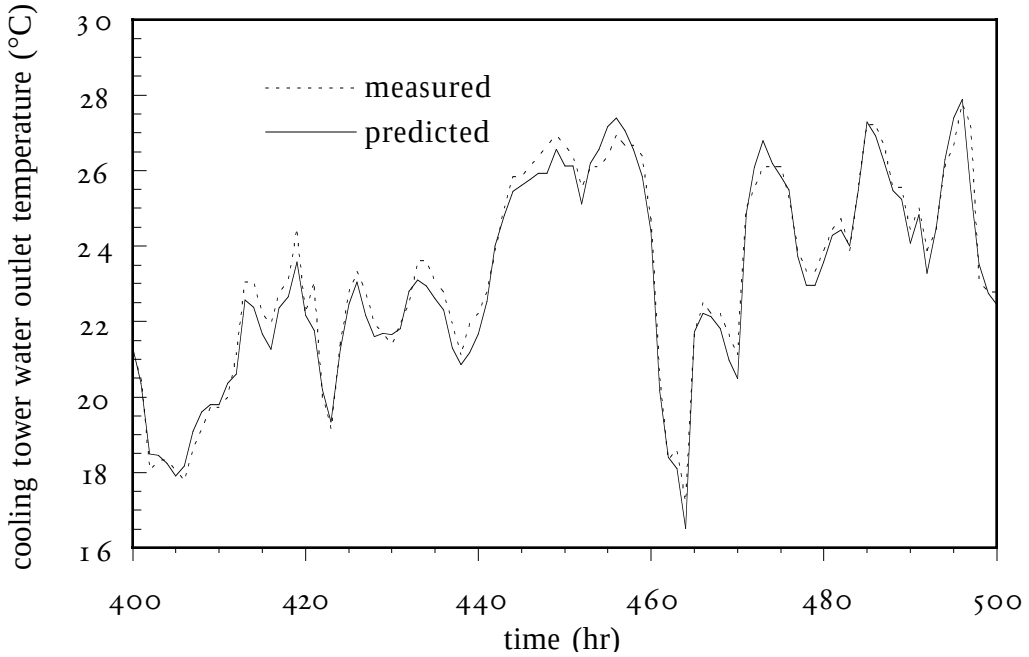

FIGURE 4.5.9: Measured and model predicted cooling tower water outlet temperature using parameters estimated from measured data.

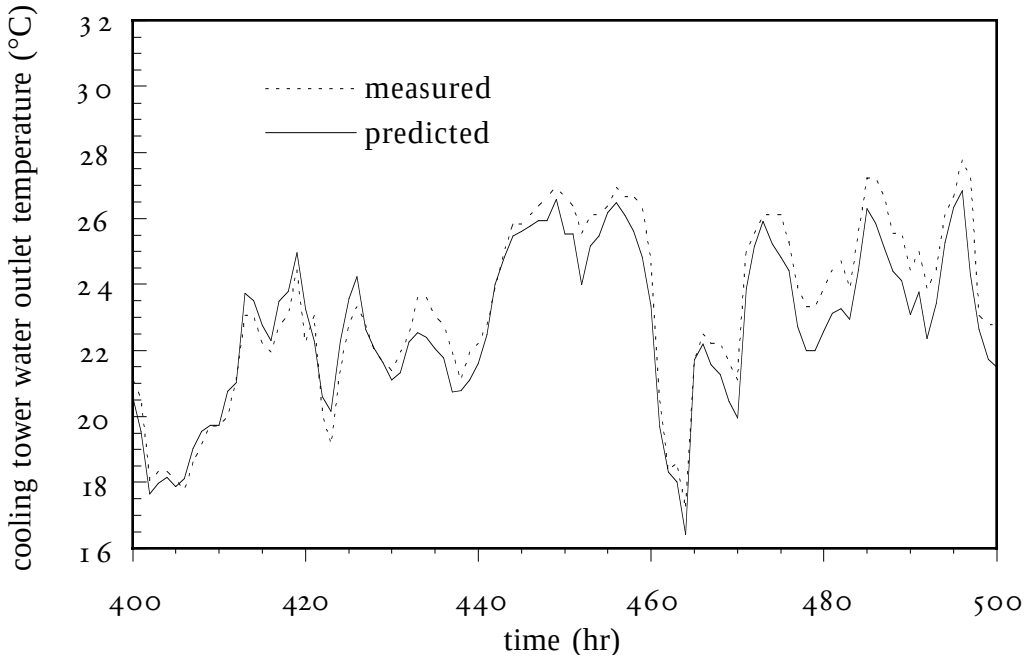

FIGURE 4.5.10: Measured and model predicted cooling tower water outlet temperature using parameters estimated from measured data.

ments are unavailable. In the interconnected subsystem models, input variables without measured data are left connected to the outputs of components that have measured data available for their inputs.

The methods presented were used to build and fit a predictive model of the Walnut Street Chilled Water Plant. Overall, the comparison of team flow rate and electric chiller power predictions with measured data not used in the parameter estimation problem demonstrates a good fit.

CHAPTER 5

Optimal Supervisory Control

With a valid model of the chilled water plant, an optimization algorithm can be applied to determine values of controlled variables that minimize energy costs. In this chapter the optimization problem for a general system is stated and then developed into an optimal supervisory control problem. The simulated annealing minimization method is presented and its implementation into the TRNSYS simulation program described.

5.1 The Optimal Control Problem

Given a chilled water system of n power consuming components, the objective is to minimize energy costs over a period of time. The problem statement is given in Equation 5.1.1 below.

The quantity to be minimized, J, is the integrated cost of energy, summed over all components, for a given time period. The power, p_i, for each of the i components is a subset of the component's output variables, y_i. Energy sources for each component have associated unit costs, $k_i(t)$, which

can be time dependent (e.g. time of day electrical rates). A trajectory of controlled variables, $c(t)$, is sought which minimizes the objective function, J, over a period of time.

$$\underset{c(t)}{\text{minimize}} \quad J = \sum_{i=1}^{n} \int_{t_0}^{t_f} k_i(t)\ p_i\Big(x_i(t), c_i(t), u_i(t), z_i(t)\Big)\, dt$$

subject to :

$$\begin{aligned}
\dot{x}_i(t) &= h_i\Big(x_i(t), c_i(t), u_i(t), z_i(t)\Big) && \text{state equations} \\
y_i(t) &= f_i\Big(x_i(t), c_i(t), u_i(t), z_i(t)\Big) && \text{output equations} \\
0 &\le g_i\Big(x_i(t), c_i(t), u_i(t), z_i(t)\Big) && \text{inequality constraints} \\
u_i(t) &= H_i\, y && \text{input/output connections} \\
p_i(t) &\in y_i(t) && \text{component power} \\
c_i(t) & && \text{controlled variables} \\
z_i(t) & && \text{uncontrolled variables} \\
k_i(t) & && \text{unit energy costs}
\end{aligned} \qquad 5.1.1$$

Component power is dependent upon the controlled variables as given by a set of state equations and output equations. The state equations represent the behavior of dynamic components, such as thermal storage elements. Output equations model the dependence of the component output variables, y_i (including power, p_i), upon component inputs and the component state. Component inputs may belong to a set of controlled variables, c_i; a set of input variables, u_i, which are outputs of other system components; or a set of uncontrolled variables, z_i. Measurable, external forcing variables such as wet bulb temperature or cooling load are included in the set of uncontrolled variables.

The connections between the inputs of a component and the outputs of others are mapped by an interconnection matrix $H_{i,}$ with elements taking a value of either zero or one. Inequality constraints may limit the feasible region of system operation. These constraints could be, for example, limits on control or output variables. Common constraints for chilled water systems include limits on chilled water temperature and condenser water temperature.

The general cost function given in Equation 5.1.1 does not include all energy associated costs charged by an energy utility. An additional cost is often charged for the highest rate of use or

"peak use" during a billing period. For example, electrical utilities commonly charge for the peak power demand. The optimal control over a billing period of time will depend upon any demand charges during the period. However, demand charges are neglected in the development of the solution to the steady state problem in this chapter. A solution to the optimal control problem including demand charges is discussed in Chapter 6.

5.2 The Steady State Optimal Control Problem

In the technical control literature, *optimal control* usually connotes a transient control problem. For example, a dynamic system may be at a certain state x_o, and a control trajectory $c(t)$ is sought which will drive the system to a desired state, x_d, in the shortest period of time. Or, a control might be sought which drives the system to x_d using the least amount of energy or energy costs. The dynamic problem can be reduced to a static or steady state problem under certain assumptions discussed below. Generally, system control includes any means of influencing a system in order to obtain some desired state or output. However, before considering the steady state approximations, it is beneficial to divide system control into two layers, one of local loop control and the other of supervisory control.

5.2.1 Local Loop/Supervisory Control

Local loop controls typically regulate a system variable by direct manipulation of a control element such as control valves, dampers and electric motors. Feedback controllers are primarily used for local loop control in chilled water systems. For example, consider the control of discharge air temperature from a chilled water coil such as shown in Figure 5.2.1. A local loop controller adjusts the flow rate of chilled water through the coil in order to keep the outlet temperature at a given set point. Changes in the inlet air temperature or air flow rate as well as the chilled water temperature or flow rate will cause the outlet temperature to deviate from the set point. The controller responds to the deviation and changes the valve position, causing an increase or decrease in the chilled water flow rate, which will then cause the discharge air temperature to decrease or increase.

The desired discharge air temperature, or set point, is determined by a supervisory controller. In the context of optimal control as used in this work, the discharge air temperature set point is a controlled variable. It is assumed that the local loop controls are stable and keep the measured

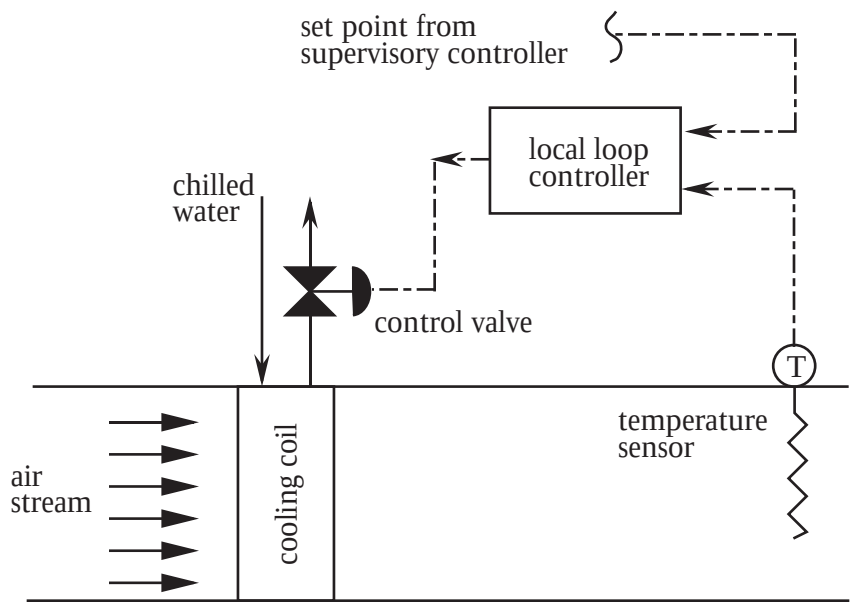

FIGURE 5.2.1: Local loop control of coil discharge air temperature.

variable sufficiently close to the desired set point. The supervisory controller provides set points to local loops controllers. In many cases of chilled water plant control, supervisory control is accomplished with a control computer typically known as an energy management and control system (EMCS). Most EMCSs can make set point changes as well as perform other duties, such as turning equipment on or off according to a programmed schedule, or monitoring energy usage.

5.2.2 The Steady State Approximation

Hackner [Hac85] demonstrated that for systems without significant thermal storage, the system dynamics of local loop controls can be neglected in the determination of optimal supervisory controls. A qualitative means of examining the applicability of steady state optimization to a system is given by Findeisen *et al*. [Fin80] Consider an optimal trajectory of a system state $\hat{x}$ from t_0 to t_1 as shown in Figure 5.2.2a. This state trajectory corresponds to some optimal control trajectory which solves Equations 5.1.1. In an chilled water system, this could be, for example, the exiting water temperature from a chiller. Rather than following the exact optimal trajectory, assume that the optimal control problem is solved and applied over discrete intervals, ΔT, as shown in Figure 5.2.2b. The resulting desired trajectory, x_d, is a step-wise changing function. The way in

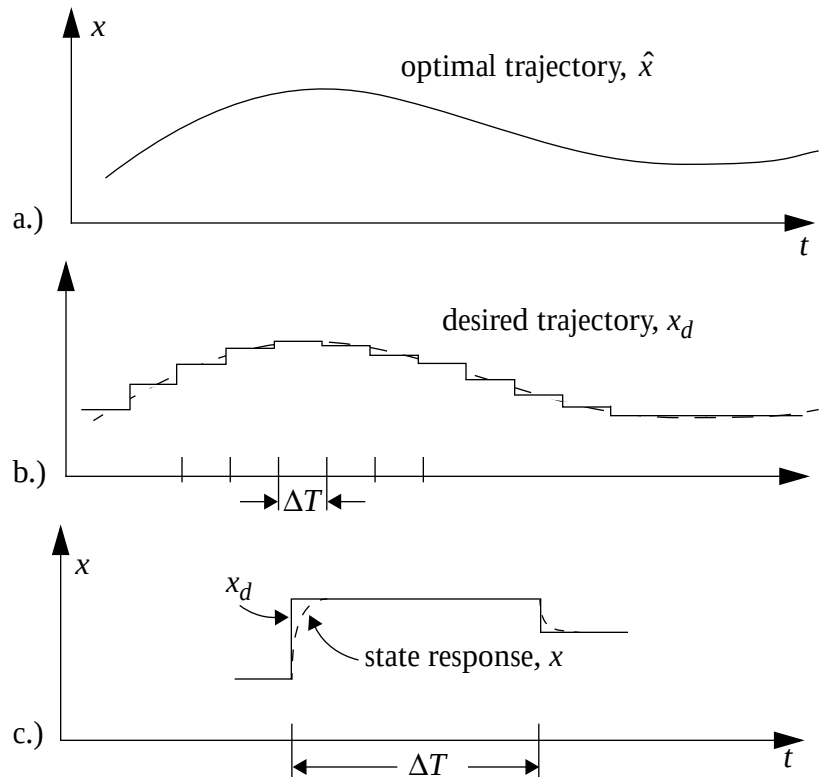

FIGURE 5.2.2: a.) Optimal trajectory of a dynamic system. b.) Discrete approximation to optimal trajectory. c.) System response showing near steady state behavior of system over interval ΔT.

which the leaving chilled water temperature (or state x) changes due to a change in chilled water set point, x_d, illustrates the relative importance of system dynamics. If the response of chilled water temperature to a change in set point is fast relative to a period ΔT (Figure 5.2.2c), the state x can be assumed to be constant over the period, and the optimal control problem solved as a steady state problem.

5.2.3 Application of the Steady State Approximation to a Chilled Water System

For most chilled water systems, the external forcing variables which cause the actual optimal trajectory to vary over time usually vary relatively slowly. For example, wet bulb temperature influences the ability of a cooling tower to reject heat and consequently influences optimal values of controlled variables in a chilled water system, but changes slowly compared to the transient

response of any individual chiller component. Another common external forcing variable is chilled water system load. Throughout the day, load changes tend to be smooth, changing with environmental conditions.

Loads can change fairly quickly, for example, in a morning start-up situation. Minimizing energy costs during a start-up situation is likely the principal case where steady state optimization can yield control far from the optimum. For example, if the building temperature has risen overnight, upon start-up local control loops in the system will begin component operation at conditions corresponding to maximum heat transfer rates. The initial chilled water return temperature will be close to the building temperature and the desired temperature as determined by the steady state optimal control solution will likely be closer to the design temperature (e.g. 7.2 °C [45 °F] for chilled water supply temperature). The local loop controller, which may be controlling compressor motor speed, will respond to this great deviation from set point by running the compressor at its maximum power until the chilled water return temperature decreases.

The energy costs required to bring the building temperature down at the fastest rate possible will exceed the costs of bringing the temperature down over a longer period of time. Also, electrical rates are often based upon a single maximum demand during a billing period. The combined effect of turning on all components at full capacity during a morning start can result in an unnecessarily high electrical demand.

Because the impact of morning start-up upon energy costs is present whether the system is optimally controlled or not, practical means are normally implemented to bring a building's temperature down over a reasonable period of time. An optimal trajectory during morning start-up can be found by solving Equation 5.1.1 if a dynamic model of the building is added to the system. However, for most systems, a simpler means is employed to bring the building temperature down before scheduled occupancy without creating undue energy rate peaks. For example, the chilled water set point may be linearly ramped down over a period of time as determined by an experienced operator or by trial and error. Many EMCSs have algorithms which determine a minimum start-up time without exceeding electrical demand limits. Parameters used in the algorithms are determined from measuring the transient response of the building temperature or chilled water

return temperature. If a schedule for gradually increasing system load during morning start up is in place, then steady state optimal control can be applied to find optimal values of other controlled variables as well during this period.

Assuming a steady state system, the optimal control problem Equation 5.1.1 can be simplified. Time derivatives are zero and the state equations need not be evaluated. What may have originally been described as a state variable can now be classified as either a controlled variable, c, or an output variable, y. As well, c, u, and y are no longer functions of time. The external forcing variables, included in $z(t)$, and the unit energy costs $k(t)$ may still vary with time. However, these variables are considered constant parameters during the time period ΔT. The integrand in Equation 5.1.1 is constant and removed from the integral. The resulting steady state optimal control problem is:

$$\begin{aligned}
&\underset{c}{\text{minimize}} \quad J = \sum_{i=1}^{n} k_i \; p_i\left(c_i, u_i\right)\Delta t \\
&\text{subject to :} \\
&\qquad y_i = f_i\left(c_i, u_i\right) \\
&\qquad 0 \le g_i\left(c_i, u_i\right) \\
&\qquad u_i = H_i\, y \qquad \text{input/output connections} \\
&\qquad p_i \in y_i \qquad \text{component power} \\
&\qquad k_i \qquad \text{unit energy costs}
\end{aligned} \tag{5.2.1}$$

Although the steady state problem requires a solution to a minimization problem just as in Equation 5.1.1, the approaches to solving the two problems are, in practice, quite different. The remainder of this report will primarily address the steady state problem, as it will be used as a foundation for solving the more difficult dynamic optimization problem in future work. Before solving either optimization problems, the output equations and inequality constraints in Equation 5.2.1 or 5.1.1 must be parametrically fit so that they represent the subject HVAC system.

5.3 Optimization Problem

Given parametric models representative of HVAC system components and a means for solving the system of equations, the optimization problem can then be addressed. Only solutions of

the steady state problem (Equation 5.2.1) are considered in this report. Solution methods for the more general dynamic problem, Equation 5.1.1, will be considered in future work.

5.3.1 Classification of the Optimization Problem

In order to have wide application, the output equations and inequality constraints in Equation 5.2.1 should represent any general HVAC system. Although the objective function is a linear combination of certain outputs (e.g. component power), the constraints will, in general, be nonlinear, and can be discontinuous. Also, some variables may only take on discrete or integer values. For example, some fans or pumps may have multiple speeds (e.g. off/low/med/high). For the general case, it is possible for the objective function to have multiple local minima.

The generality of the problem restricts the number of available solution methods. One method for solving optimization problems with both continuous and integer variables is mixed integer nonlinear programming (MINLP). However, this method is not generally applicable to problems exhibiting discontinuities (other than the discontinuity between integers) or multiple local minima. Relatively recently, a global optimization method called simulated annealing has demonstrated success in solving both combinatorial problems (e.g. mixed integer problems) and functions of continuous variables. Simulated annealing's general applicability make it an appealing method for solving the general HVAC system optimization problem.

5.4 Simulated Annealing

5.4.1 Background

The name, *optimization by simulated annealing*, was coined by Kirkpatrick *et al.* who originally proposed the application of an earlier method of simulating a collection of atoms in equilibrium to solving optimization problems. [Kir83] The earlier method was used as a simulation tool to find a configuration of an ensemble of atoms which minimized the total energy at a given temperature. [Met53] From some given configuration, an atom is given a small displacement and the resulting change in system energy, ΔE, is calculated. If the energy has decreased, the new configuration is accepted as the starting point for the next step. If the calculated energy is higher, however, a probabilistic means is used to determine if the point should be accepted. A probability P of the higher energy configuration is given by $P(\Delta E) = \exp(-\Delta E/k_B T)$, where k_B is the Boltzmann

number and T is the ensemble temperature. A random number between 0 and 1 is generated and compared to the calculated probability. If the random number is less than P then the new configuration is accepted as a new starting point. The probability as defined above results in the system evolving into a Boltzmann distribution.

The algorithm was used to investigate what happens to a system of atoms as the temperature is lowered. Of interest is the determination of the ground state and how the atoms may solidify, becoming a crystalline solid or a glass. Experimental methods for exploring the low temperature states of matter involve gentle annealing, where the substance is first melted, and then the temperature slowly lowered. If cooled too fast, the system may get out of equilibrium and form a crystal with many defects or a glass without crystalline order. The algorithm which simulates the process of annealing should result in finding a configuration of atoms with a minimum energy state. The probabilistic means used in arriving at the minimum energy state is the key feature used in the optimization problem. In optimization by simulated annealing, rather than searching for a configuration of atoms which minimizes energy, values of dependent variables which minimize an objective function are found.

Kirkpatrick originally used the method to solve combinatorial problems such as optimization of circuits on a computer chip and the traveling salesman problem. Corana *et al.* modified the simulated annealing algorithm to handle functions of continuous variables. [Cor87] Goffe *et al.* used the continuous variable implementation to compare simulated annealing to conventional algorithms in determining parameters for econometric models. [Gof94] Goffe also introduced extensions to the Corana algorithm which help in reducing execution time.

5.4.2 Methodology

The implemented algorithm explores a region of the range space by generating trial points randomly within a step length v_i from a fixed point, x_i. Individual moves from the fixed point are made in only one coordinate direction at a time. For example, if x is a three dimensional vector, a move is first made in the x_1 direction, then in the x_2 direction and then in the x_3 direction. At each move the objective function, f, is calculated. If the new objective function value, f', represents a decrease, then that point is accepted as the new x_i. The unique feature of the simulated

annealing algorithm is that another check is made before moving to another point. If the objective function increases due to the move, then the "Metropolis criteria" is used, where a probability function analogous to the Boltzmann probability is calculated:

$$p = \exp\left(\frac{f_i - f'}{T_k}\right) \qquad 5.4.1$$

The probability, p, is compared with a random number in the range [0,1]. If the probability is greater than the random number the point is accepted as the new x_i. Consequently, the algorithm has the ability to move out of local minima. At the beginning of the algorithm the "temperature," T_k, is relatively high and many points resulting in higher objective function values may be accepted. But as the algorithm proceeds, T_k decreases incrementally as determined by a user set parameter, and the probability p tends toward zero for any increase in objective function.

The step size, v_i, within which points are generated is adjusted after a given number of cycles of random moves, N_s. The adjustment is made so that approximately half of the generated moves are accepted. If too many moves are rejected, then the trial points are too far from the current point. If too few moves are rejected, the search is being made over too small a region. As the algorithm progresses, the step size decreases due to decreases in the temperature, T_k. After a temperature reduction, the step length that resulted in half of the moves being rejected at the previous temperature will cause more moves to be rejected at the new lower temperature. The step length will then be shortened to bring the ratio back to near 1:1.

A flowchart of the algorithm is shown in Figure 5.4.1. After parameter initialization, random points are generated sequentially in each of the coordinate directions over a number of cycles, N_s. Each point is accepted or rejected according to whether the objective function decreased or the Metropolis criteria discussed above was met. During these moves, any point encountered which results in a lower value of objective function than any previous point is recorded as the optimum. The step length, v_i, is adjusted after N_s cycles such that the ratio of rejected to accepted moves is approximately 1:1. The number of times the step is adjusted, N_T, is another user-defined parameter. After $N_T \times N_s$ cycles, the temperature is reduced by a user-defined factor, r_T, set between 0 and

1. The algorithm will stop if after a number of temperature reductions, N_ε, the optimal value of objective function has not changed more than a tolerance, ε.

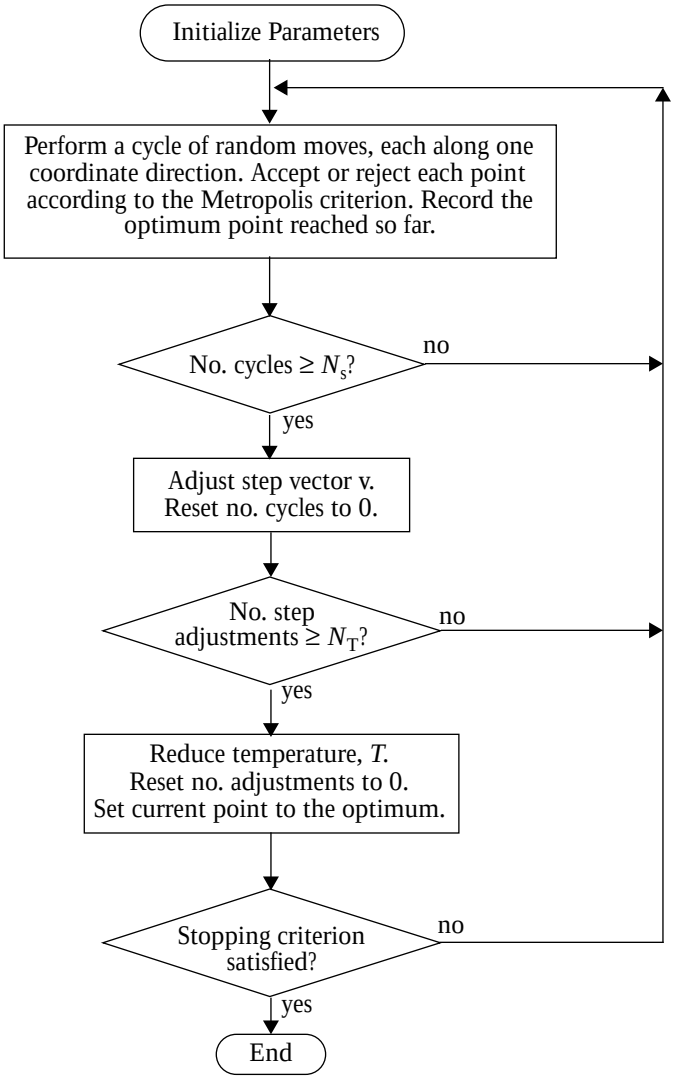

FIGURE 5.4.1: The simulated annealing algorithm given by Corana *et al.* [Cor78]

5.4.3 Implementing Simulated Annealing with TRNSYS

A simulated annealing subroutine written by Goffe *et al.* [Gof94] was modified and incorporated into the TRNSYS simulation package. For the purpose of describing the implementation, TRNSYS may be considered a "black box" function where a set of controlled variables, c, a set of uncontrolled variables, z, and a set of parameters, β, as shown in Figure 5.4.2 together represent

the input; and the resulting sum of component costs, J, represents the output. For the given input variables and parameters, TRNSYS attempts to converge upon a stable set of outputs. It is worthwhile to note that the component models are not generally represented by continuous functions, but are FORTRAN subroutines which may include a number of logical statements that could make the output discontinuous or nonsmooth. Also, there may be constraints built into the subroutines such that outputs never exceed some upper or lower bounds. The discontinuities and nonsmooth relationships between component inputs and outputs limit the choice of optimization algorithms to only the most robust, such as simulated annealing.

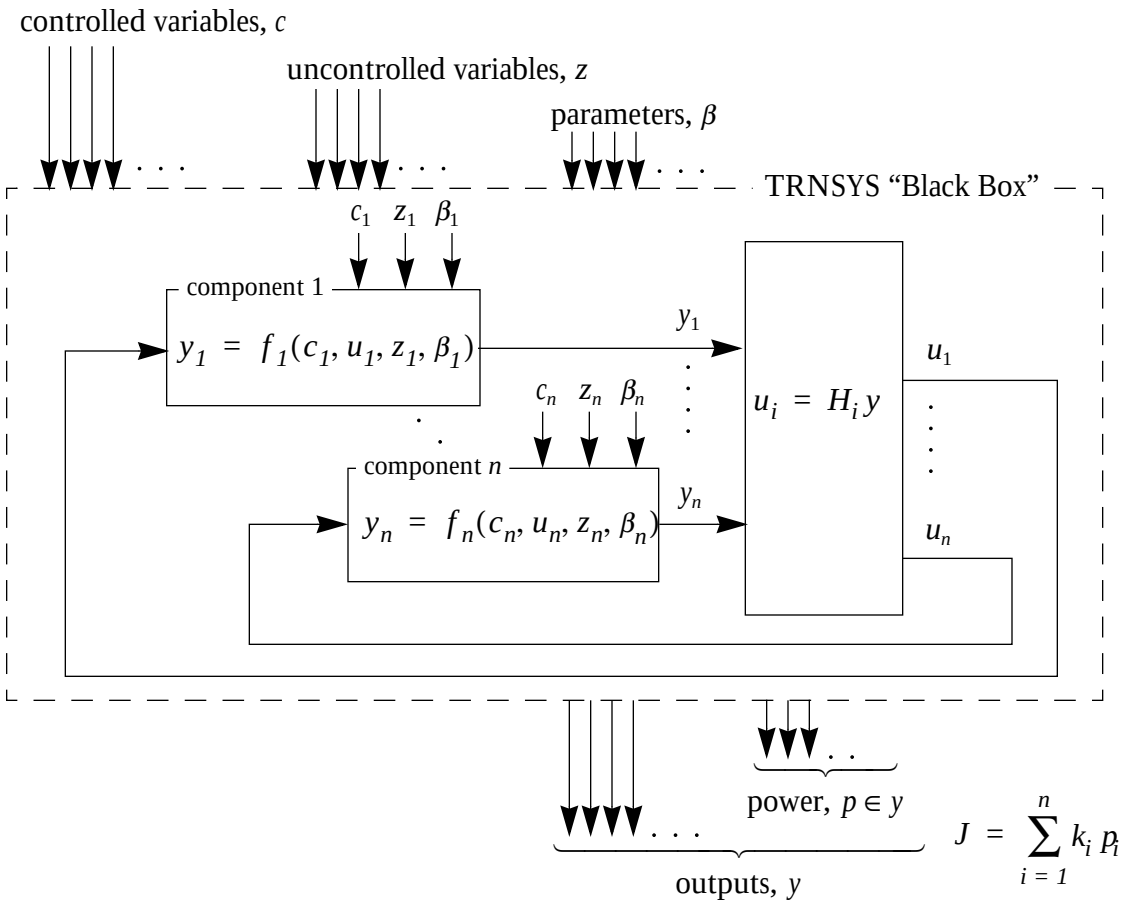

FIGURE 5.4.2: System of HVAC components within TRNSYS.

The simulated annealing program, SIMANN, was originally written as a subroutine which calls a user-defined subroutine for calculating the objective function. Rather than calling an objec-

tive function subroutine, SIMANN returns program control to TRNSYS when an objective function must be evaluated. After TRNSYS converges to a solution, inequality constraints are evaluated. If the constraint is violated, a penalty is added to the objective function to force SIMANN to search only in a feasible region. A flowchart showing the SIMANN implementation with TRNSYS is given in Figure 5.4.3.

5.4.4 Constraints

The relationships between component inputs and outputs given by the component models can be considered *equality constraints,* maintained as TRNSYS converges upon a set of outputs for a given set of controlled and uncontrolled inputs, $y = f(c,z;\beta)$ (For a more convenient representation, let x represent the inputs in general, and assume β constant, i.e. $y = f(x)$). This set of component equations, however, does not constrain the problem in the sense of decreasing the number of degrees of freedom since an output variable, y, is added for each additional equation. The component equations serve to define the functional relationship between the objective function J and the variables subject to control, c.

There may be other constraints which are not representative of a single component. For example, in the application considered in this chapter, the constraint on average or mixed chilled water temperature from all chillers is an operational requirement. The mixed chilled water temperature constraint can be included in the problem formulation by identifying as controlled variables all but one of the chilled water supply temperatures. The remaining one temperature is then calculated from an energy balance so that the mean flow temperature is at its constrained value. The calculated chilled water temperature is constrained by upper and lower bounds corresponding to the warmest and coldest temperature attainable by the chiller. If the calculated temperature is beyond the bounds, a simple barrier function is used where a cost orders of magnitude higher than any possible operating cost is returned to the minimization algorithm.

5.5 Implementation of Optimal Control in a Chilled Water System

With a means for arriving at a set of controlled variables which minimize energy costs in a modeled system, these optimal controls can then be applied in a real system. Control application

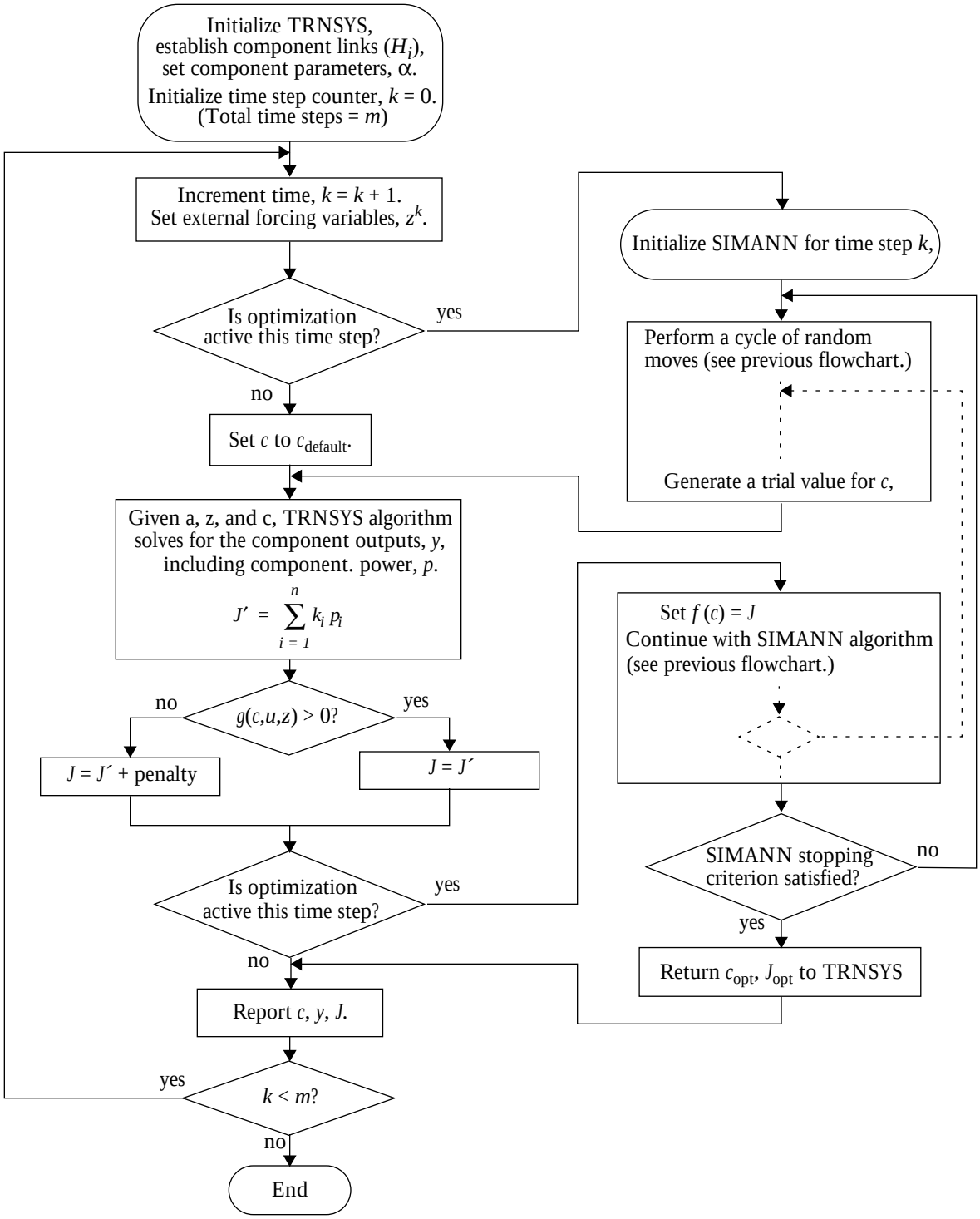

FIGURE 5.4.3: Implementation of SIMANN optimization algorithm with TRNSYS.

may be classified according to how often the parameter estimation and optimization problems are solved. In on-line parameter estimation and control, system parameters are updated after each real system measurement is taken, then the optimization problem is solved with the new parameters, and the resulting optimal set points are applied to the system. In off-line parameter estimation, a fixed set of system data is used to determine representative parameters. For example, the data may have been taken while exercising the real system over a wide range of operating conditions to improve the predictive capabilities of the parametric models. Given a set of parameters β, the optimal control variables, c^*, depend only upon the external, driving variables z (e.g. load, wet bulb temperature). The optimal controls may be found by solving the optimization problem on-line every time a new set of values for z is measured. Alternatively, a model of the dependence of the optimal control variables upon the external variables may be constructed from the results of system simulations. The model could be in the form of equations, graphs (maps), or tables.

There are advantages and disadvantages associated with both on-line and off-line control. Continuously updated parameters found in on-line control may result in a more accurate system model as the parametric models adapt to the current operating conditions. A more accurate system model will yield more accurate optimal control variables. However, the cost associated with installing and maintaining the computational equipment required for on-line control may be substantial. Also, a problem in parametric estimation may arise if the external variables remain nearly constant over an extended period of time. For example, if the parametric estimation problem is used with data taken over a period where the external variables were near constant, the dependence of the model output upon these external variables cannot be discerned.

5.6 Summary

A method for determining values of control variables which minimize energy costs of an chilled water system has been presented. Essentially, the proposed method includes fitting real system data to a parametric model of the subject chilled water system, and then using the parametric model in an optimization algorithm to determine minimum energy costs. An optimization algorithm, simulated annealing, is implemented with the TRNSYS simulation program to determine values of control variables which minimize energy costs.

CHAPTER 6

Optimal Supervisory Control - Walnut Street Plant

The model of the Walnut Street Plant used in the parameter estimation studies in Chapter 4 is used in optimization studies in this chapter. Results from solving the optimization problem with and without demand charges are presented and discussed. In addition, some general optimal strategies for operating the Walnut Street plant are developed.

6.1 Problem Description

The objective is to minimize the system energy costs for the two chillers (one steam driven and one electrically driven), four cooling tower fans, two chilled water pumps and two condenser water pumps. Steam cost is estimated by physical plant personnel to be \$7.74/1000 kg. Electrical costs are dependent upon the time of day of usage. During "peak rate" usage hours (10:00 a.m. through 9:00 p.m. weekdays) the cost is \$0.0440/kW·hr, and the cost is \$0.0264/kW·hr during the "off-peak" hours. An additional electrical demand charge of \$7.00/kW is levied for the highest power demand during on-peak hours in the one month billing period.

System energy costs depend upon the six independent variables and six control variables listed in Table 6.1.1. In the calculations for optimal control, new values of the independent variables are

TABLE 6.1.1: Independent and Control Variables

Independent Variables	T_{chwr}	chilled water return temperature
	T_{wb}	ambient wet bulb temperature
	T_{db}	ambient dry bulb temperature
	p_{inlet}	available steam inlet pressure
	k_{steam}	steam cost
	k_{elec}	electricity cost
	k_{demand}	peak electrical demand charge
Control Variables	$T_{\text{chws \#3}}$	steam chiller (#3) water supply temperature
	$T_{\text{chws \#4}}$	electric chiller (#4) water supply temperature
	γ_1	cooling tower fan #1 speed
	γ_2	cooling tower fan #2 speed
	γ_3	cooling tower fan #3 speed
	γ_4	cooling tower fan #4 speed

taken from the measured data at each hour and input to the model. The optimization algorithm then searches over all values of the control variables for the minimum in total energy costs for that hour.

Certain loads served by the chilled water plant have a high limit on chilled water supply temperature. The water temperature from the plant is constrained to not exceed the limiting temperature. For example, if water flow rates through the individual chillers were equal and the limiting combined water temperature is 4.6 °C, a chilled water temperature of 5.6 °C from one chiller would constrain the temperature from the other chiller to no greater than 3.6 °C. This constraint is applied inside the TRNSYS model where $T_{\text{chws \#4}}$ (maximum) is calculated via an energy balance as a function of the combined chilled water supply temperature and $T_{\text{chws \#3}}$. Since supplying a lower chilled water temperature than the maximum always increases energy costs, the constraint effectively removes $T_{\text{chws \#4}}$ as a control variable. ($T_{\text{chws \#4}}$ is always at its maximum).

The four cooling tower fan motors can individually be run at zero, half, or full speed. Although 81 different combinations of fan speed settings are possible, only nine of these combinations need to be searched. Since fan power increases in cubic proportion to fan speed, the change in power from half to full speed is greater than the power required at half speed. Also, the increase in cooling tower effectiveness is less from half to full speed than from off to full speed. Thus, the combinations having a fan off simultaneously with a fan on at full speed will always use more power and result in less cooling than both fans at half speed. Since all four cells of the cooling tower have equivalent performance, the particular combination or order of operating cells makes no difference. The 72 combinations that have one fan off when one is at full speed are eliminated from the search. The problem was further simplified by using a single control variable (having eight discrete values between 0 and 1) to represent the particular combinations of fan speed.

The resulting optimization problem is a nonlinear function of one continuous variable ($T_{\text{chws \#3}}$) and one discrete variable (fan speed control). The continuous control variable, chilled water supply temperature for chiller $_{\#3}$, $T_{\text{chws \#3}}$, has a lower bound of 3.3 °C (lowest safe operating temperature according to plant operators). The upper bound for $T_{\text{chws \#3}}$ is the warmest water temperature that forces the chilled water temperature out of chiller #4 to its minimum (also 3.3 °C) in order to meet the required combined flow temperature.

6.2 Conventional Control

A sequence of 31 days of data, beginning with July 1, is established as a period for comparing optimal control strategies with the actual control. Costs for conventional operation were estimated using the Walnut Street Plan model and the measured data for the period. In the simulation, the chilled water supply temperatures from both electric and steam driven chillers were set to match the average measured values over the period. The cooling tower fans were set at speeds indicated by the measured data.

The operators' existing strategy for operating the plant is to supply chilled water between 4.4 °C and 6.1 °C (40.0 °F and 43.0 °F). Operators will normally set the chillers' controls to a fixed set point of 4.4 °C and monitor the mixed chilled water temperature leaving the plant. Operators will add an available chiller if the chilled water leaving the plant reaches 6.1 °C. The measured

chilled water supply and return temperatures for both chillers average 4.6 °C (40.3 °F) and 9.30 °C (48.7 °F) respectively for July.

Cooling tower fans are manually controlled by the operators. Generally, fans are added or fan speed increased if the water temperature from the cooling tower exceeds about 21.1 °C (70.0 °F). However, with manual control, fan operation does not tightly follow in response to cooling tower water temperature. Measured data shows all fans on at full speed for cooling tower water temperature above 23.3 °C (74.0 °F), and fans somewhere between all at half speed and all at full speed for temperatures from 17.8 °C to 23.3 °C (64.0 °F to 74.0 °F). There is inconsistent correlation between the operators' choice of fan speed and cooling tower temperature in the 17.8 °C to 23.3 °C range.

A simulation of the plant operating at the measured values of control variables (conventional control) is used as a basis for comparing the costs under optimal control. A plot of estimated steam and electricity costs over the period is shown in Figure 6.2.1. The periodic reduction in electricity costs after every five peaks (five days) is due to the reduced off peak rate of electricity applying during all hours of the weekend. Summing over the month, the steam, electrical and total energy costs are $63,444, $95,034 and $158,478 respectively. Measured chilled water supply temperatures are shown in Figure 6.2.2. Although both chillers had a constant controller set point of 4.4 °C (40.0 °F) over the period, the measured temperatures show some variation. Measured temperature from the electric chiller is more steady over time than that from the steam driven chiller. The apparent noise in the measured temperatures from the steam driven chiller is due more to instability in the control of the chiller than to measurement noise. The mean mixed supply temperature over the period is 4.6 °C (40.3 °F). Cooling tower fan control during the period is shown in Figure 6.2.3. Fan speeds over the period varied between all on at half speed and all on at full speed.

6.3 Optimal Supervisory Control Results

In the optimization calculations, values of the two control variables ($T_{\text{chws \#3}}$ and γ_{ct}) that minimize energy (steam and electricity) costs for each hour are found. The chilled water tempera-

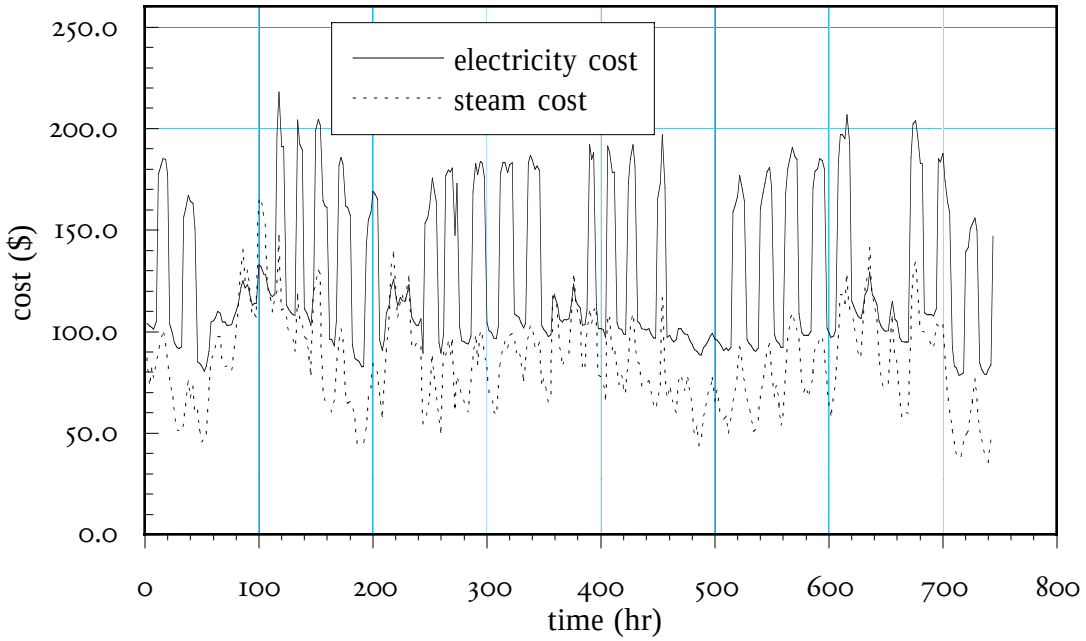

FIGURE 6.2.1: Steam and electricity costs under conventional control.

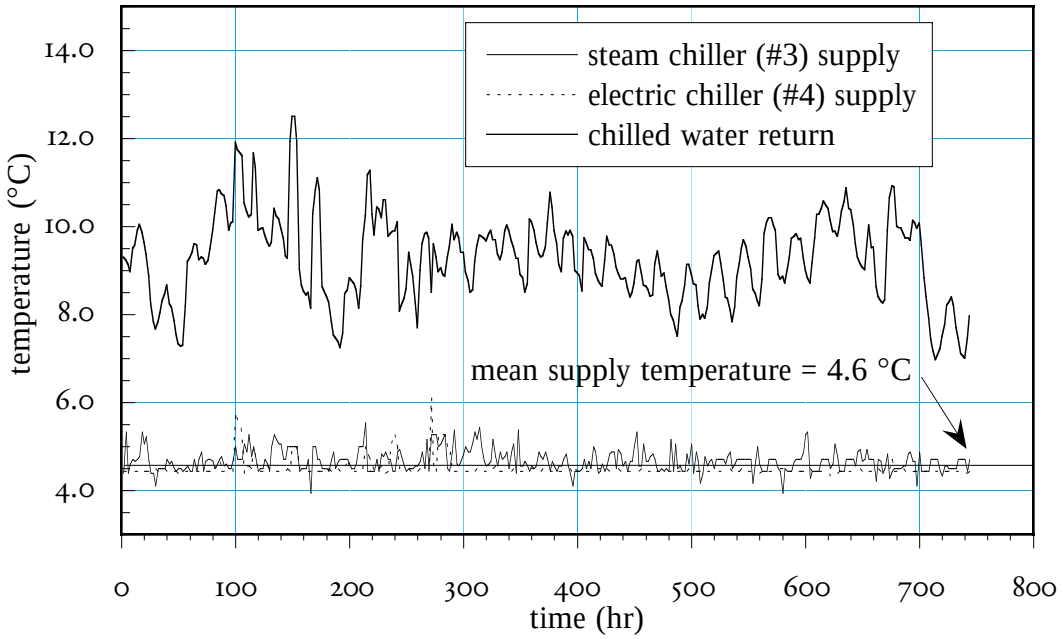

FIGURE 6.2.2: Chilled water return temperature and supply temperatures from the steam and electric chillers (#3 and #4) under conventional control.

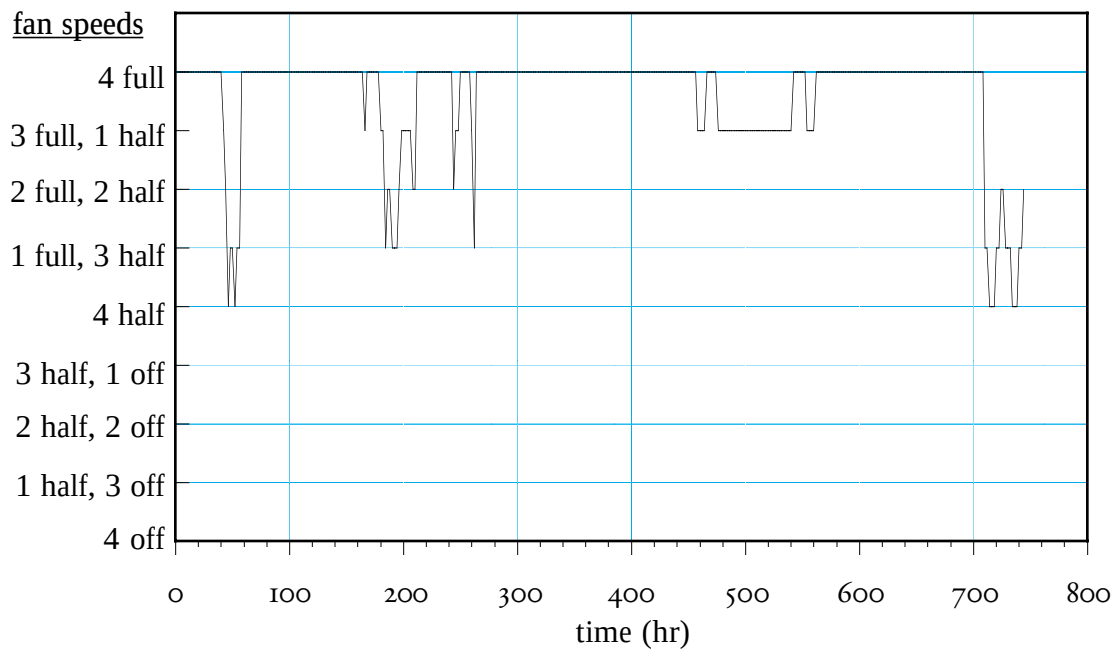

FIGURE 6.2.3: Cooling tower fan speeds under conventional control.

ture from the electric chiller ($T_{\text{chws \#4}}$) is constrained such that the mixed water temperature is at the set point of 4.6 °C (40.3 °F). Over most of the period, optimal control favored using the electric chiller (#4) for the majority of the load.

In Figures 6.3.1 and Figures 6.3.2 optimal chilled water supply temperatures from chiller #3 are plotted against chilled water return temperature. At lower return water temperatures (less than 10.4 °C), the electric chiller is run at its minimum allowable temperature (fully loaded) and the steam chiller takes on the remainder of the load. Figure 6.3.1 includes those points calculated with an electric kW·hr cost of $0.0444 and Figure 6.3.2 includes the points calculated with a cost of $0.0264. The minimum allowable supply temperature for either chiller is 3.3 °C (38.0 °F). The optimum strategy during the higher electric rate period, disregarding demand costs, is to base load the electric chiller (run at minimum supply temperature) and carry the rest of the load with the steam driven chiller except for high loads (chilled water return temperatures above 10.4 °C).

The plots in Figures 6.3.3 and 6.3.4 illustrate that the minimum total cost occurs with either the steam chiller or electric chiller fully loaded. The dependence of total cost upon steam chiller

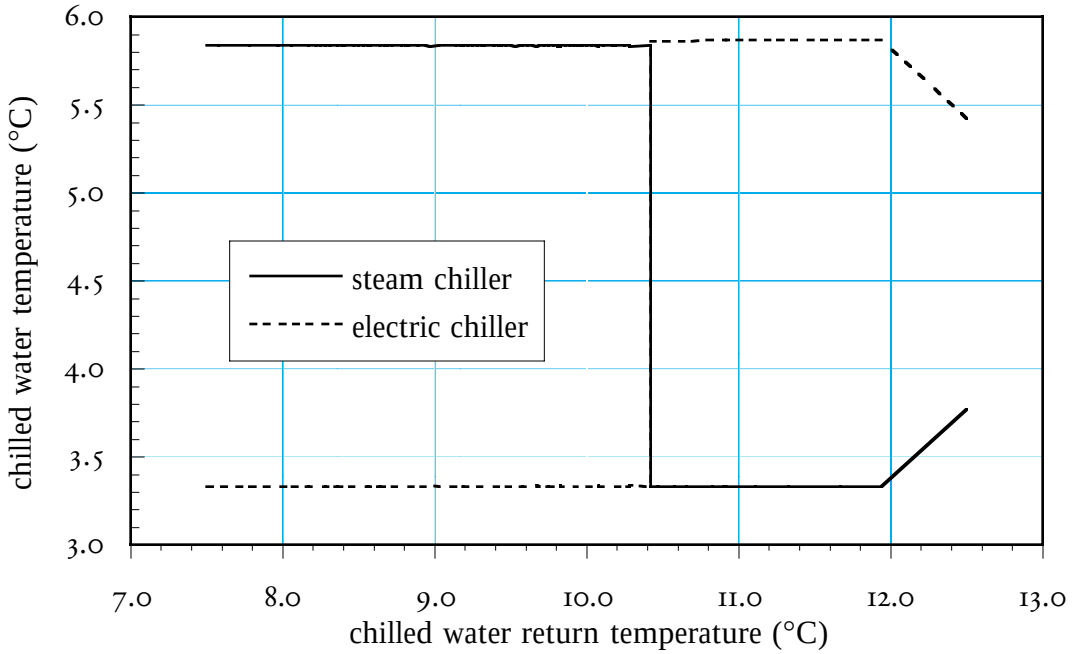

FIGURE 6.3.1: Optimal chilled water temperatures from both chillers as a function of chilled water return temperature. Electric costs are 4.40¢/kW·hr.

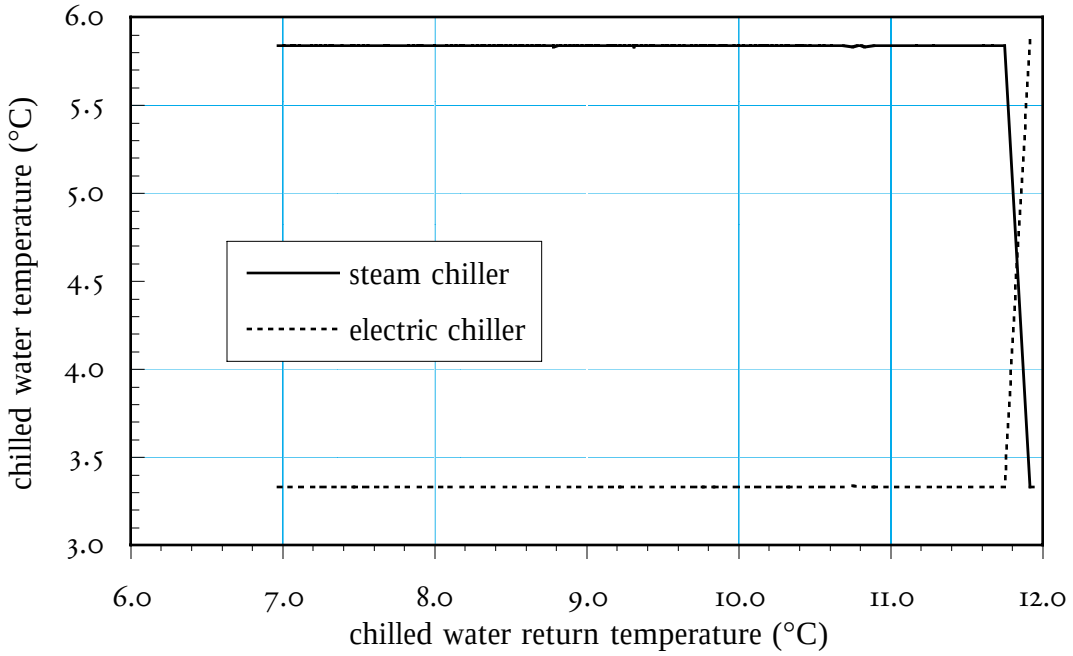

FIGURE 6.3.2: Optimal chilled water temperatures from both chillers as a function of chilled water return temperature. Electric costs are 2.64¢/kW·hr.

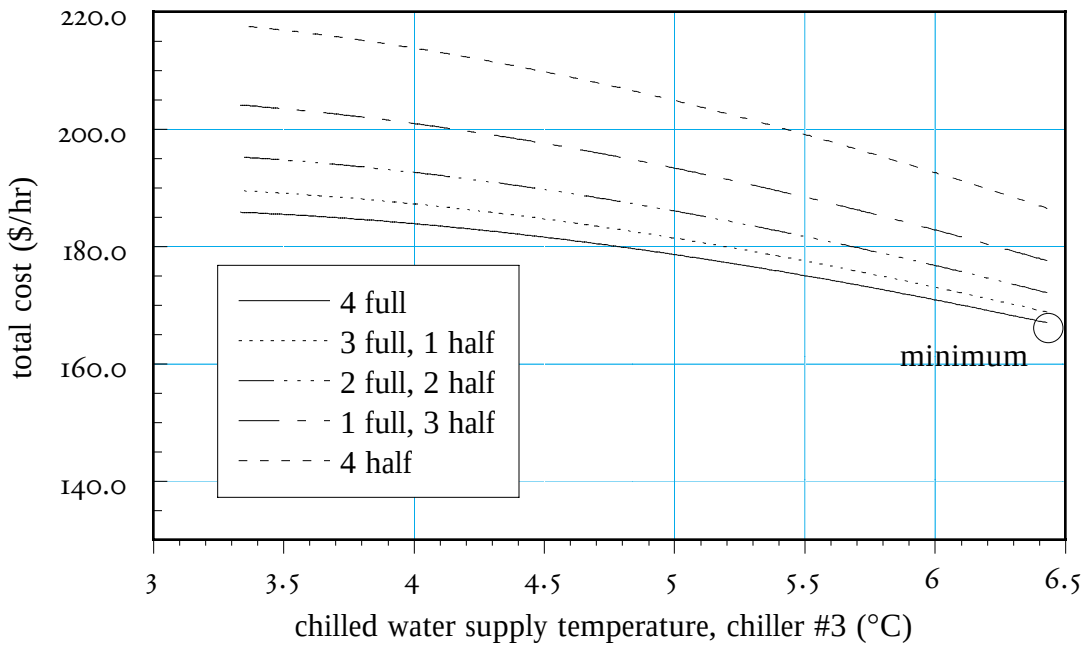

FIGURE 6.3.3: Total cost as a function of $T_{\text{chw \#3}}$ at different cooling tower fan speeds. Independent variables: T_{chwr} = 9.2 °C, T_{wb} = 18.3 °C, k_{elec} = \$0.0264/kW·hr.

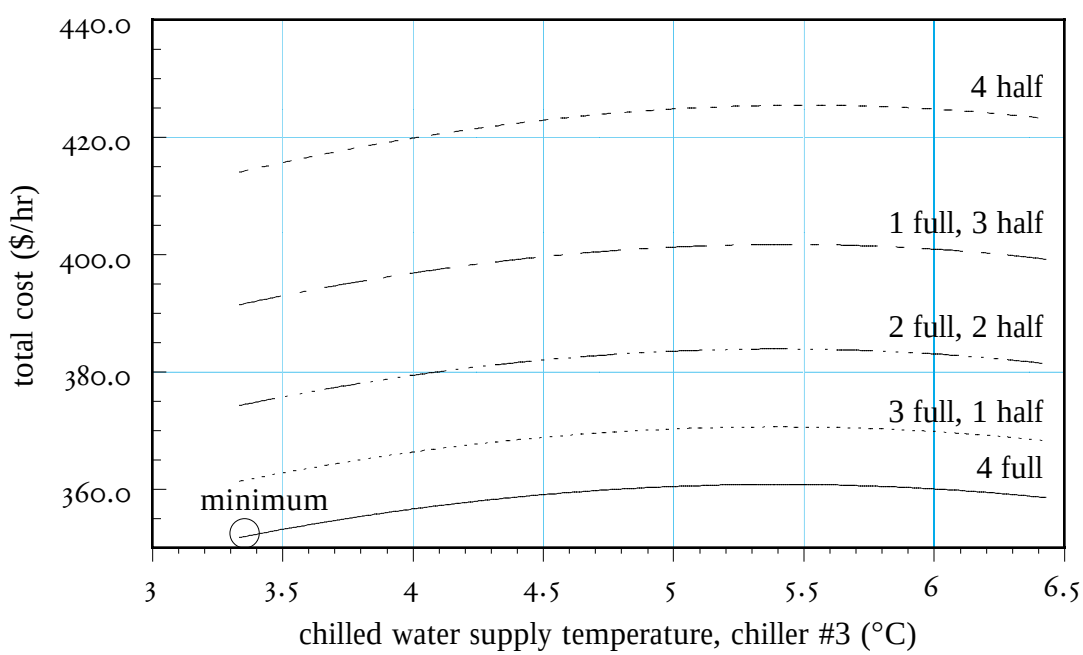

FIGURE 6.3.4: Total cost as a function of $T_{\text{chw \#3}}$ at different cooling tower fan speeds. Independent variables: T_{chwr} = 11.3 °C, T_{wb} = 25.6 °C, k_{elec} = \$0.0444/kW·hr.

water temperature and cooling tower fan speed is shown for two different hours (different values of independent variables). In Figure 6.3.3, the cost is calculated with a low load, cool wet bulb and low electrical rate. Figure 6.3.4 is for a high load, warm wet bulb and high electrical rate. At the lower load and lower electrical rate (Figure 6.3.3), the optimum control is to run the steam chiller at the higher temperature limit and the cooling tower fans at full speed. The costs in Figure 6.3.4 are calculated at a high chilled water load and high wet bulb temperature. Under this high load and at the higher electrical energy rate, the optimum control changes to running the steam chiller at its lower temperature limit and all cooling tower fans at full speed.

The concavity in total cost versus $T_{\text{chws \#3}}$ apparent in both figures results in the optimum control occurring at either the lower or upper boundary on $T_{\text{chws \#3}}$. Due to the mixed temperature constraint, the upper bound on $T_{\text{chws \#3}}$ is fixed by the lower bound on $T_{\text{chws \#4}}$. Individual chiller costs for the case with all fans at full speed shown in Figures 6.3.4 (labeled "4 full") are replotted in Figure 6.3.5. The plot shows that the concavity of the curve in Figures 6.3.4 is due pri-

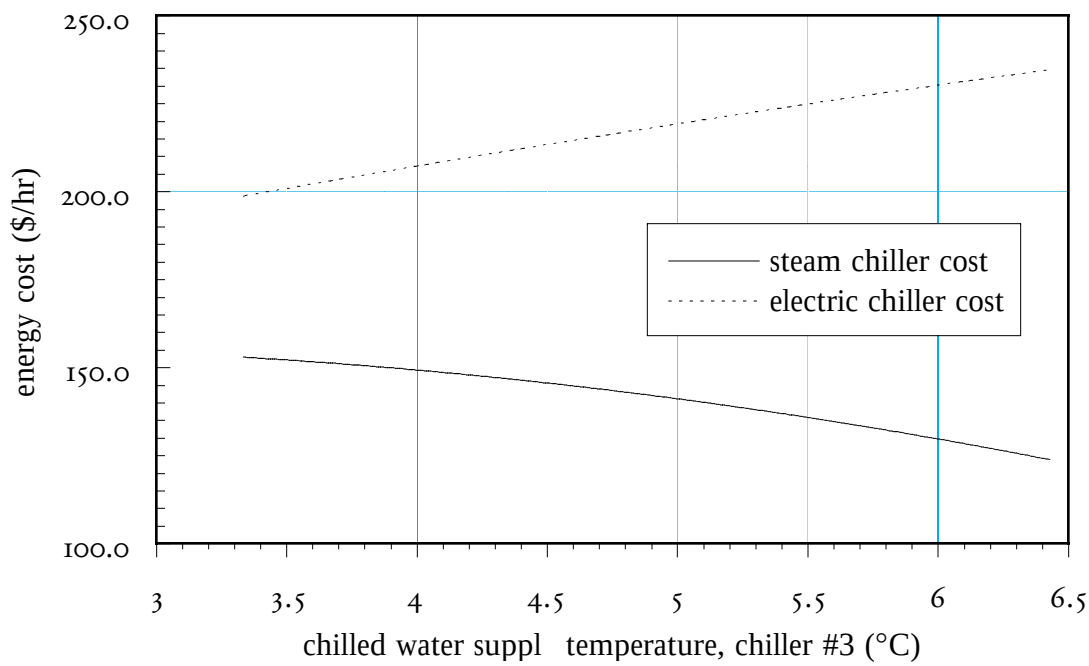

FIGURE 6.3.5: Steam and electric chiller energy costs with cooling tower fans at full speed. Independent variable values are the same as given in Figure 6.3.4.

marily to the performance of the steam driven chiller (chiller #3). The electric chiller costs are nearly linear with respect to load. Note that as $T_{\text{chws \#3}}$ increases (steam chiller load decreases), the supply temperature from the electric chiller, $T_{\text{chws \#4}}$ must decrease (electric chiller load increases). Since the return water temperature is constant in Figures 6.3.3, 6.3.4 and 6.3.5, changes in $T_{\text{chws \#3}}$ correspond to changes in load for the individual chillers. The concavity in steam chiller costs indicates that the chiller's COP increases as the load increases. The near linear electric chiller performance indicates its COP is nearly constant. The influence of the shape of a chiller's "part load" performance curve upon optimal control is discussed in Section 6.8.

A plot indicating optimal cooling tower fan settings at various combinations of chilled water return and wet bulb temperatures at the lower electrical rate is given in Figure 6.3.6. The overlapping groupings of particular fan speed settings demonstrate dependence upon both return and wet bulb temperature. When operating at the higher electrical rate, switching to a higher fan speed setting occurs at a slightly warmer chilled water return temperature. As shown in Figure 6.3.7, the switch up from two fans at full speed and two at half at the higher electrical rate occurs at approximately 8.3 °C and at approximately 8.0 °C at the lower rate.

The operators' cooling tower fan control decisions are also shown as a function of wet bulb and chilled water return temperature in Figure 6.3.8. Although scattered, the operators' settings somewhat coincide with the optimal values. When asked how he decided when to increase fan speed, a senior operator at the Walnut Street Plant revealed that he could tell from the sound and vibration of a chiller that a cooler condenser temperature is needed.

An hourly plot of total cost savings of optimal over conventional operation in shown in Figure 6.3.9. With optimal control, the steam and electricity costs are reduced to $52,770 and $99,930 respectively. The total energy cost for the month is $152,700 for a savings of $5,778 (3.6%) over conventional control. Average savings per day is $186.49.

6.4 Demand Charges

Typically, an electrical utility will charge not only for energy used, but also for the largest power required (peak demand) over a billing period. During periods of high cooling loads, the

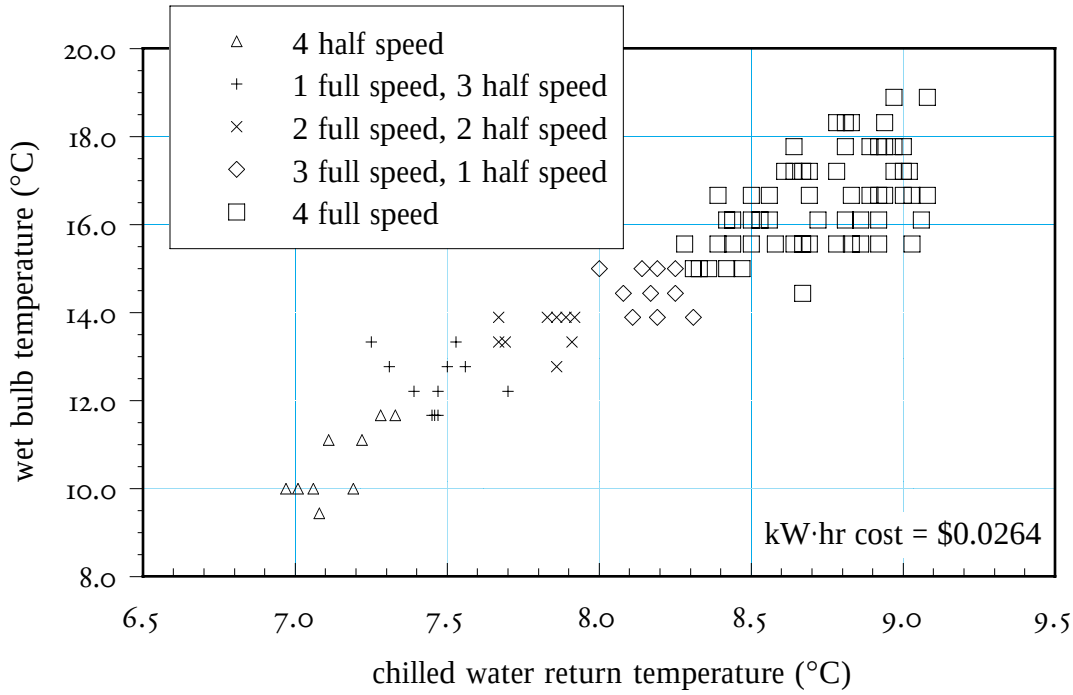

FIGURE 6.3.6: Optimal cooling tower fan speed control vs. chilled water return temperature and wet bulb temperature. Electrical cost is $0.0264/kW·hr.

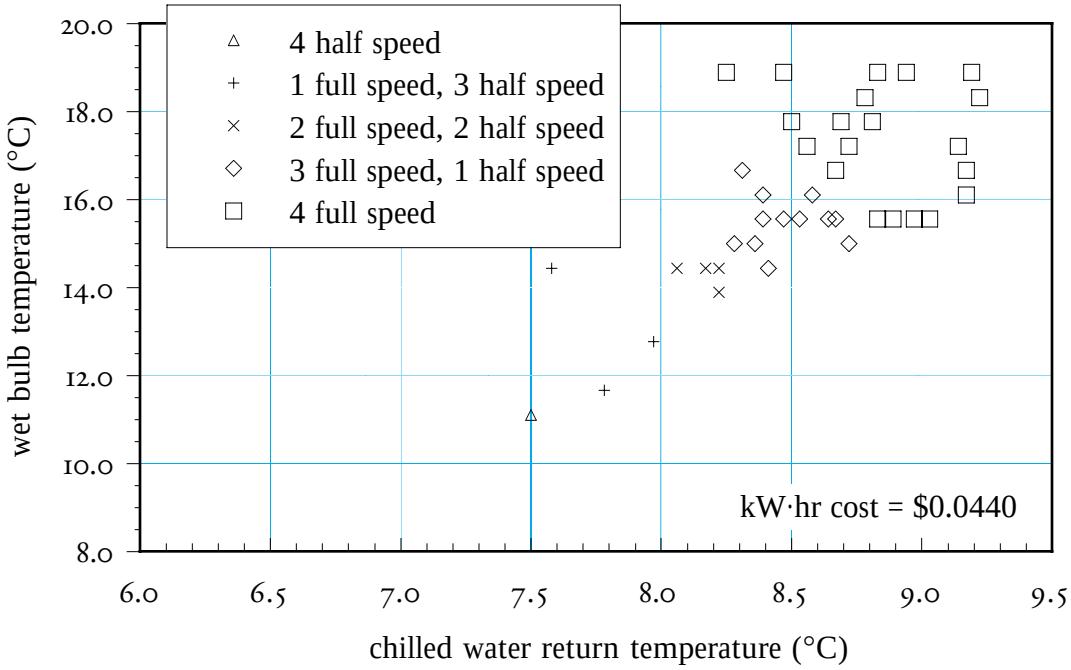

FIGURE 6.3.7: Optimal cooling tower fan speed control vs. chilled water return temperature and wet bulb temperature. Electrical cost is $0.0440/kW·hr.

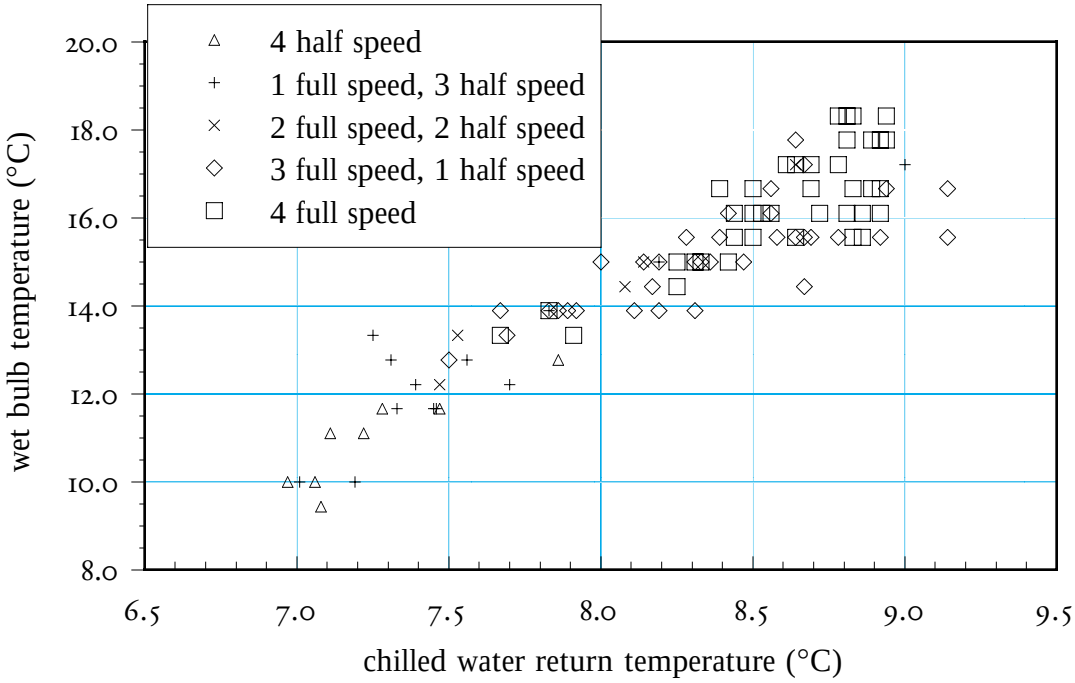

FIGURE 6.3.8: Conventional cooling tower fan speed control vs. chilled water return temperature and wet bulb temperature.

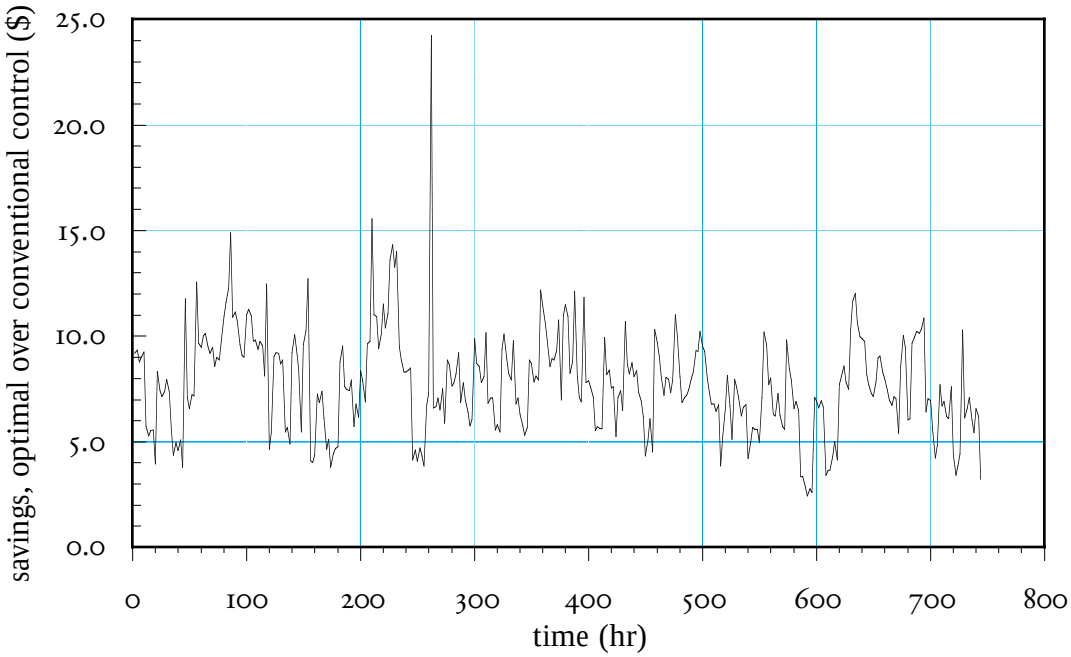

FIGURE 6.3.9: Hourly savings of optimal control over conventional control.

power used at the Walnut Street Plant can have a substantial impact on the University's electrical bill. The power used in operating the electric chiller at full load during a peak period represents approximately $25,000 in monthly demand charges.

In comparing demand costs, it is assumed that the remainder of the University's electrical load (other than the chilled water plant) is relatively flat. With a flat "base" load, all peaks and valleys in the recorded electrical demand is attributed to demand from the chilled water plant.

The peak electrical demand under conventional control is 5,439 kW, corresponding to $38,074 in peak demand charges. The peak demand in the optimal control given in Section 6.3 is 5,646 kW, an increase of $1,449 in demand costs. The savings in optimal over conventional control including demand costs is reduced to $3850 for the month, 2.0% of the total energy and demand costs under conventional control. Almost half of the optimal savings are offset by increased demand charges. To find the minimum monthly energy cost for the chilled water plant, the demand charge must be included in the optimization.

One strategy for reducing peak demand costs is to minimize electricity use during an anticipated high cooling load period. For example, at the Walnut Street Plant, electrical energy could be reduced by moving as much of the load as possible to the steam driven chillers, unloading the electrically driven chiller. Knowing when a peak load occurs impacts the operators' decisions in loading the chillers. If a large peak was to occur later in the billing period, or if the peak had already passed, operators would not take the peak charges into account when operating the plant during periods of lower loads. But the true peak load for the billing period is uncertain until the end of the billing period, and operators must make predictions of future load based on expected weather conditions.

In an actual implementation, determining an optimal control strategy to minimize both energy and demand costs requires weather and load predictions for the billing period. Using historic measured data of weather and loads over a month for the Walnut Street Plant, what would have been the optimal control can be determined after the fact.

6.5 Optimal Supervisory Control with Demand Charges

Given the measured data for July from the Walnut Street Plant, the optimal control strategy which would have minimized costs for that billing period can be determined. For hours with relatively small chilled water loads, the optimal control is not influenced by peak demand charges. The optimum control at lower loads is the same as the results from solving the optimization problem without demand charges (See Section 6.3). To simulate the presence of demand charges, the chiller plant model includes an additional cost at each hour for any power increment above a user set "demand limit" parameter. This demand limit parameter could be set to the highest demand previously calculated during the period or an expected peak demand for the period. If the limit was 4,000 kW, electrical costs for that hour would include energy use costs (for kW·hrs) plus the demand charges for use exceeding 4,000 kW. At relatively large loads, this limit will influence the optimum control solution for that hour.

The effect of adding a cost for exceeding a set demand limit is demonstrated in Figure 6.5.1. The data presented are identical to those presented in Figure 6.3.3 except that the cost calculations include an electrical demand charge. Figure 6.3.3 shows that without demand charges, the lowest total cost for the hour is $167.03. This minimum cost occurs at a steam chiller supply water temperature of 6.4 °C and an electrical demand of 4,095 kW. In Figure 6.5.1 the demand limit is set at 3951 kW, lower than the demand of 4,095 kW at the minimum point in Figure 6.3.3. With the demand charge for exceeding 3,951 kW, the optimum steam chiller supply temperature falls to 5.6 °C, indicating the steam chiller is taking on load from the electric chiller. (The temperature of the combined flow is constrained to 4.9 °C.) The sharp upturn in total costs toward the right of Figure 6.5.1 is due to the relatively high demand charge ($7.00/kW) added when exceeding the limit. The electrical demand at the new minimum is the same as the demand limit, 3,951 kW.

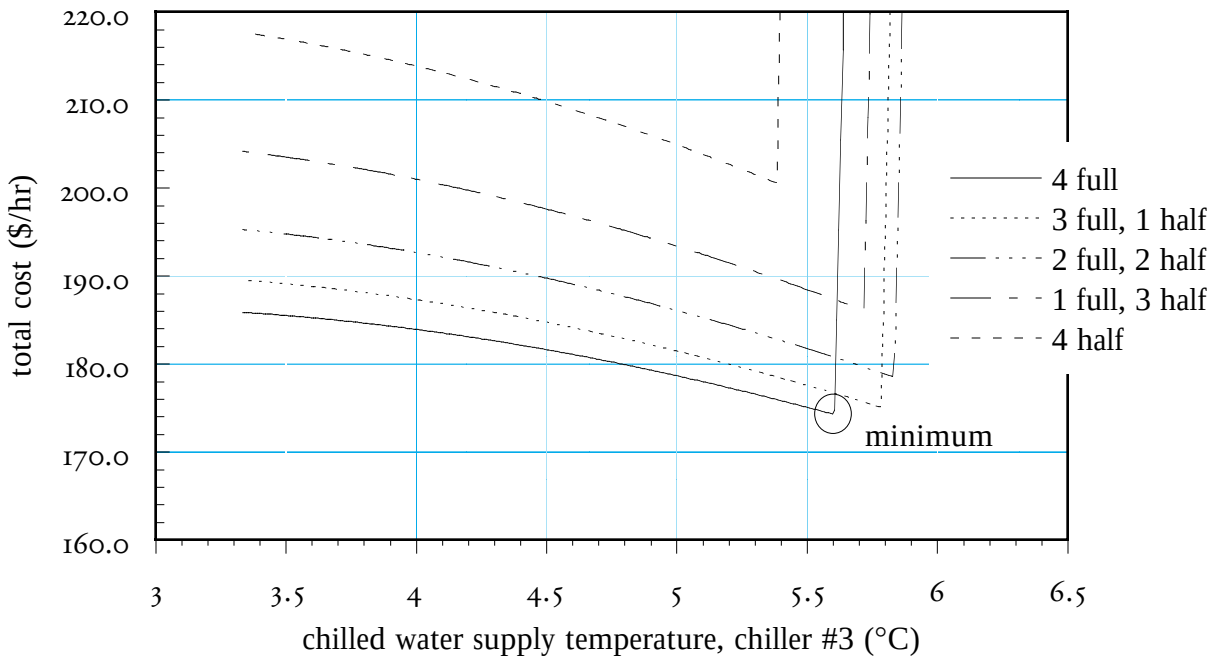

FIGURE 6.5.1: Total cost versus chilled water supply temperature from chiller #3. In this case, there is a demand charge for electric power requirement exceeding 3951 kW.

Without demand charges, the minimum monthly cost can be found by minimizing steam and electric cost as a function of $T_{\text{chws \#3}}$ and γ_{ct} at each ith hour, then summing over all n hours.

$$\phi^*_{month} = \sum_{i=1}^{n} \left\{ \min_{T_{chws\,\#3,i},\ \gamma_{ct,i}} \left(\dot{m}_{\text{steam,i}}\, k_{\text{steam}} + p_{\text{i}} k_{\text{elec}} \right) \Delta t \right\} \qquad 6.5.1$$

With demand charges, a cost is added for the maximum power required during the billing period. The optimization problem is then to find control variables for each hour, $T_{\text{chws \#3, i}}$ and $\gamma_{\text{ct, i}}$, that minimize the total monthly cost:

$$\phi^*_{month} = \min_{T_{chws\,\#3,i},\ \gamma_{ct,i}} \left\{ \sum_{i=1}^{n} \left(\dot{m}_{\text{steam,i}}\, k_{\text{steam}} + p_{\text{i}} k_{\text{elec}} \right) \Delta t + \max\left(p_1, p_2, \ldots, p_n \right) k_{\text{demand}} \right\} \qquad 6.5.2$$

The minimum monthly cost cannot be found by separately minimizing energy (kW·hr and steam) costs at each hour, then adding the demand cost for the individual hour having the peak

electrical demand. At the hour having the largest optimal power demand, the plant could have been operated at a lower power usage. The decreased power use can only increase the otherwise optimal energy (kW·hr and steam) costs. However, the savings in demand costs can be much greater than the increased kW·hr and steam costs.

The dimension of the minimization problem as stated in Equation 6.5.2 is $2n$. The scope of the problem can be reduced by considering $p_i \leq p_{\max}$ as a constraint applied over all n hours. The problem in Equation 6.5.1 is then minimized as a function of $p_{\max}$.

$$\min_{p_{\max}} \left\{ \sum_{i=1}^{n} \left(\min_{\substack{T_{chws\#3,i},\ \gamma_{ct,i} \\ s.t.\ p_i \leq p_{\max}}} \left(\dot{m}_{\text{steam,i}}\, k_{\text{steam}} + p_{\text{i}} k_{\text{elec}} \right) \Delta t \right) + p_{\max}\, k_{\text{demand}} \right\} \qquad 6.5.3$$

$$s.t.\ p_{\max} \leq p_{\max\, u.b.};\ p_{\max} \geq p_{\max\ l.b.}$$

For the greater minimization problem, the upper bound, $p_{\max\, u.b.}$, can be found by solving the problem without demand charges, Equation 6.5.1. The largest hourly demand from this solution is the upper bound in Equation 6.5.3. A lower bound on demand exists because at each hour, there exists some minimum power required to meet the load, regardless of the cost. The largest of these minimums is the lower bound on maximum power demand.

As $p_{\max}$ decreases from its upper bound, the sum of the minimum hourly costs can only increase and the $p_{\max}\, k_{\text{demand}}$ term decrease. If at an unbounded minimum, the optimum value of $p_{\max}$ will occur when the derivative of the argument in Equation 6.5.3 is zero, or equivalently

$$\frac{\partial}{\partial p_{\max}} \left(\sum_{i=1}^{n} \min_{\substack{T_{chws\#3,i},\ \gamma_{ct,i} \\ s.t.\ p_i \leq p_{\max}}} \left(\dot{m}_{\text{steam,i}}\, k_{\text{steam}} + p_{\text{i}} k_{\text{elec}} \right) \Delta t \right) = -k_{\text{demand}} \qquad 6.5.4$$

Total power use for each hour optimized without demand charges is plotted in Figure 6.5.2. The hours have been rank ordered by hourly power use. The optimum peak demand which solves Equation 6.5.4 may be approximated by progressively lowering the demand limit in successive

optimization runs until the incremental savings in reduced demand costs is less than the additional energy (steam and kW·hr) costs. At relatively high demand charges (compared to kW·hr cost), the savings in lowering the peak will always be greater than the increased energy costs and the optimum will be at the lower bound on demand. By rank ordering the hours by power demand, only the first few of n hours need to be minimized with the changing $p_{\max}$ constraint. Optimum control values at hours having an optimum power demand (resulting from the solution of Equation 6.5.1) less than $p_{\max}$ are not affected by the constraint and need not be recomputed.

The lower bound on demand is found by minimizing electrical use each hour rather than energy cost. The largest minimum power requirement over the month for the Walnut Street Plant is 5,062 kW. Rerunning the optimization including a demand cost for power exceeding 5,062 kW influences the optimal control during eight of the highest load hours. Rank ordered hourly demand from the demand limited run is replotted in Figure 6.5.3. The savings in demand charges compared to optimizing without regard to demand is $4,086. The increase in energy charges during those high load hours is $8. For the Walnut Street plant, the optimum peak demand during the month is at its lower bound.

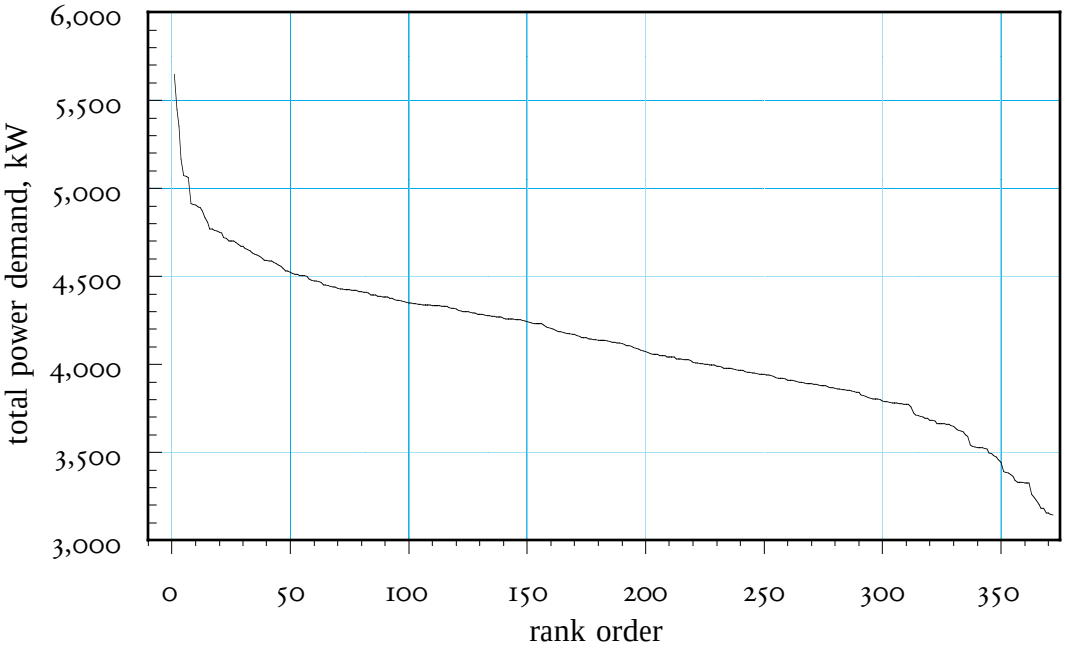

FIGURE 6.5.2: Rank ordered optimal hourly power demand. No demand charges were included in the optimization.

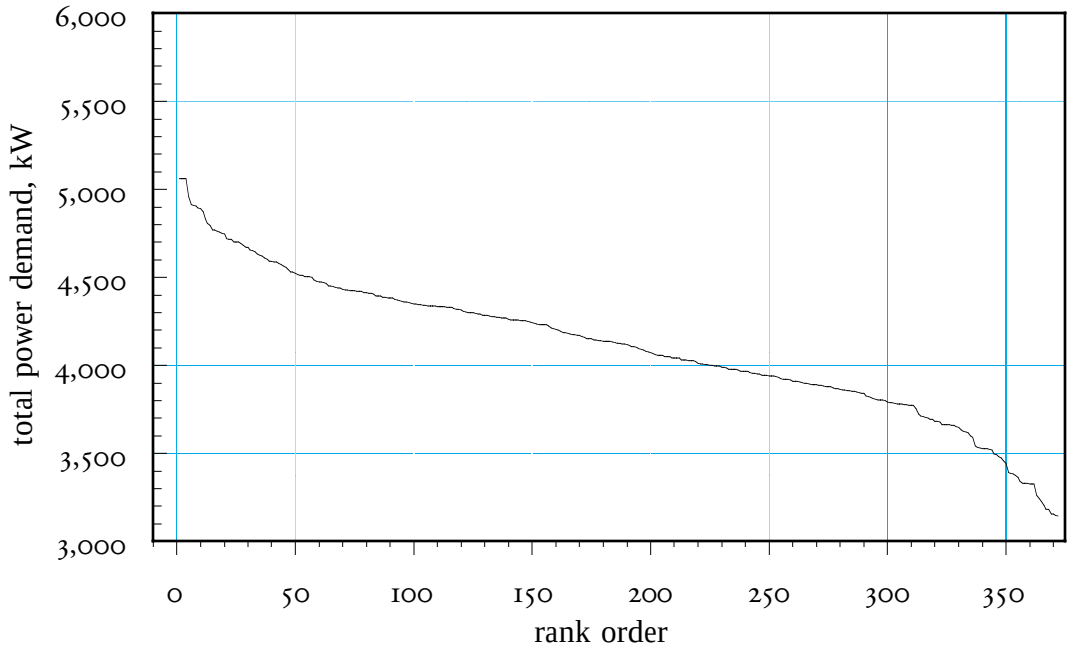

FIGURE 6.5.3: Rank ordered demand with optimal peak demand limit included in the optimization.

Comparing optimal costs and conventional costs including demand charges, the savings is $8,406 for the month, averaging $271 per day. This represents a 4.3% decrease in the monthly energy bill. The percentage savings is not very large, but because yearly energy costs are in the millions of dollars, the absolute savings is substantial. The small percentage in cost savings is primarily due to the small range of possible individual chiller supply temperatures. The required mixed water temperature of 4.6 °C is only 1.3 °C greater than the minimum allowable temperature, leaving approximately a 2.6 °C range of operation. A larger range for possible individual chiller supply temperatures would allow for increased savings. Optimal control allowing a warmer chilled water supply temperature is discussed in Section 6.7 below.

6.6 Priority Control

Two other commonly implemented control strategies were simulated for comparison. In one, the steam driven chiller is given "priority" and takes on as much of the chilled water load as possible before using the electric chiller to provide the remaining cooling. In the other mode the electric chiller is given priority.

With fixed water flow rates through both chillers, the only control over loading the chillers is by varying the chilled water supply temperatures. The maximum load either chiller can supply is limited by the minimum allowed chilled water supply temperature. A plot of both chillers' supply temperatures and fraction of total load under steam priority control is shown in Figure 6.6.1. At chilled water return temperatures below 12 °C (53.6 °F), the chilled water return temperature is not warm enough to fully load either chiller and the priority chiller's supply temperature remains at its minimum value. Above a return temperature of 12 °C, the chiller's maximum load is reached and the priority chiller's supply temperature rises above its minimum. The non-priority chiller then supplies a lower chilled water temperature to meet the required mixed temperature of 4.6 °C (40.3 °F).

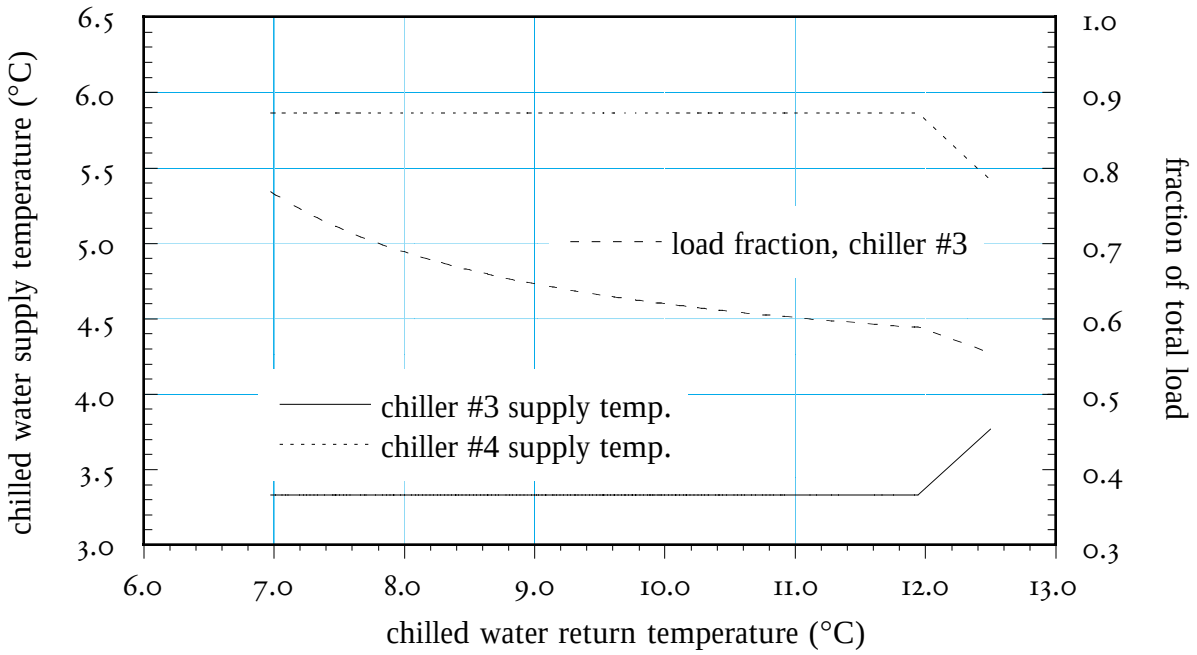

FIGURE 6.6.1: Chilled water supply temperatures and load fraction for steam priority chiller control.

Total monthly costs when running the plant in steam priority mode are approximately the same as when run in conventional mode. Increased steam costs for operating with steam priority were offset by lower demand and kW·hr costs. Running the plant under electric chiller priority

increased total costs by 4.8%, the greatest increase coming from greater kW demand cost. Costs for conventional, optimal and priority control strategies are given in Table 6.7.1.

Optimal control for the Walnut Street is a priority control that switches from electric chiller priority to steam chiller priority depending upon the load and the electric rate. As shown in Figures 6.3.1 and 6.3.2, priority switches to the steam chiller at T_{chwr} above 10.4 °C during on peak electrical rates, and at T_{chwr} above 11.7 °C during off peak rates.

6.7 Optimal Control with T_{chws} = 7.2 °C (45.0 °F)

In the design of facility air conditioning systems, a chilled water temperature of 7.2 °C (45.0 °F) is commonly assumed to be available for meeting the largest cooling load. For purposes of comparison, conventional and optimal control were recalculated with the plant required to supply 7.2 °C instead of 4.6 °C chilled water. The return water temperature was set to be 2.4 °C (4.6 °F) higher so that the chilled water load would be approximately the same as indicated in the measured data. With the warmer mixed chilled water supply temperature the individual chillers can operate over a wider range of temperatures.

Under conventional control at the warmer supply temperature, steam and electrical energy costs are $60,450 and $91,050 respectively. Adding the power demand charge of $34,741 results in a total cost of $186,231. Optimal control reduces the total cost to $160,002 if demand costs are not considered in the optimization. Limiting the power demand (to the largest minimum required hourly demand) reduces demand costs by $4,116 and increases steam and kW·hr costs by $258. The total monthly cost of $156,144 is a 16.2% savings over conventional control.

The larger percentage savings of optimal over conventional control is possible with the warmer supply temperature because the individual chillers can operate over a wider range of supply temperature. Optimal supply temperatures at the higher electric kW·hr rate ($0.044/kW·hr) are plotted in Figure 6.7.1. As return water temperature increases, optimum operation switches from loading the steam chiller to loading the electric chiller at about 11 °C, then back to the steam chiller at temperatures greater than about 13 C.

Examining the corresponding plot of load in Figure 6.7.2 allows a better understanding of why the favored chiller switches. At low loads, below 11 °C T_{chwr}, only the steam chiller is operated. At about 11 °C, the steam chiller reaches its minimum allowed supply temperature and two chillers must be operated to meet the load.

With both chillers on, the steam driven chiller disproportionately contributes to the heat rejected at the cooling tower because of the heat removed from the steam condenser. Consequently, the water temperature from the cooling tower increases as load is moved to the steam chiller. Increased water temperature from the cooling tower reduces the COP of both chillers. If two chillers must be run at low load conditions, it is more economical to move as much load as possible to the electric chiller.

The small jump in load above 11 °C T_{chwr} is due to the minimum operating load required before a chiller can be operated. In the transition region near 11 °C T_{chwr}, the optimum operation switches from favoring one chiller to the other. Two data points in this range have high wet bulb temperatures compared to other points having approximately the same chilled water return temperatures. At high wet bulb temperature, the cooling water temperature entering the refrigerant and steam condensers rises. Because of the steam condenser, steam driven chiller performance is relatively more sensitive to changes in wet bulb temperature than the electric chiller. At the two points near 11 °C having high coincident wet bulb temperature, meeting the load with the electric chiller is more economical that meeting it with the steam driven chiller.

Further increasing T_{chwr}, the electric chiller supply temperature remains at its minimum until it reaches its maximum load (about 21,000 kW at 12.2 °C T_{chws}). As the chilled water return temperature increases from 12.2 °C, the electric chiller remains fully loaded and its supply temperature rises. While the electric chiller remains fully loaded, the steam chiller takes on the additional load, decreasing its supply temperature to meet the required 7.2 °C mixed supply temperature. Above approximately 13.1 °C T_{chwr}, it is more economical to fully load the steam chiller. The curve of total cost versus steam chiller supply temperature changes from a minimum at the higher bound

(see for example, Figure 6.3.3) to a minimum at the lower temperature bound (e.g. Figure 6.3.4).

TABLE 6.7.1: Comparison of costs under different operating strategies

operating strategy			savings over conventional control	total cost, $	kW demand cost	subtotal, kW·hr and steam costs	kW·hr cost	steam cost
T_{chws} = 4.6 °C	conventional control		-	196,554	38,074	158,478	95,034	63,444
	priority control	steam chiller	711	195,843	35,437	160,408	88,470	71,938
		electric chiller	-9,507	206,061	53,423	152,638	100,600	52,038
	optimal control	without demand constraint	4,333	192,221	39,523	152,700	99,930	52,770
		with demand constraint	8,407	188,147	35,437	152,708	99,818	52,890
T_{chws} = 7.2 °C	conventional control		-	186,231	34,731	151,500	91,050	60,450
	priority control	steam chiller	13,206	173,025	32,315	140,710	68,790	71,920
		electric chiller	21,182	165,049	36,891	128,158	96,890	31,268
	optimal control	without demand constraint	26,229	160,002	36,432	123,570	93,186	30,384
		with demand constraint	30,087	156,144	32,316	123,828	92,706	31,122

6.8 Chiller Part Load Performance and Optimal Control

A curve of typical centrifugal chiller part load performance given in manufacturer's catalog literature is shown in Figure 6.8.1. The curve is convex with COP improving as the chiller is loaded, reaching a maximum at about 70 to 80 percent of full load. A chiller having maximum COP at less than full load is beneficial in most applications where the chiller is fully loadedonly a small fraction of total operating hours. Minimum electrical cost for two identical chillers with part load performance as shown in Figure 6.8.1 would occur with each chiller operating at part load and the same chilled water supply temperature.

In the case of the Walnut Street Plant, the optimal solution includes operating either of the two chillers at a maximum load or minimum chilled water supply temperature boundary. Optimal operation occurs at these boundaries because of the convex total cost curve as given for example in Figure 6.3.4. The part load performance of the Walnut Street Plant chillers differs from

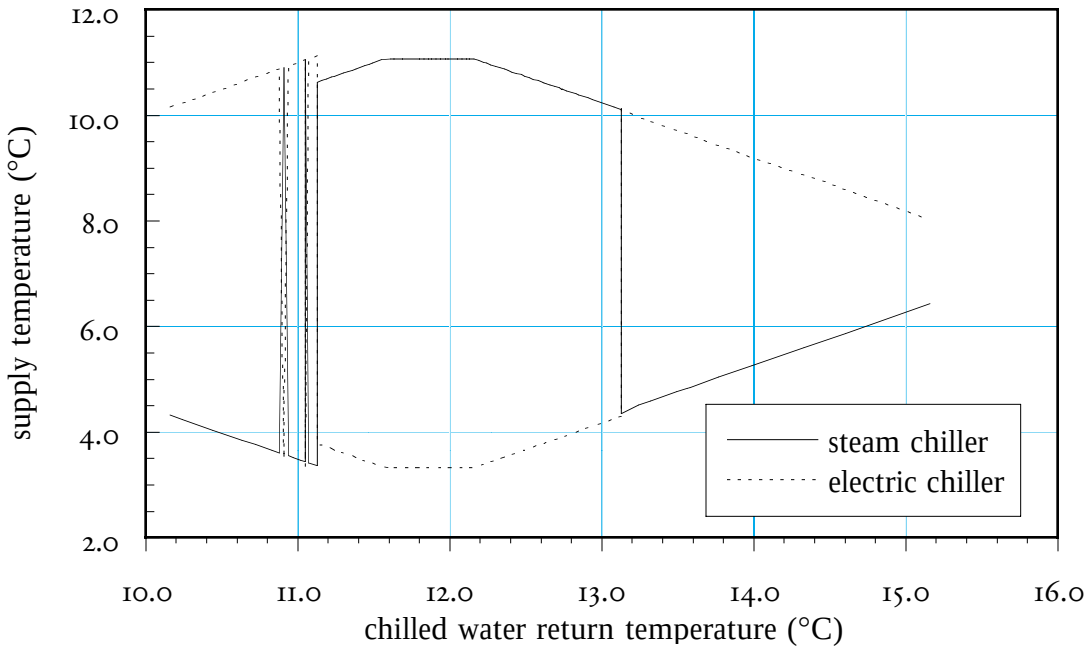

FIGURE 6.7.1: Optimal chilled water supply temperatures of the steam and electric chiller versus chilled water return temperature. The mixed chilled water supply temperature is fixed to be 7.2 °C.

typical electric chiller performance for a number of reasons. The steam chiller's atypical decrease in COP at part load is largely due to the means of load control. Part of the control mechanism for unloading the steam driven chiller is to throttle the inlet steam. Although the refrigeration cycle efficiency may improve at part load, the losses in the turbine associated with throttling the inlet steam result in an overall decrease in system efficiency.

The typical part load curve assumes a constant entering condenser water temperature. The nearly linear electric chiller part load performance shown in Figure 6.3.5 includes an increasing condenser water temperature with decreasing load. Shifting load to the steam chiller results in a rise in entering condenser water temperature. The temperature increases because the steam turbine/chiller combination must reject more heat per unit of refrigeration than the electrically driven chiller. Improvement in cycle performance associated with increasing evaporator temperature is countered by the increasing condenser temperature.

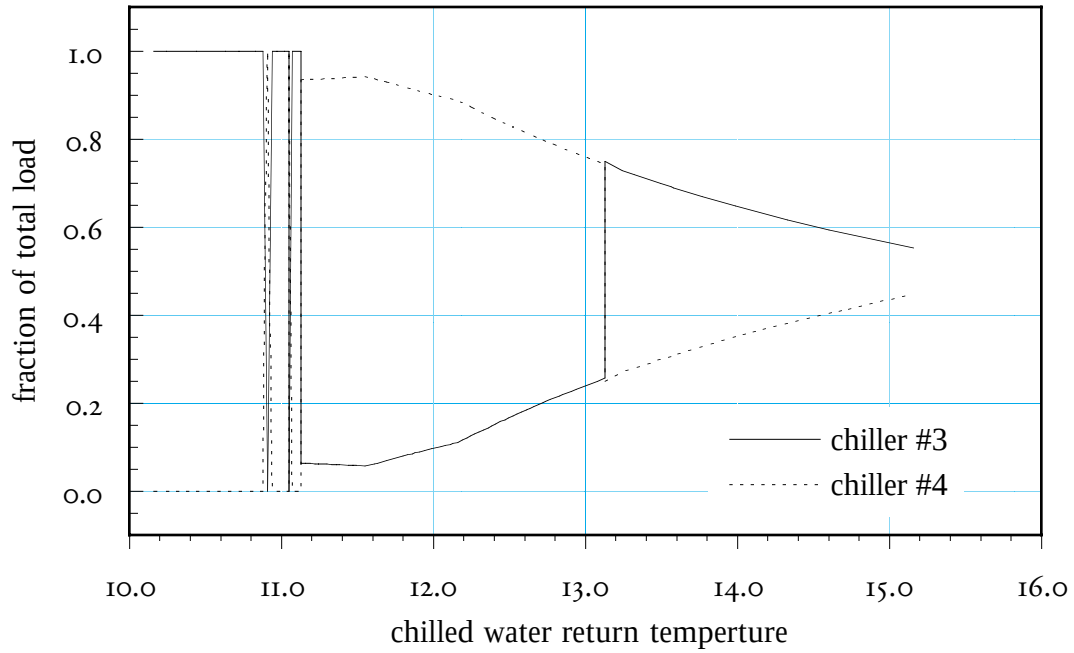

FIGURE 6.7.2: Optimal fraction of total load met by chillers #3 and #4 versus chilled water return temperature.

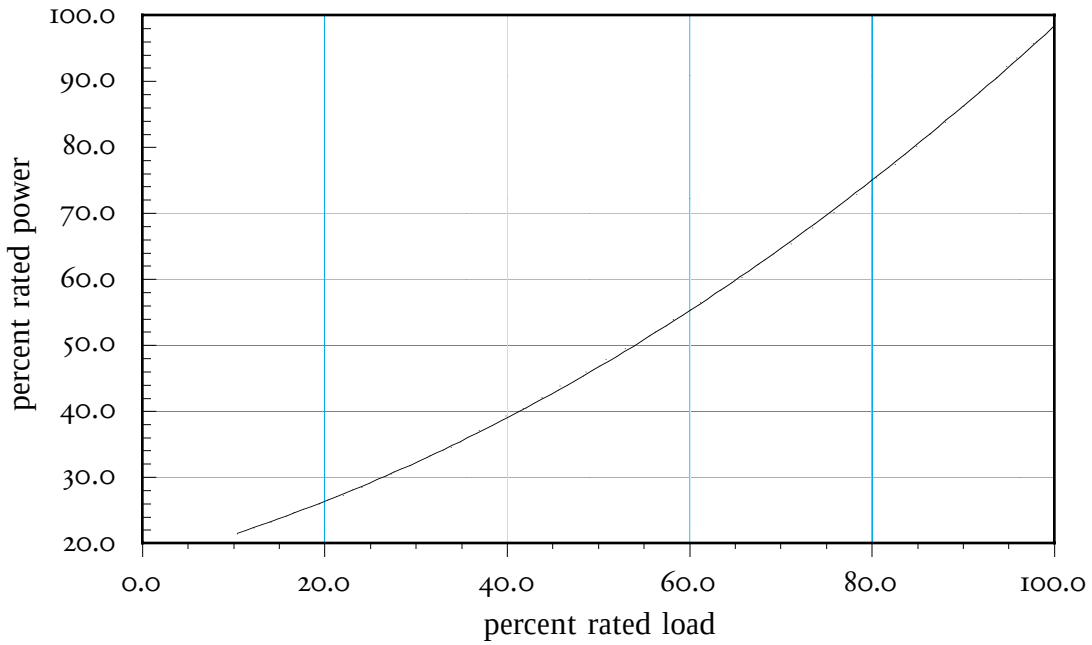

FIGURE 6.8.1: Typical part load performance for an electrically driven chiller at constant entering condenser water temperature.

The atypical part load behavior evident in the measured data has been reported in other published works. In Ng's paper on performance evaluation of centrifugal chillers, decreasing COP at decreasing loads is apparent in his measured data. [Ng94] Other works presently in publication have also found atypical part load performance of centrifugal chillers. [Brn98]

6.9 Summary

In this chapter optimal supervisory control of the Walnut Street Chilled Water Plant is predicted. Optimal control for the chilled water plant results in a 4.3% cost savings over conventional control. The savings are limited due to the required chilled water supply temperature (4.6 °C [40.3 °F]) being very close to the minimum allowed supply temperature from the individual chillers. If supplying a warmer chilled water temperature of 7.2 C (45.0 °F), optimal control savings increase to 16.2 % over conventional control.

Optimal operation includes running one chiller at maximum load with the other chiller meeting the remainder of the required load (priority control). At lower plant loads, the electric chiller should be run at maximum load. The point at which it becomes optimal to priority load the steam chiller depends upon the chilled water return temperature and the electrical rate. Optimal cooling tower fan speed increases with increasing load and increasing wet bulb temperature.

Costs for chiller priority control are compared to optimal and conventional control costs. Due to plant part load performance characteristics, optimal control is priority control where the switch point depends upon chilled water return temperature and electricity cost.

CHAPTER 7

Conclusions

In this work, methods were developed for fitting a chilled water system model with measured data and for determining optimal supervisory control using the plant model. Parameter estimation methods for multivariate nonlinear models were investigated and applied to the problem of fitting a chilled water system model. A minimization algorithm was used with the system model to determine optimal supervisory control of the plant. In this chapter, conclusions concerning the methods of parameter estimation and optimization as well as the results of their application will be presented.

7.1 Modeling and Parameter Estimation

At the outset of this investigation, it was anticipated that the optimization problem would be the more formidable task compared to the problem of estimating model parameters. The TRNSYS chilled water plant model is a multiresponse, multiparameter and nonlinear system. Finding parameter estimates for the plant model was as difficult or more so than the optimization problem. A comment quoted in a regression text [Sen90] gives a daunting outlook: "Nonlinear estimation is an art. One-parameter estimation is minimalist, multiparameter is rococo. There are

numerous booby traps (dependencies, discontinuities, local minima, etc.) which can ruin your day." [Wil87]

7.1.1 Modeling

A mechanistic model can have advantages over other models (polynomial equations, neural nets, etc.) in extrapolating model predictions. The mechanistic model, in general, constrains the relationships between inputs and outputs to adhere to conservation laws and energy transport relationships observed in physical phenomena. Thus the mechanistic type model for the chilled water plant is advantageous over interpolative type models when the optimal plant operation occurs at control values not present in the measured data.

In determining the optimum supervisory control for the Walnut Street Plant (Chapter *6*), the model extrapolated responses as the minimization algorithm searched for optimal values of the control variables. The optimal control is to fully load one chiller (operate it at the minimum allowable chilled water supply temperature) and use the other chiller to meet any remaining load. This optimal control usually caused both chillers to operate at a chilled water supply temperature a few degrees outside the range of measured data used in the fit. Although the accuracy demonstrated for the interpolated predictions is not guaranteed for the extrapolated values, using the mechanistic models gives some confidence that the variable values conform to physical laws. With arbitrary curve fits or neural nets, any prediction outside the region of the data used in the fit is highly suspect.

7.1.2 Regression Methods

In order to begin the regression a scalar quantity representing the difference between model prediction and the measured data must be defined. Using a sum of squared residuals from all responses is an extension of the least squares method used in single response cases. It is important to scale all responses (usually scaled by the response's mean value in the set of observations) because of the differences in magnitudes of the measured values.

In multiresponse regression theory, individual responses should be weighted before summing the squares. The weight for a particular response should be proportional to the inverse of its esti-

mated variance. Weights can be estimated in an iterative method by first solving the problem with no weighting preferences for the responses. The resulting set of residuals for each response will demonstrate some measure of variance. A set of weights can be constructed from the variance found in the previous solution and the weighted least squares problem resolved, iteratively, until the change in weights fall below some tolerance. According to regression theory, an alternative to weighting the responses is to minimize the determinant of the matrix formed by multiplying the residual matrix by itself.

For the chilled water plant model and data used in this work, using either a weighting matrix or the determinant criterion did not result in any significant improvement in model predictions. The lack of improvement in predictions does not, however, imply that weighting is not necessary in any other case. It can only be concluded that measurements used in this work have approximately uniform error.

While adding power measurements to the regression would have yielded a significant improvement in parameter estimates, because of problems associated with collinear responses, (discussed in Chapter 3) adding too many responses can be detrimental to the fit. For the Walnut Street Plant model, regression results varied when the combination of responses were changed. Even after removing all obvious collinear responses, it was found that a smaller set of responses resulted in a better fit. The response set resulting in the best fit was determined by repeated solution of the parameter estimation problem using various combinations of responses.

7.1.3 Walnut Street Plant Parameter Estimation

A total of 22 parameters in the composite Walnut Street Plant model require estimates. Subjecting the composite model to a parameter estimation algorithm required the minimization of an objective function of 22 dimensions. Several regressions were made with the composite model to compare different parameter estimation methods. Significant differences or variance in some parameter estimates were evident in results from multiple resgressions having approximately the same level of fit. The differences in parameter estimates over the multiple regression indicate over-parameterization in the composite model. Large variances in parameter estimates were also demonstrated with the example problem examined in Chapter 3.

Dividing the composite model into three subsystems allowed the solution of three lower dimensional problems. Parameter estimation problems could be solved for the electric chiller and cooling tower models separately because measurements were available for all model input and output variables. However, measurements were missing for some interconnected input and output variables between the steam driven chiller, steam turbine and condenser models. Parameter estimates were found by considering the three models to be combined as a single subsystem model. Separately solving parameter estimation problems for the three individual subsystems yielded a better fit than solving for the 22 parameters simultaneously with the composite model.

Overparameterizaion was also evident in the steam turbine/chiller/surface condenser subsystem model and in the separate electric chiller model. Considering the relative amounts of variance found among all model parameters, the seven parameters in the chiller model are more than are needed to adequately model chiller performance indicated in the data. The overparameterization problem is not necessarily inherent in chiller model but is rather more due to the small range of values present in the measured data. For example, the chilled water supply temperature measurements demonstrate relatively small variation as the chiller control system and the operators tried to maintain a constant temperature. Chiller power does depend upon the chilled water supply temperature, but that dependence (and any parameters that model the dependence) cannot be determined unless the chilled water temperature varies. Despite the large variance in some model parameters, the model does show a reasonable fit to data used in the regression and a separate data set recorded later in the month.

7.2 Optimization

7.2.1 The Optimization Problem

Many minimization algorithms and software packages are available for solving different classes of optimization problems. [Mor93] The majority of available methods are applicable to convex problems with continuous variables. Integer programming methods are available for solving problems with discrete variables, and these methods have been combined with algorithms that minimize convex functions to solve problems having both discrete and continuous variables. The control variables in the general chilled water plant model considered in this work include both

continuous and discrete variables. The objective function may be convex or concave in any particular region of the space spanned by the control variables. The general nature of the problem led to the application of the robust but relatively slow simulated annealing minimization algorithm.

7.2.2 Simulated Annealing Method

The simulated annealing method employed in this work performed well in determining minimum operating costs. Minimization methods that use gradients to find a local minima would have had problems with the concave objective function curve discussed in Chapter 6. The disadvantage of using simulated annealing is that it requires relatively large number of function calculations compared to gradient methods. Also, the method requires more function calls than integer programming methods when searching over the discrete variables.

In the application of simulated annealing in Chapter 6, the objective function was minimized with respect to two control variables. With the two control variables, the algorithm took approximately twenty computer processing unit (CPU) seconds using one processor (of 16) on a Cray C90 "supercomputer" to determine the optimal supervisory control per set of independent variable values (per simulated hour). The code was not optimized for vector performance and the computing time is comparable to what would be required on a conventional unix workstation. To optimize the entire Walnut Street Plant, a total of five control variables are required. Optimizing with respect to five control variables would require approximately two minutes of CPU time. Determining optimal control values over a month of hourly data would require approximately 24 hours of CPU.

If it were certain that the objective function surface was concave with respect to the continuous variables, a conventional gradient search combined with an integer programming method has the potential to significantly reduce computational time.

7.2.3 Optimal Control of the Walnut Street Plant

The estimated savings from optimally controlling the Walnut Street Plant was only 4.3 percent over conventional control. The small decrease in energy costs is primarily due to a required plant chilled water temperature of only 1.3 °C warmer than the minimum allowable temperature

leaving an individual chiller. To illustrate the impact of a low limit for temperature, the estimated savings increase to 16.2 percent over conventional control if the plant were operated at 7.2 °C (45 °F) rather than 4.6 °C (40.3 °F) chilled water temperature.

The optimal control strategy is to operate the chillers in a "priority" mode where one chiller operates at its maximum possible load (priority loaded) and the other chiller meets any remaining load. Which chiller should be given priority is a function of the chilled water return temperature. At the higher time of day electrical rate of $0.044/kW·hr, the electric chiller should be given priority control at chilled water return temperatures below 10.4°C (50.7 °F). At higher chilled water return temperatures, the steam chiller should operate at maximum load. At the lower electrical rate of $0.0264/kW·hr (off-peak hours), the switch between electric and steam chiller priority occurs at a chilled water return temperature of 11.7 °C (53.0 °F).

The optimal control strategy of fully loading one of the chillers rather than running both at part load is attributed to the concave shape of the chiller part load curve. For the chiller system modeled in this work, individual chiller performance (COP) improves with increasing load and the maximum efficiency occurs at full load. According to conventional centrifugal chiller manufacturers, the typical part load curve is concave, with a maximum COP at about 70 percent load. Previous guidance toward optimally controlling multiple chillers has been to operate all chillers at the same chilled water temperature. [Bra88] Maintaining equal chilled water supply setpoints coincides with optimal operation for identical chillers having the typical part load performance. However, given two identical chillers having a concave part load curve (maximum efficiency at full load), controlling both at identical chilled water temperatures is the least efficient operation.

The concave part load performance curve is not unique to the chillers studied in this work. Other investigations have found similar performance for operational chillers. One conclusion that should be carried forward from this work is, that for multiple chiller systems, equivalent chilled water setpoints does not always result in near optimal operation. The part load performance of individual chillers should be considered before implementing conventional control strategies.

7.3 Summary

In the example problem considered in Chapter 3, parameter estimates resulting in a close fit were found using simulated data and an exact model. The methods examined in Chapter 3 were applied in Chapter 4 using the same component models and actual measured data from the Walnut Street Plant. Although the mechanistic models used in the TRNSYS simulation do not exactly model the performance of actual plant components, a successful predictive model of the Walnut Street Plant was determined.

Considering the second law thermodynamic losses associated with mixing flows of different temperature, the predicted optimal operation of the Walnut Street Plant is counterintuitive. The predicted optimal control is also counter to results and recommendations of previous optimal control studies. Optimal control for any given plant is dependent upon particular component performance and configuration. Near optimal control will seldom be self-evident and the results from optimal control studies on other chilled water plants can result in far from optimal control of even a similarly configured plant. The disagreement with previous control studies does not suggest that those studies are in error or invalid; it rather emphasizes the importance and value of the methods of modeling, parameter estimation and optimization given in this work.

CHAPTER 8

Recommendations

In this work, methods for solving the parameter estimation and optimization problem were proposed and demonstrated on a chilled water plant model. There remains, however, a number of areas requiring further investigation. Demonstration of the methods upon real as well as simulated systems is needed to validate the methods. Areas recommended for further investigation are summarized here.

8.1 Modeling and Parameter Estimation

8.1.1 Data Acquisition

For the Walnut Street Plant, installation of new instrumentation and a modern data acquisition system would be of great benefit to monitoring performance and to controlling the plant. Adding an automatic data acquisition system would contribute to measurement accuracy by removing error associated with the current method of observing an instrument display then transcribing the measurement to a written log. A data acquisition system could also record all measured values simultaneously, removing the time delay present in the manual recordings and would allow observation of transient responses.

Flow meters should be added in the chilled water and condenser water loops. In this work flow rate had to be estimated from pressure differential measurements across chilled water and condenser water pumps. Manufacturers' pump curves were then used to estimate flow given the pressure drop. Data collected from calibrated flow meters would be more accurate and would not rely on pump curves.

Currently, power used in driving the steam turbine driven chiller at the Walnut Street Plant is not measured. Chiller power is a response of the chiller model and an input to the steam turbine model. Because calculated chiller power is dependent upon a number of parameters, having measurements of steam turbine power would have resulted in better parameters for both the steam turbine and chiller models.

8.1.2 Model Comparisons

The capability of greater accuracy in extrapolating responses was cited as a reason for using mechanistic component models instead of arbitrary polynomial equations or a neural net. The advantages of using a mechanistic model should be substantiated by a study comparing mechanistic model extrapolations with other methods. A study could compare other aspects of the different modeling techniques such as selecting initial values for the model parameters.

The parameter estimation methods used with the different models could also be compared. Several packaged software programs (commercial and public domain) are available for solving linear parameter estimation problems and for training neural nets.

The goal of having a single model that can accurately predict system performance over all possible ranges of operation should be reconsidered. The ISOPE method discussed in Section 8.1.5 below uses models that may be accurate only in a smaller region local to current values of system variables. Model parameters are updated as the system moves into different regions of operation.

8.1.3 Overparameterization and Parameter Variance

The results from parameter estimation studies with the Walnut Street Plant model indicate some overparameterization in the model. Detection and removal of redundant parameters from the estimation problem can reduce variance and improve accuracy in the remaining parameters.

Reducing the number of parameters also reduces the dimension of the minimization problem solved in the regression. Overparameterization can be identified using the method discussed in Section 3.4.1. Methods for identifying model parameters that should be fixed and removed from the estimation problem should be further investigated.

8.1.4 Updating Parameter Estimates

In this work the problem of parameter estimation was considered separately from the optimization problem. The only relationship between the two problems was that the goal of the parameter estimation problem was to obtain a model that best predicted cost related responses (e.g. steam flow rate and electric power).

In an initial implementation of optimal control in an actual plant, there is an interaction between the optimization and parameter estimation problems. Unless the plant was already optimally controlled, the predicted optimal control will force the plant into a new region of operation (i.e. at values of control variables not present in previously measured data). As the plant operates in the new region, data can be collected and the parameter estimation problem solved again. Improvement in the model as a result of using the new data will result in an improved prediction of optimal control.

Determining the frequency of resolving the parameter estimation problem with newly acquired data is yet another question. Also, the range and number of measurements used in the regression must be identified. One approach would be to resolve the parameter estimation problem (during the initial implementation) until the model demonstrates some arbitrarily established level of accuracy. After establishing a plant model that satisfactorily predicts performance over some range of operation, the parameter estimation problem would not be resolved.

Over time, physical changes in the plant (e.g. fouling of heat exchanger surfaces, or installation of a new pump) would reduce the accuracy of a static plant model. In order to maintain optimal plant control, plant model parameters must be updated to reflect the changes in the actual plant. The updating of parameters could be initiated if some level of sustained bias were detected in model predictions.

Before updating parameters to reflect physical changes in the plant, it would be beneficial to determine if the physical changes in the plant were due to some acceptable reason (e.g. gradual degradation of individual component performance or the replacement of a component) or due to an unacceptable "fault." Detecting changes in model parameters is one method of detecting possible faults.

8.1.5 Integrated System Optimization and Parameter Estimation

In integrated system optimization and parameter estimation (ISOPE), the parameter estimation problem is solved in combination with the optimization problem. [Ell88] One ISOPE method uses an adaptive-model approach where model parameters are updated as the system moves toward a region of optimum operation. The approach used in ISOPE methods makes use of the most recently acquired data to update model parameters. The system model used in ISOPE may use linear or polynomial equation(s) rather than a mechanistic model. Although the simplified models may not accurately predict system performance over a wide range of operation, they can adequately predict operation within a limited range of current system operation as their parameters are kept updated using current data.

Current application of ISOPE methods is limited to cases having continuous variables and a differentiable objective function. Extending ISOPE methods to the optimal control of systems with discrete control variables may reveal another practicable approach to the optimal control of chilled water plants.

8.2 Optimal Control

8.2.1 Optimal Control Strategies

The optimal control strategy determined for the plant in this work was to fully load either the steam driven chiller or electric motor driven chiller, depending upon chilled water return temperature and kW·hr cost. This strategy can be presented to plant operators with simple "If-Then" rules. For example, if the time of day is between 10 a.m and 9 p.m. and the chilled water return temperature is above 10.4°C, then the steam driven chiller should be fully loaded.

As the plant operates over a day, the optimally favored chiller can change as the chilled water return temperature increases or decreases. Although the optimal control may indicate the change in loading, it may not be economically optimum because of costs associated with the unloading of one chiller and loading of the other. If a cost of switching can be estimated, the optimization algorithm can consider the additional costs in determining the optimal control. The optimization algorithm would need a load model since the decision to switch will depend upon energy cost savings predicted over the duration of the switch.

The existing method of cooling tower fan control is to manually switch the fans on or off based upon an operator's decision. While the recorded fan speeds did, on average, follow the trends predicted in the optimal control, automatic fan speed control would be more consistent and cost effective than human control.

8.2.2 Demand Charges and Dynamic Optimization

The steady state optimization problem with demand charges was solved by embedding the minimization without demand problem within a minimization problem with respect to the upper limit on electrical demand (See Section 6.5). This approach can also be used to solve the problem of optimizing a dynamic system subject to demand charges, such as a plant with thermal storage elements.

One primary reason for installing and operating a thermal storage system is to reduce peak demand charges. During very high or peak loads the chilled water load can be met with water chilled with the storage elements. The optimal control problem for systems with thermal storage elements is usually solved by the dynamic programming method. [Bra88, Hen97] However, if an energy demand charge is incorporated into the objective function, the problem cannot be solved directly by dynamic programming.

Dynamic programming is founded upon Bellman's principle of optimality: An optimal set of control actions has the property that no matter what the previous control actions have been, the remaining control actions must constitute an optimal set of control actions with regard to the state resulting from those previous control actions. [Lew95] The problem with the peak electrical

demand charge is that peak demand is a function of all the control decisions over a billing period, not just the future decisions:

$$p_{\text{peak}} = \max\left(p_{t=1}, p_{t=2}, \ldots, p_{t=k}, \ldots, p_{t=n-1}, p_{t=n}\right). \tag{8.2.1}$$

The peak power demand is not known until the end of the period after all control decisions have been made. Thus a control decision at stage k to limit demand would not be optimal if the peak demand occurred at some future stage $k+j$. Conversely, not limiting demand at stage k would not be optimal if, at the end of the period, it were determined that peak demand occurred at stage k.

The dynamic programming problem can be solved if a constraint on maximum power, $p_{\max}$, is observed over all stages. Then the dynamic programming problem can be embedded in a minimization problem with respect to $p_{\max}$, as was done for the static optimal control problem in Section 6.5.

8.2.3 Extension of Optimal Control Methods

This work should be extended toward application of the optimal control strategy at the actual plant. Only half of the Walnut Street Plant was modeled in this work. The remaining plant includes two other steam driven chillers and another six-cell cooling tower. An optimal control strategy for the plant should include chilled water set points for the additional chillers and fan speed settings for the additional cooling tower. Improved instrumentation for these additional components is required to obtain measurements that can be used to estimate model parameters.

Another chilled water plant, the Charter Street Plant, operates along with the Walnut Street Plant to meet campus chilled water requirements. Minimizing total campus costs for chilled water requires a model of the Charter Street Plant chilled water system as well. Adding the boiler and cogeneration unit at the Charter Street Plant would result in a more complete and more interesting optimization problem. Exhaust from the steam turbine that drives the generator is a primary source of the steam consumed at the Walnut Street Plant and three additional chillers at Charter Street (a 7,000 ton chiller and two 3,500 ton chillers). The dependencies between the boiler, the steam driven electric generator, the steam driven chillers and the electric driven chiller make it almost impossible to postulate a favorable control strategy. However, an optimum strategy can be

predicted with a complete model of the campus chilled water system and an optimization algorithm.

The last step toward making a complete model of the campus chilled water system is a model of the load. The campus chilled water load is a strong function of weather (primarily incident solar radiation, wet and dry bulb temperature) and some deterministic schedules (e.g. in-session schedule). A time dependent load model is needed to account for the significant amount of energy storage in the chilled water distribution system. Large electric motor driven variable speed circulation pumps are used to maintain pressure in the chilled water distribution system. A model of the chilled water flow rate as it varies with load is needed to determine pumping costs.

Optimal control of the combined plants and chilled water loop is a challenging but solvable problem. Plant models can be created from interconnected component models and parameters estimated with the methods given in Chapters 3 and 4. Although a chilled water load model was not addressed in this work, means for creating a stochastic model of load as a function of weather and occupancy schedules are abundant in the technical literature. Electrical demand costs can be addressed as discussed in Section 6.5. The scale of the minimization problem makes it a formidable challenge. Including the energy storage in the chilled water model yields a time dependent system. However challenging, the means for modeling the complete system exist as well as methods for determining model parameters. Combining available static and dynamic optimization methods along with increasingly powerful computers put the goal within reach.

8.2.4 Recommended Application of Optimal Control Results

Although the two chiller plant model studied in this work does not represent all components of the Walnut Street Plant, the optimal supervisory control results in Chapter 6 are still useful. At times of high plant load, all four chillers in the plant are operated. Thus, there is a part of the total plant load that must be met by chillers #3 and #4 (steam driven and electric driven). At the high load conditions, plant personnel should implement the recommended priority loading for chillers #3 and #4. Also, the optimal cooling tower control maps given in Figures 6.3.6 and 6.3.7 should be used to guide cooling tower fan speed control.

The optimal control strategy can be validated by comparing measured energy use, while under optimal control, to historical measurements of energy use of the two chillers and cooling tower when operated during the same loads and wet bulb temperatures.

Bibliography

[Aus93] S. Austin. Chilled water system optimization. *ASHRAE Journal*. July, 1993.

[Bar74] Y. Bard. *Nonlinear Parameter Estimation*. Academic Press, New York. 1974.

[Bat88] D. Bates and D. Watts. *Nonlinear Regression Analysis and Its Applications*. John Wiley and Sons, New York. 1988.

[Bog90] P. Boggs and J. Rogers. Orthogonal distance regression. *Contemporary Mathematics*. Vol. 112. 1990

[Bog92] P. Boggs, R. Byrd, J. Rogers and R. Schnabel. *User's Reference Guide for ODRPACK Version 2.01*. National Institute of Standards and Technology Report, NISTIR 92-4834. 1992.

[Box73] G. Box, W. Hunter, J. MacGregor and J. Erjavec. Some problems associated with the analysis of multiresponse data. *Technometrics*, **15**(1), 1973.

[Bra88] J. Braun. *Methodologies for the Design and Control of Central Cooling Plants*. Ph.D. Thesis. University of Wisconsin-Madison. 1988.

[Bra89] J. Braun, S. Klein, W. Beckman and J. Mitchell. Methodologies for optimal control of chilled water systems without storage. *ASHRAE Transactions*. **95**(1), 1989.

[Bra90] J. Braun, G. Diderrich. Near-optimal control of cooling towers for chilled-water systems. *ASHRAE Transactions*. **96**(2), 1990.

[Brn98] M. Brandemuehl. Implementation of on-line supervisory control of cooling plants without storage. ASHRAE Research Project 823-RP. Interim report presented at the ASHRAE Annual Meeting on 18 January 1998 in San Francisco.

[Chu82] C. Chun and N. Norden. Computer Optimization of Refrigeration Systems in a Textile Plant: A Case History. *Automatica*, **18**(6), 1982.

[Cor87] A. Corana, M. Marchesi, C. Martini and S. Ridella. Minimizing Multimodal Functions of Continuous Variables with the "Simulated Annealing" Algorithm. *ACM Transactions on Mathematical Software*. **13**(3). 1987.

[DOE97] United States Department of Energy, Energy Information Administration. *Monthly Energy Review*. Publication No. DOE/EIA 0151(97/05). Washington, D.C. 1997.

[Ell88] J. Ellis, C. Kambhampati, G. Sheng and P. Roberts. Approaches to the optimizing control problem. *International Journal of Systems Science*. **19**(10). 1988.

[Ent84] L. Enterline, A. Sommer and A. Kaya. Chiller Optimization by Distributed Control to Save Energy. *ISA Transactions*. **23**(2), 1984.

[Fin80] W. Findeisen, F. Bailey, M. Brdyś, K. Malinowski, P. Tatjewski, A. Woźniak. *Control and Coordination in Hierarchical Systems*. Number 9, Wiley IIASA International Series on Applied Systems Analysis. John Wiley & Sons, New York. 1980.

[Gil81] P. Gill, W. Murray, and M. Wright. *Practical Optimization*. Academic Press, London. 1981.

[Gof94] W. Goffe, G. Ferrier and J. Rogers. Global optimization of statistical functions with simulated annealing. *Journal of Econometrics*. Vol. 60. 1994

[Gol89] M. Golden and B. Ydstie. Adaptive Extremum Control Using Approximate Process Models. *AIChE Journal*. **35**(7). 1989.

[Hac84] R. Hackner, J. Mitchell and W. Beckman. HVAC System Dynamics And Energy Use In Buildings–part I. *ASHRAE Transactions*. Paper KC-84-09, 1984.

[Hac85] R. Hackner, J. Mitchell and W. Beckman. HVAC System Dynamics And Energy Use In Buildings–part II. *ASHRAE Transactions*. **91**(1), 1985.

[Hen97] G. Henze, R. Dodier, M. Krarti. Development of a predictive optimal controller for thermal energy storage systems. *International Journal of Heating, Ventilating, Air-Conditioning and Refrigerating Research*. **3**(3).

[Hic87] T. Hicks, Editor. *Power Generation Calculations Reference Guide*. (The MacGraw-Hill engineering reference guide series). McGraw-Hill, New York. 1987.

[Jon85] G. Johnson. Optimization Techniques for a Centrifugal Chiller Plant Using a Programmable Controller. *ASHRAE Transactions*. **91**(2), 1985.

[Kan90] G. Kang and D. Bates. Approximate Inferences in Multiresponse Regression Analysis. *Biometrika*. **77**(2), 1990.

[Kir83] S. Kirkpatrick, C. Gelatt, M. Vecchi. Optimization by Simulated Annealing. *Science*. **220**(4598). 1983.

[Lau85] A. Lau, W. Beckman, J. Mitchell. Development of Computerized Control Strategies for a Large Chilled Water Plant. *ASHRAE Transactions*. **91**(2), 1985.

[Lew95] F. Lewis and V. Syrmos. *Optimal Control*. John Wiley and Sons, New York. 1995.

[Lip77] B. Lipták. Optimizing Plant Chiller Systems. *Instrumentation Technology.* September 1977.

[Ols90] R. Olson and J. Liebman. Optimization of a Chilled Water Plant Using Sequential Quadratic Programming. *Engineering Optimization*. Vol. 15, 1990.

[Pie86] D. Pierre. *Optimization Theory with Applications.* Dover Publications, Mineola, New York. 1986.

[Mac93] J. MacArthur. A Novel Predictive Strategy for Cost-Optimal Control in Buildings. *ASHRAE Transactions*. **99**(1), 1993.

[Mah82] R. Mah and A. Tamhane. Detection of Gross Errors in Process Data. *AIChE Journal*. **28**(5). 1982

[McL79] D. McLean, D. Pritchard, D. Bacon and J. Downie. Singularites in Multiresponse Modelling. *Technometrics*, **21**(3), 1979.

[Met53] N. Metropolis, A. Rosenbluth, M. Rosenbluth, A. Teller and E. Teller. Equation of State Calculations by Fast Computing Machines. *Journal of Chemical Physics*. **21**. 1953.

[Mor93] J. Moré and S. Wright. *Optimization Software Guide*. Society for Industrial and Applied Mathematics, Philadelphia. 1993.

[Nel65] J. Nelder and R. Mead. A Simplex Method for Functional Minimization. *Computer Journal*. Vol. 7. 1965.

[Ng94] K. Ng, T. Bong and H Chua. Performance evaluation of centrifugal chillers in a n air-conditioning plant with the building automation system (BAS). *Proceedings of the Institution of Mechanical Engineers. Part A, Journal of Power and Energy.* 208(A4). 1994.

[Seb89] G. Seber and C. Wild. *Nonlinear Regression.* John Wiley and Sons, New York. 1989.

[Sen90] A. Sen and M. Srivastava. *Regression Analysis: Theory, Methods, and Applications.* Springer-Verlag, New York. 1990.

[Spe85] P. Spethmann. Optimized Control Of Multiple Chillers. *ASHRAE Transactions*. **91**(2), 1985.

[Tam85] A. Tamhane and R. Mah. Data Reconciliation and Gross Error Detection in Chemical Process Networks. *Technometrics*. **27**(4). 1985.

[Thi83] D. Thielman.Chiller Optimization by Energy Management Control Systems. *ASHRAE Journal*. November 1983.

[Wil87] L. Wilkinson. *SYSTAT: The System for Statistics.* SYSTAT, Inc., Evanston. 1987.

[Zim76] H. Zimmer. Chiller Control Using On-line Allocation for Energy Conservation. *ISA Annual Conference Proceedings*, No. 522, 1976.